Response to the Referees

Comments from Referees are written in *italic* and our replies are in blue.

Anonymous Referee #1

Review of "New technique for high-precision, simultaneous measurements of CH_4, N_2O and CO_2 concentrations, isotopic and elemental ratios of N_2, O_2 and Ar, and total air content in ice cores by wet extraction" by Oyabu, I. et al. AMTD.

General:

The manuscript discusses a significantly improved extraction method for sample size without compromising precisions of several important paleo-proxy parameter. The multi-proxy approach is very helpful for improving not only the resolution due to the lower sample amounts necessary, but also regarding the comparison among the different parameters analysed. This again improves the issues with timing, since all the parameters are measured on the same sample, as well as the intercomparison of parameter because only one laboratory and one method is used.

The manuscript is very nicely written with detailed information how the method works and how it is used for standard and sample analyses. Furthermore, the authors show tests that only a very limited number of corrections are necessary which is obviously due to the in depth selection and preconditioning of all materials used in the extraction, split and measurement lines. They further state how the values are calibrated.

It was easy to read the manuscript and I would like to congratulate the authors. I have only a few rather minor comments and suggestions. I suggest to publish it once these comments have been taken into consideration.

Thank you very much for your review. Our replies are in blue.

Minor points:

You often used subscripts rather than superscripts in the text. This need to be changed, i.e. $\delta^{15}N$ rather than $\delta_{15}N$, or cm^3 rather than cm_3. Please check any such issues.

They were due to unexpected errors of the MS Word application when the word file was converted to the PDF file. We use a different conversion software to solve the issue and checked all the descriptions.

Line 137: New header (Description of method and manipulations)

We added a new header there, and we also added two more headers under section 2.1., as the following.

Line 120 (in the revised manuscript with track changes): **2.1.1 Extraction line and its pre-treatment**

"A schematic diagram of our extraction system is……".

Line141 :**2.1.2 Preparation of apparatus and ice samples**

"For routine air extraction, the sample tubes and extraction line are…….".

Line 170: **2.1.3 Manipulations for air extraction**

"Up to six vessels, thus prepared, are brought to our laboratory room at……..".

Line 211: Flame Ionization Detector not Frame

We correct it (line 257).

Line 293: How are the coefficients d, e, and f calculated, how do they relate to a, b and c?

For the FIDs, the relationship between peak area and pressure (for the same standard gas) is found to be almost linear over a wide pressure range, but it is slightly nonlinear towards lowest pressures within the range of the ice core measurements. Also, the response of ECD detector is generally nonlinear. We thus interpolate the three calibration points for each of three standard gases by a quadratic fit (the determination of a, b, and c for each gas). The relationship between the concentration and area at any given pressure is also slightly nonlinear, and thus we interpolate the three calibration points on the area-concentration space (from three standard gases, at the pressure of the sample gas) also with a quadratic fit (the determination of d, e, and f). A three-point calibration with quadratic fit is a common practice in precise atmospheric observations. The a, b, and c should be closely related with d, e, and f (after compensating for different units, for the same molar abundance of a gas of interest) because they both represent the same nonlinear responses of the same detectors. However, the coefficients would not necessarily be identical because of uncertainties unrelated to the detector characteristics, such as those from pressure measurement, standard gas scale, and deviation of actual pressure-area relationship from the quadratic function.

We added a figure (Fig. 5) based on the above explanation and some more description (line 332 – 343).

Eq. 6, lines 380ff: what about the sample loss during the first evacuation after loading the sample? Is this neglectable?

We indeed take into account the sample loss during the evacuation as follows, although it is small. After all the extractions for a day, the mass of Trap 1 is measured to obtain the total mass of sublimated ice during the first-stage evacuations. The typical amount of ice is 0.5 – 1.5 g for four to six samples (each with ~90-min evacuation). To account for the additional loss during the second evacuation after switching the line to the transfer line (~30 min), the mass of ice in Trap 1 is multiplied by 4/3 (120 min/90 min). The ice loss for each sample is estimated by simply dividing the total ice loss by the number of samples, and it is typically 0.1 – 0.3 g. We added this explanation in lines 208 – 210 and 432 – 437 in the revised manuscript.

Eq. 8: Why is the normalization made to direct atmospheric air and not to a standard that is well linked to the outside air at a given time.

The normalization of the sample is indeed made to the reference can, which is determined against the atmosphere from time to time. We revised the text as lines 558 – 575.

Line 548: …is impossible to be of atmospheric origin…

We corrected it (line 619).

Line 603ff: you might cite Huber et al., EPSL 2006

We added Huber et al. (2006, EPSL) and Severinghaus et al. (2009, Science), and revised the text following the comment by another reviewer (lines 710 – 713).

Referee #2 (Jochen Schmitt)

General remarks:

The paper by Ikumi Oyabu and co-authors presents a new technique to extract and subsequently measure a large suite of key parameters on a single ice core sample. Since so many and diverse parameters are obtained from this new device, this paper is quite extensive. Not only the technique is described, but also new results for several parameters are presented and compared with previous records. Thanks to the fact that the manuscript is both well-structured and clearly written, the reader is not overwhelmed and can find the necessary information without too much effort.

The introduction provides the reader with sufficient information of the key applications of the individual parameters that are obtained with the new device. This chapter nicely captures the general advantages of multi-species measurement systems, i.e. to save precious ice and, more importantly, to obtain a large suite of parameters from the same piece of ice. Obviously, this feature is advantageous to improve the palaeo-climatic interpretation (no age difference between parameters), it is also very useful for troubleshooting and scrutinizing the parameters. As the ice core community continuously improves the precision and accuracy of these parameters, more and more previously unknown effects (e.g., production of species in the ice or preferential loss of some gas species from the ice) emerge from the noise level that alter the archived information of the ice core. Multi-species methods that provide a wide array of parameters without compromising the individual precisions are the key techniques to help identify and quantify those effect. In that sense, the new method presented by Oyabu and co-authors is very welcome and sets a new standard for these analyses.

Overall, the paper is already in good shape and below I commented only on minor issues to improve the accessibility of the text and figures.

Thank you very much for your very detailed and thorough review, including a number of specific suggestions on the manuscript. We took them into consideration in revising the manuscript. Below, we reply to your comments in blue.

Minor comments on the text:

Line 77: Beginning of Chapter 2. You immediately start describing your procedure and then you compare/discuss it afterwards with other options to extract air with wet extraction techniques. While OK, you may add a short introductory section to briefly discuss the different wet techniques and point out their advantages and drawbacks. This may help readers not familiar with wet extraction techniques to put your technique into a wider perspective; e.g. …three different types of wet extraction techniques have been developed that…1) melt-refreeze techniques (you already mention it with their drawbacks) 2) melting under vacuum with the vessel closed, with subsequent helium purging (takes long and consumes lots of helium often used for isotope work on greenhouse gases e.g. Bock et al. 2014, AMT); 3) melting under vacuum with immediate removal of the released air (Kawamura et al., Schmitt et al. 2014, AMT, Bereiter et al. 2018). Method 3) is the preferred way to achieve sufficiently high extraction efficiencies for precise values of soluble trace gases (e.g. N_2O, Xe) and high-precision ratios of atmospheric main components (e.g. O_2/N_2).

We modified the first paragraph of Chapter 2 in the revised manuscript (lines 83 – 98 in the revised manuscript with track changes).

Line 83: please clarify: "Also, the pressure over the meltwater is relatively low (~100 – 200 Pa),…" The reported 100 to 200 Pa is not the air pressure over the meltwater (within the vessel) as this value is measured far away downstream at P1, after the water traps, if I got it right. The air pressure after the first water trap is modulated by the individual flow resistances of the tubing etc. between the vessel, the water trap, and the He cryostat. To my knowledge, there is no simple solution to come up with a robust estimate of the air pressure over the meltwater. One option would be to install a pressure sensor close to the vessel and before the first water trap and measure the total pressure (pH_2O at 0°C around 600 Pa plus the air pressure) and subtract the water vapour pressure. Using bubble-free ice as a comparison allows to get an estimate of the actual pH_2O while the ice melts, which might be warmer than 0°C since you melt the ice quite quickly with the hot water bath.

As you point out, the pressure (~100 – 200 Pa) is the reading of P1 and thus probably much lower than the air pressure over the meltwater in the vessel. We simply removed "(~100 – 200 Pa)" from the text. It would be interesting and informative if we can actually measure the air pressure in the vessel, but we have not done such experiments considering the fact that it would not help to improve the method itself, and that it requires significant cost (a dedicated pressure sensor, some modification to the system, and time and effort to establish the experimental procedures and precision). Together with the prior sentence, we modified the text as the following (lines 108 – 113).

Line 108: you might add here that this $H_2O + O_2$ pre-treatment is sufficient for the (relatively short) extraction step. However, O_2/N_2 ratios are not stable in these sample tubes over a longer time, therefore we use a different set of dip tubes after splitting (GEPW tubes).

We added a sentence (lines 138 – 140).

.

Line 111: you might remove this extra info "(i.e., on weekends and holidays)" to help keep the paper short.

We deleted it (line 144).

Line 122: remove "highly". unclear: "the surface of ice samples". Actually, the fractionation happens on the exposed outer parts of the stored ice core sections (for me the term "ice sample" refers to the piece of ice that is prepared prior to the measurement in the lab).

We moved most of the paragraph to the beginning of section 5.2 (discussion of gas-loss fractionation), and modified according to your suggestions (this and the next two suggestions were taken into account) (lines 695 – 701).

Line 123: "… removed to precisely measure" add: … and accurately the archived composition for these ratios.

See above.

Line 127: "… not important for greenhouse gas …large molecular size…". This sentence could be better phrased to prevent misunderstanding. For example, CO_2 concentrations could indeed be biased by gas loss if O_2 (or if O_2, N_2, Ar, are lost without relative fractionation) is preferentially lost from the ice, while CO_2 is preserved due to its larger diameter. Consequently, CO_2 conc. would be biased higher as CO_2 conc. is just the ratio of CO_2 against total amount of (remaining) air. This process might occur but it is not yet visible due to limitations in the measurement precision. Gas loss biases for CO_2 were discussed as a potential option to explain the observed offsets among different ice cores

of the same age (e.g. Eggleston et al. 2016 doi:10.1002/2015PA002874).
See above.

Line 133: remove the word vessel after Dewar.
We removed "vessel" (line 167).

Line 137: "laboratory room", remove the word room after laboratory;
We removed "room" (line 171).

Line 144: regarding the impact of the ice + gas loss during sublimation on TAC: can you estimate how much ice is lost due to sublimation (e.g. weighing the sample before and after 90 +30 min of pumping?
We take into account the sample loss during the evacuation as follows, although it is small. After completing all extractions for a day, the mass of Trap 1 is measured to obtain the total mass of sublimated ice during the first-stage evacuations (all samples combined). The typical amount is 0.5 – 1.5 g for four to six samples (each with ~90-min evacuation). To account for the additional loss during the second evacuation after switching the line to the transfer line (~30 min), the mass of ice in Trap 1 is multiplied by 4/3 (120 min/90 min). Then, the ice loss for each sample is estimated by simply dividing the total ice loss by the number of samples, and it is typically 0.1 – 0.3 g. We added this explanation to the text (lines 208 – 210 and 432 – 437).

Line 149: "After the evacuation, all vessels, except for one for the first extraction, are…" please rewrite
We rewrote as line 183.

Line 156: "The hot water bath is removed after the completion of ice melting." At that point, I wondered how the operator detects when the ice is gone because the vessel where the ice is melted is full metal, thus there is no visual control of that point. I guess it is done via a sudden drop in the pressure reading at P1? Also, all valves of the entire system are manually operated, right?
We found that the pressure at P1 is not a good guide for knowing the timing of the completion of ice melting, so we rely on the senses of the operators on the noise from the vessel and temperature at the bottom of the vessel. Popping noise can be heard during the ice melting (especially if it is clathrate ice), and it changes to higher frequency noise, which could originate in the boiling of meltwater under vacuum. However, the difference in noise is not always clear, thus we also sense the temperature at the bottom of the vessel by temporarily removing the hot water bath and touch the bottom for a few seconds. The rapidity of temperature decrease sensed by hand can tell if the ice is melted away (if ice still exists, we quickly feel icy coldness). We added a brief description to the manuscript (line 191).
All valves of the extraction and split lines are manually operated.

Line 159: "The time required for melting the ice sample is <~3 minutes, and the total time for the air transfer takes ~10 min (including the ice melting)." Perhaps it is easier for the reader if you write that the ice melting takes ca. 3 min and the pumping step after melting is completed takes additional ca. 7 min (i.e. the duration of the individual steps).
We changed the text (line 195).

Also: convert the mTorr unit into Pa to use only one pressure unit throughout the paper.
We unified the units (line 194).

Line 163-165: this sentence could benefit from rephrasing. I am not sure if I got it.
We changed the text (lines 199 – 202).

Line 170: "one night" perhaps just write the hours that are physically needed for this equilibration step and not "one night"
We changed it to "15 – 24 hours" (line 207).

Line 173: Does that mean you measure two sets of 6 samples each day?
No, we can operate only one set of 6 samples in a day. We changed the text (line 210).

Line 182: "…depletion of the O_2/N_2 ratio" just to be on the save side, explicitly say that O_2 is consumed at the metal surfaces leading to lower O_2/N_2 values (to exclude the option that extra N_2 causes lower O_2/N_2 ratios)
We added it as line 223.

Line 184: perhaps add a sentence stating that the stainless steel sample tubes lead to an unacceptable trend in the O_2/N_2 ratio as O_2 is consumed (perhaps provide numbers if available so the reader gets a handle on the size of this O_2 depletion).
We added a sentence (lines 225 – 228)

Line 187: delete "(e.g., during nights and weekends)",
We deleted it (line 231).

Line 191: replace "(measured at the head of a turbomolecular pump with an ionization gauge) with (P3)
We corrected it (line 236).

Line 198: perhaps add the reason for the -196°C cold trap: ..to remove CO2 and N2O…
We added it (line 242).

Line 201: is the lowering of the tube by a few cm an essential step or rather precautionary or does it speed up the process?
This step is a precautionary procedure, at least for our routine analysis with small samples (~1 mL_{STP}).

Line 204: unclear "Sometimes the samples are measured on the following day of the splitting".
We deleted the sentence and modified the prior sentence as line 249.

Line 209: "the air left in the original sample tube" can you roughly provide the reader with an estimate of how much the rest is (e.g. fraction of the original amount)? You provide this info (80% vs 20%) only in the conclusion.
We corrected this part as "the remaining air in the original sample tube (~80 % of the extracted air)..." in line 254.

Line 211: FID = flame ionization detector
We corrected it (line 257).

Line 223-: This GC section is nicely written too, yet due to the inherent complexity of the system it still took me a while to jump from one valve to the next and figure out which way the gas goes. It is hard to come up with a better description but you could help the reader by optimizing details, e.g. you write "we use small sample loops (1/16" o.d., 0.5 cm3, Valco)" here, it would help that you use the same unit as in Fig. 3 (rather than 0.5 cm^3 in the text and 500 µL in the figure)…write e.g. we use two 500 µL sample loops (Loop 1 and 2 in Fig. 3 [mentioning the names Loop 1 and 2 helps the reader locate the object quicker])
We use the same units (mL) and modified the explanation according to the suggestion (line 268).

Line 229: 400 – 600 hPa…
We added it (line 274).

Line 241: let? "At 1.74 min, V2 is switched to lead CO_2 from column 1 to pass through…"
We corrected it (line 286).

Line 346 : "… but the first cycle is discarded and only the latter 16 values are used." Delete "and only the latter 16 values are used" as this should be clear already.
We deleted it (line 394).

Line 351: "…by simply opening the tube valve". Just curiosity: is the valve opened quickly?
We open the valve as quickly as possible.

Line 359: (at ΔP = 0, +100 and -100 ‰). In line 347 you write "… imbalancing the sample pressure by ± 10 %". It is already clear that the ± 10 % refer to the +100 and -100 ‰, but using the same "unit", either % or ‰, could save a few seconds for some readers.
We use "10%" (line 407).

Line 437: "The standard gas thus transferred to the sample tubes is (are) measured …" check is/are.
We corrected from "are" to "is" (line 492).

Line 465: as you assume that a constant amount of O_2 is consumed independent of the sample size you could use a Keeling plot style fit (i.e. 1/V) and work with a linear system instead of the exp function.
We tried the Keeling plot and the linear fit, but the goodness of fit turned out to be poor (figure below), and the magnitude of correction seemed to change too rapidly at low volumes. It might imply that O_2 consumption may not

strictly be independent of sample size, and we would like to keep the exponential function that gives the better fit.

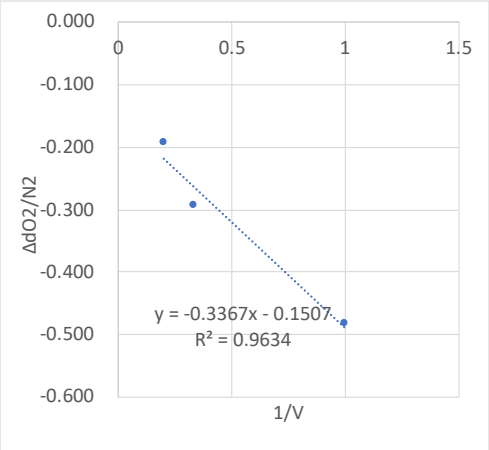

Line 501: please rephrase this sentence

We modified this part as lines 558 – 562.

Line 511: "…112.88 – 157.81 m (bubbly ice, 2.0 – 0.2 kyr BP)," please arrange order, the same a line below for the NEEM core

We corrected (lines 581 and 583).

Line 551: "In any case, we exclude these anomalously high concentrations from the calculation of pooled standard deviation and comparison with other ice core records". Perhaps rephrase: I am not so convinced by your statement that these anomalies should not be compared with other records as CH_4 anomalies have been observed for NEEM and GISP2, therefore these anomalies are valuable and important observations. You might also cite and have a look in Mitchel et al. 2013, Supplement figure S1: there are several instances where GISP2 shows elevated CH4 that are not an analytical artefact but features of the ice (see Rhodes et al. papers 2013, 2016).

We agree with the reviewer and changed this part as lines 624 – 631.

Just my curiosity: 2 out of three of anomalous samples from 361 m show also elevated CO_2 values. Do the corresponding dO_2/N_2 values for these samples also deviate from their neighbours (e.g. lighter values due to microbial O_2 consumption)?

We checked CH_4, CO_2 and $\delta O_2/N_2$ around 361 m and 418 m, where CH_4 concentrations are anomalously high. The $\delta O_2/N_2$ are indeed ~3 ‰ lower in the samples with higher CH_4. However, $\delta O_2/N_2$ neighboring samples in the vertical direction can vary by a similar amount (for example at ~190 m where CH_4 values are normal), so the hypothesis of microbial O_2 consumption is not easy to test. We attach expanded figures below (not included in the manuscript).

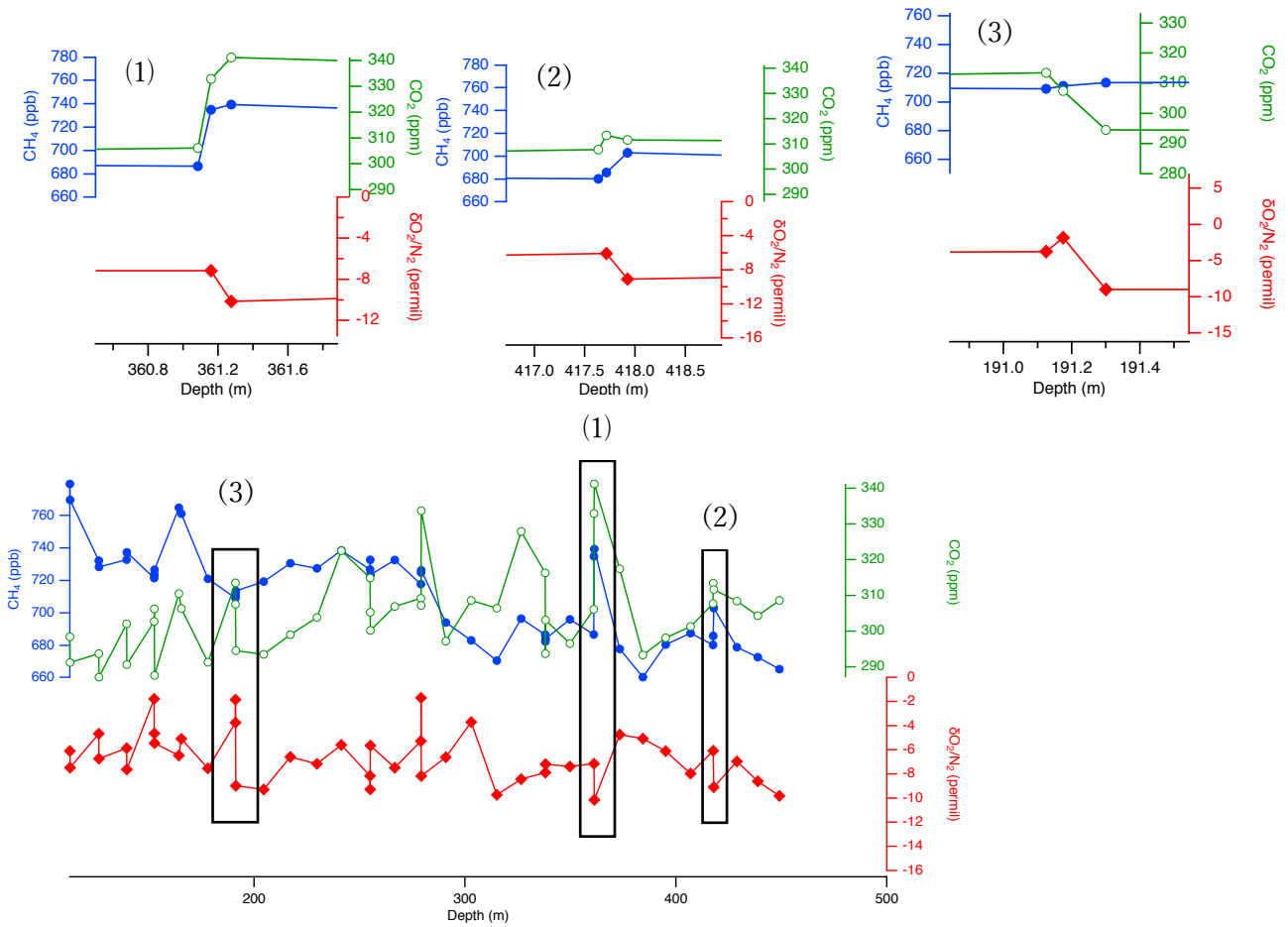

Line 561: The comparison of your N_2O measurements with previous measurements can be improved (especially in Fig. A1) as many records exist and the evolution during the Late Holocene is rather flat with only little fine structure. To make this comparison easier for the reader, you might use the Late Holocene Monte Carlo N_2O spline with 2s error envelopes and compare your DF and NEEM records with that spline as in Figure 4 of Fischer et al. 2019, Biogeosciences, doi: 10.5194/bg-16-3997-2019.

https://www.ncdc.noaa.gov/paleo-search/study/28890, the direct link to the Late Holocene N_2O spline is: https://www1.ncdc.noaa.gov/pub/data/paleo/icecore/fischer2019/fischer2019spline3k-2o.txt

We added the spline curve from Fischer et al. 2019 and also newly published N_2O data (NEEM and Styx Glacier cores) (Ryu et al. 2020, Global Biogeochemical Cycles) to the main figure (Fig. 10, error bars are summarized in a box for better visibility of the data points). We keep the original data points in Figure A1 but delete the lines connecting data points for better visibility. We added a discussion based on the new comparison as lines 644 – 660.

Line 578: to be complete, you might add "... generally measured with mechanic dry extraction techniques (references) and sublimation (Schmitt et al. 2011, doi:10.5194/amt-4-1445-2011).

We added the phrase and reference according to your suggestion (lines 674 – 675).

Line 585 and the following line: It might be better to mention in an introductory sentence that reliable atm. CO_2 reconstructions are only possible in Antarctic ice cores because impurity levels in Greenland are too high and lead

to excess CO_2 (refs). …so it is no wonder that your NEEM data also shows higher values.
We added a sentence at the end of the paragraph (lines 684 – 689).

Line 595: "…outer ice pieces were…"
We will add "pieces" between " ice" and "were" (line 704).

Line 599-601: these two sentences have almost the same meaning, combine.
We modified the second sentences as lines 710 – 713.

Line 601: "…indicating significant size-dependent fractionation in the outer ice". Without further information, the reader has no clue why you immediately state that these observations are due to a size-fractionating process. May be O_2 has a higher permeation rate due to solubility in the ice matrix compared to N_2. Either provide more background or just write e.g. gas species-dependent gas loss
We added some information (see above).

Line 603: "…but not for N_2, in the outer ice." Unclear: because N_2 is not lost at all.
We would like to keep the original sentence because it is possible that some N_2 is also lost from ice cores, but our analytical precision is not good enough to detect its isotopic fractionation. To clarify, we changed "significant" to "detectable" (line 714).

Line 609: please better specify what is plotted in Fig. 14: While it is clear that Fig. 13 shows the differences between samples with 5 or 8 mm removed this is not so clear for Fig. 14.
We changed the sentence as line 720.

Line 612: "…more than 8 mm is sufficient" message not clear: is 8 mm enough?
8 mm was sufficient in our tests, so we changed the text as line 724. We also added that we decided to cut 9 mm for the routine ice-core measurements, to have a safety margin (line 725).

Line 624 : "$\delta O_2/N_2$ as originally trapped…can be reconstructed (delete measured) from the 20-year old samples. Also, the overall match of the corrected old data and the new data is a good sign that the relatively large gas-loss correction was accurately done at that time.
We changed "measured" to "reconstructed" in the sentence (line 736), and add a phrase ", and that the relatively large gas-loss correction by Kawamura et al. (2007) was rather accurate" at the end of the sentence.

Line 625: regarding the $\delta^{18}O$ values in Fig. 15b it seems that the old values that experienced gas loss (thus mass-dependent fractionation of the O_2) are consistently heavier and is thus in line with the idea of the mass-dependent fractionation during the O_2 loss from the ice (a scaled correction factor that was used to correct the O_2/N_2 data from gas-loss effects might work as well).
We checked the relationship between $\delta^{18}O$ and storage period or O_2/N_2 and found no significant correlation. A reason for the lack of correlation may be that the magnitude of $\delta^{18}O$ fractionation (expected to be ~0.1 per mil) is one order

of magnitude smaller than the atmospheric variations (~1 per mil). Because the old data does not have any duplicated measurements, it is also impossible to examine pair differences, as conducted by Severinghaus et al., (2009). Another possible reason for the bias in the data is the underestimation of the gravitational correction by $\delta^{15}N$ (old data is generally lower than the new data). The old data also have much larger measurement errors (0.02 per mil for $\delta^{15}N$ and 0.05 per mil for $\delta^{18}O$ as one sigma) due mainly to a small number of measurement cycles (8 cycles x 1 block). Due to these limitations, it is difficult to discuss the nature of bias in the old $\delta^{18}O$ data, so we would like to keep the original text here.

Comment regarding the $\delta^{15}N$ values: The new measurements of the clathrate ice look, on average, ca 0.03‰ higher than the old Kawamura values. This systematic offset is not visible for the young ice, thus calibration is not the reason. Yet for gas loss, the sign is in the wrong direction.

We do not think it is safe to say that the offsets only exist in the clathrate hydrate ice because there are actually not many data points in the Holocene. There are two reasons we can think of for the offset between the new and old data, although it is difficult to conclude.

1) The old method did not split the sample for the MS measurement. It first measured the sample gas with GCs, and then the air that remained in the sample tube was measured with MS. There is a possibility that the sample gas was fractionated during the GC measurements.

2) The old method did not remove CO_2 before the MS measurements, thus a correction on $\delta^{15}N$ for the interference of fragmented CO_2 (by CO) was applied to $\delta^{15}N$ data. The correction factor was determined only once during the measurement campaign and could have had some bias.

Line 648 : technique?

We corrected it (line 761).

comments on the figures and tables:

Fig. 1 typo in the scheme: "He ditector", should read detector. Note, the schematic is quite large and in the final version it might get squeezed a bit to fit the page. To allow readability of the labels please increase the font size a bit (in most cases the distances allows that).

We increased the font size in the figure and corrected "He ditector".

Fig. 2: you might help the reader find the "small volume (1.4 cm3) between the valves" by adding colors to this section.

We added color to this section.

Fig. 3: the ":" symbol in the legend seems not necessary. electronforming (without n); explain SuS

We removed ":". "SUS" is a word from the Japan Industrial Standard for stainless steel, so we changed it to Stainless Steel (SS).

Fig. 4: I guess the y-axes are arbitrary units, please add any label to that axes. CH_4 panel, please add labels to the O_2 and CH_4 to make it more intuitive for the reader which peak is what. Since your paper has many figures (15) and

tables you might want to save a bit space here and try plotting Fig. 4 more compactly, e.g. plotting all three gases on one x-axis without showing the others (like you did in Fig. 5)
We modified the figure according to the suggestions.

Fig. 5: there seems to be a typo at the x axis labels (16.7.1), also Fig. 7. To better differentiate the symbols (filled vs open markers), you might increase the symbol size.
We used a standard format for the x-axes and increase the symbol size (Fig. 6 and 8).

Panel c. For the O_2/N_2 ratio is seams that with each new filling of the reference can the trends get smaller, i.e. less O_2 is consumed for a certain time interval. Is this an indication that consumption ceases over time as all of the oxygen-reactant is consumed?
We have four reference cans, so what we see in the graph is the differences of drifts between the different cans. It is possible that the O_2 consumption ceases over time (in every can) as you speculate, but we need more time (more rotations of the cans) before we can discuss it.

Fig. 6: there is a typo in the equation: there is + and - before 0.078802, equation (7) says -0.078802.
you may add the equation into the figure rather than in the caption
We corrected it and added the equation in the figure (Fig. 7).

Fig. 8: it looks like that the new CO_2 measurements are slightly higher between 100 and 150 m and after 1800 m compared to the old ones? perhaps calc. the difference of means for the 100-150 m. Is it due to better extraction efficiency (or lower headspace pressure air reducing CO_2 solution in the meltwater) or longer reaction time for the chemical CO_2 production pathway in the meltwater?
We think both of your suggestions are possible. The final headspace pressure should be lower in the new method (the reading at P1 is <0.1 Pa compared with <1 Pa in the old method). The transfer time is probably longer in the new method (as we wait for lower pressure). We don't discuss it in this paper because we would need dedicated experiments to draw a definite conclusion.

Fig. 9: Caption: remove "from other groups". Panel c: you don't need the connecting lines for South Pole and EDML and WDC. just keep it for Law Dome.
We deleted "from other groups" in the caption (line 1132). Please see above for the figure (Fig. 10).

Fig. 10: Caption: write "The line connects the blue markers..." since there is only one line, therefore, there is no need to specify this line it as "dotted line (blue)" Actually, I am not sure if you need the blue line at all as the next neighbouring points to the right side are quite a bit older and thus outside of the gas age distribution. For me this situation with the artefact samples is convincing already as the age difference of the plotted data is smaller than the NEEM gas age distribution. Additionally, you might indicate these two artefact depth levels already in Fig. 9 panel a) e.g. with a red circle around the artefact samples that you zoom in in Fig. 10.
We removed the blue line in the figure and add markers to indicate the two artefact depths in Fig. 10.

Fig. 11: caption. unclear statement: "For single (non-duplicate) measurements, "a" piece is not cut.". I am not sure if I got it right. If you do a single measurement, piece "b" is measured only, but you need to do the cut between a and b anyway? Further, how did you cut the curvature between the inner and outer pieces?

We only cut out the "b" piece for the single measurement (cut at (2)), so the "a" and its outer part remain as the main ice body. We usually cut the outer part at red lines by a bandsaw and shave off the rest by a ceramic knife.

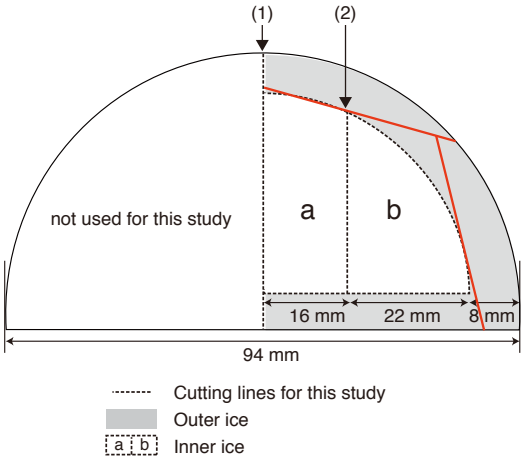

Fig. 12: you might consider producing a single figure (as e.g. nicely done in Fig. 15) out of the four panels because you don't need four-times Depth(m) and the depth scales. The same applies to Figs. 13 and 14. Also, you might consider using a Δ symbol (e.g. Δ δAr/N2 to indicate the "pair differences" to prevent too long y-axis labels every time and write this in the caption (Pair differences (Δ) between the inner and outer ice piece.

We corrected the figures (Figs. 13, 14 and 15).

Fig. 14: figure: go for the same design: the dashed line at zero is plotted as a thick line in d) while thin for a, b, c. please chose one thickness, e.g. the thin line style. Caption line 955: add pieces: between the two inner ice pieces: and also specify if it is a-b or b-a.

We corrected the figure and added the phrase as your suggestion (line 1170).

Fig. 15: figure top x-axis label: replace Air age with Gas age because you use gas age throughout your manuscript. Legend between panel c) and d) the names for the grey and red crosses are switched, the red symbols refer to the values After gas loss correction?

The figure was corrected (Fig. 16).

caption line 1001: delete dotted lines, because there are none (crosses connected with dotted lines, Kawamura, 2000; Kawamura et al., 2007).

We deleted it (line 1176).

Table A1: typo: TALDICE not TALDAICE; the Eurocore ice core and project is mostly written Eurocore (in some cases EUROCORE, but EURO core would be new)

We corrected TALDICE and removed the Eurocore data from the Fig. A1 because the Eurocore data covers only the

last 800 years.

Fig. A1:

panel a) this panel is a bit busy. you might consider plotting more records without the connecting line (EDML, TALDICE Schilt, Siple Dome) typo. EDML (Schilt et all. 2010), et al. And for the legend, TALDICE add a blank between 4.06 and ppb.

panel b) this is a busy panel and you might consider plotting only some records (your data and perhaps NEEM from Prokopiou et al) with a connecting line while removing the line for others (Eurocore, GRIP, GISP2, EDC, TALDICE, EDML)

We corrected your points.

Finally, a few technical things:

Most of your subscripts and superscripts in your manuscript have been moved up or down.

They were due to unexpected errors of the MS Word application when the word file was converted to the PDF file.

We will use a different conversion software to solve the issue and check all the descriptions.

Please check but the usual style convention for AMT papers is that the units % and ‰ are written without a blank, e.g. 0.23‰, while all others come with a blank. Also, the unit litre is written L, e.g., 25 mL.

We use a capital letter for a liter (L).

We found the statement “Spaces must be included between number and unit (e.g., 1 %, 1 m).” in the Figure content guidelines, so we do not remove a blank before % and ‰.

New technique for high-precision, simultaneous measurements of CH_4, N_2O and CO_2 concentrations, isotopic and elemental ratios of N_2, O_2 and Ar, and total air content in ice cores by wet extraction

Ikumi Oyabu[1], Kenji Kawamura[1,2,3], Kyotaro Kitamura[1], Remi Dallmayr[4], Akihiro Kitamura[5], Chikako Sawada[6], Jeffrey P. Severinghaus[7], Ross Beaudette[7], Anaïs Orsi[8], Satoshi Sugawara[9], Shigeyuki Ishidoya[10], Dorthe Dahl-Jensen[11,12], Kumiko Goto-Azuma[1,2], Shuji Aoki[13], Takakiyo Nakazawa[13]

[1] National Institute of Polar Research, Tokyo 190-8518, Japan
[2] Department of Polar Science, The Graduate University of Advanced Studies (SOKENDAI), Tokyo 190-8518, Japan
[3] Japan Agency for Marine Science and Technology (JAMSTEC), Yokosuka 237-0061, Japan
[4] Alfred Wegener Institute, Am Alten Hafen 26, Bremerhaven 27568, Germany
[5] Labosoltech LLC, Tokyo 190-0003, Japan
[6] Atmosphere and Ocean Research Institute, University of Tokyo, Tokyo 277-0882, Japan
[7] Scripps Institution of Oceanography, University of California San Diego, La Jolla, CA 92093, USA
[8] Laboratoire des Sciences du Climat et de l'Environnement, LSCE/IPSL, CEA-CNRS-UVSQ, Université Paris-Saclay, 91191, Gif-sur-Yvette, France
[9] Miyagi University of Education, Sendai 980-0845, Japan
[10] National Institute of Advanced Industrial and Technology (AIST), Tsukuba 305-8569, Japan
[11] University of Copenhagen, Tagensvej 16, Copenhagen 2100, Denmark
[12] University of Manitoba, 66 Chancellors Circle, Winnipeg, Manitoba, R3T 2N2, Canada
[13] Tohoku University, Sendai 980-8577, Japan

Correspondence to: Ikumi Oyabu (oyabu.ikumi@nipr.ac.jp)

Abstract. Air in polar ice cores provides ~~various~~ unique information on past climatic and atmospheric changes. We developed a new method combining wet extraction, gas chromatography and mass spectrometry, for high-precision, simultaneous measurements of eight air components (CH_4, N_2O and CO_2 concentrations, $\delta^{15}N$, $\delta^{18}O$, $\delta O_2/N_2$, $\delta Ar/N_2$ and total air content) from an ice core sample of ~60 g. The ice sample is evacuated for ~2 hours and melted under vacuum, and the released air is continuously transferred into a sample tube at 10 K within 10 minutes. The air is homogenized in the sample tube overnight at room temperature, and split into two aliquots for mass spectrometric and gas chromatographic measurements. Care~~s~~ ~~are~~ is taken to minimize 1) contamination of greenhouse gases ~~with~~ by using a long evacuation time, 2) consumption of oxygen during sample storage by a passivation treatment on sample tubes, and 3) fractionation of isotopic ratios with a long homogenization time for splitting. Precisions are assessed by analysing standard gases with artificial ice~~,~~ and ~~by~~ duplicate measurements of the Dome Fuji and NEEM ice cores. The overall reproducibility (one standard deviation) ~~from~~ of duplicate ice-core analyses are 3.2 ppb, 2.2 ppb and 3.1 ppm for CH_4, N_2O and CO_2 concentrations, 0.006, 0.010, 0.09 and 0.12 ‰ for $\delta^{15}N$, $\delta^{18}O$, $\delta O_2/N_2$ and $\delta Ar/N_2$, and 0.67 ~~ml$_{STP}$~~ mL_{STP} kg^{-1} for total air content, respectively. Our new method successfully

combines the high-precision, small-sample and multiple-species measurements, with a wide range of applications for ice-core paleoenvironmental studies.

1. Introduction

Measurements of gas components ~~of~~ in polar ice cores have provided valuable information on past climatic, atmospheric and glaciological changes. For example, CH_4, N_2O and CO_2 are important greenhouse gases with natural and anthropogenic variations. CH_4 concentration (defined as a dry air mole fraction in this paper) in deep ice cores is useful for detecting abrupt climate changes and to synchronize age scales of different ice cores (e.g., Blunier and Brook, 2001; Brook et al., 1996; WAIS Divide Project Members, 2015). The isotope values $\delta^{15}N$ of N_2 and $\delta^{40}Ar$ of Ar provide information on past firn thickness and surface temperature (Huber et al., 2006b; Kobashi et al., 2011; Kobashi et al., ~~2008~~2008a; Orsi et al., 2014; Severinghaus and Brook, 1999; Severinghaus et al., 1998). The $\delta O_2/N_2$ values in some ice cores are proxies for local summer insolation and used to constrain age scales by orbital tuning (Bender, 2002; Kawamura et al., 2007). $\delta^{18}O$ of O_2 records the variations of terrestrial hydrological cycles and is used for dating as well as detection of abrupt climate changes (Bazin et al., 2013; Extier et al., 2018; Landais et al., 2010; Seltzer et al., 2017; Severinghaus et al., 2009). Total air content (TAC) is affected by atmospheric pressure, temperature, and firn porosity at bubble close-off (Martinerie et al., 1994; Martinerie et al., 1992), and is used for reconstructing ice sheet surface elevation (NEEM community members, 2013) and orbital tuning (Bazin et al., 2013; Lipenkov et al., 2011; Raynaud et al., 2007).

Reduction of sample size and improvement of analytical precision are both desired for ice core studies, ~~Capabilities of both reducing the sample size and improving the analytical precision of ice core analyses are desired,~~ especially for deep ice cores from low accumulation sites ~~to acquire~~that require high-resolution data. For example, the inter-polar difference (IPD) of CH_4 for the Holocene is ~30 – 50 ppb (Beck et al., 2018; Chappellaz et al., 1997; Mitchell et al., 2013), thus analytical uncertainty of a few ppb is required for reconstructing subtle changes in IPD. Uncertainty of < ~0.01 ‰ would be required for $\delta^{18}O$ of O_2 (after correcting gravitational fractionation by $\delta^{15}N$) to detect the changes ~~for~~ during Heinrich events (Seltzer et al., 2017; Severinghaus et al., 2009). The smallest amplitude of the local summer insolation variation at the precession band is a few %, and the corresponding amplitude of $\delta O_2/N_2$ may be < 0.5 ‰.

High precision~~s with~~ in relatively small samples ~~have~~ has already been achieved for some species; ± 2.8 ppb for CH_4 with ~60 g of ice by Oregon State University (OSU) (Mitchell et al., 2013), ± 1.5 ppb for N_2O with ~20 g of ice by Seoul National University (SNU) (Ryu et al., 2018), and 0.005 ‰ for $\delta^{15}N$ and 0.01 ‰ for $\delta^{18}O$ with ~15 g of ice by Scripps Institution of Oceanography (SIO) (Seltzer et al., 2017; Severinghaus et al., 2009). However, a total of ~100 g of ice and more than one laboratory are required to measure all species. Multiple-species measurements combining gas chromatography (for greenhouse gases) and mass spectrometry (for major gas ratios) have been ~~applied~~ pioneered by Tohoku University (Kawamura, 2001;

Kawamura et al., 2003, 2007), but with lower precisions than the values mentioned above~~above-mentioned values~~ and larger samples (> 200 g).

Here, we present a new method developed at National Institute of Polar Research (NIPR) to measure eight air components ($\delta^{15}N$, $\delta^{18}O$, $\delta O_2/N_2$, $\delta Ar/N_2$, concentrations of CH_4, N_2O and CO_2, and TAC) using a 60 g piece of ice with high precision~~s~~. This method has the technical advantage~~s~~ of reducing the sample size without sacrificing precision. It also has the advantage ~~of~~ for paleoclimatic studies that all the measured species can be compared without any age difference. The method is also desired for very old ice cores from the Antarctic interior, with ~~the~~ expected resolution for 1.5-million-year ice near bedrock ~~is expected to be on the order of~~ of order10 kyr m^{-1} (Parrenin et al., 2017).

This paper is structured as follows. Chapter 2 describes the air extraction from ice and the splitting of the extracted air for the analyses by respective instruments. Chapter 3 describes the measurements of the sample air with two gas chromatographs and a mass spectrometer. The system performance and precisions are evaluated by various tests with standard gases (Chapter 4) and comparisons of our data from ~100 ice-core samples (Dome Fuji and NEEM) with published records from other laboratories.

2. Air extraction and split

Four types of wet extraction techniques have been developed by different laboratories: 1) ice is melted and slowly refrozen in a closed vessel to expel dissolved gas from the meltwater (so-called melt-refreeze technique, e.g., Brook et al., 2005; Chappellaz et al., 1997; Flückiger et al., 1999; Severinghaus et al., 2009; Sowers et al., 1989; Lipenkov et al., 1995 (air content)), 2) ice is melted in a closed vessel with subsequent agitation during transfer to extract dissolved gas (Severinghaus et al., 2003; Kobashi et al., 2008b), 3) ice is melted in a closed vessel with subsequent helium purging to extract dissolved gas (e.g., Bock et al. 2014), and 4) ice is melted in a vessel open to a sample tube to transfer the extracted air immediately (e.g., Bereiter et al. 2018; Kawamura et al., 2003; Nakazawa et al., 1993a; Schmitt et al. 2014). Method 1 is most widely used with small ice samples (~10 to 50 g) for measuring basic gas components for paleoclimatic reconstructions such as CH_4 and N_2O concentrations, or the isotopic and elemental ratios of N_2, O_2, and Ar with high precisions. The method requires a relatively long time for refreezing (up to several tens of minutes), and thus possibly elevates trace gas concentrations in the extracted air by degassing from the inner wall of the vessel, as well as alter the air composition by gas-dependent dissolution in meltwater and incomplete degassing during refreezing. Method 2 is used with larger ice samples (50 to 100 g) for N_2 and noble gases. Method 3 is used with much larger ice (several hundred grams) for measuring isotopic ratios of greenhouse gases. It takes a long time and consumes a large amount of helium. Method 4 is typically used with samples with intermediate or large size (one to several hundred grams) for measuring multiple gas species. It is also a preferred way to achieve both high extraction

efficiencies for soluble trace gases (e.g., N_2O and Xe) and high-precision ratios of N_2, O_2, and Ar.~~e.g., Brook et al., 2005; Chappellaz et al., 1997; Flückiger et al., 1999~~~~In order to~~

To measure CH_4, N_2O and CO_2 concentrations, isotopic and elemental ratios of N_2, O_2 and Ar, and TAC from ~~one~~a small ice sample with high precision, we modified ~~the wet extraction and measurement techniques~~Method 4 that was originally developed at Tohoku University (Kawamura et al., 2003; Kawamura et al., 2007; Nakazawa et al., 1993a; Nakazawa et al., 1993b). ~~Briefly~~In our new method, an ice sample of 50 – 70 g is melted under a vacuum, and the released air is immediately and cryogenically transferred into a sample tube at < 10 K (cooled with a closed cycle refrigerator) without refreezing the meltwater. It requires a relatively short time (< 10 minutes) for melting ice and transferring extracted air, minimizing contaminations due to degassing from the inner walls of the ~~vessel and line. Also, the pressure over the meltwater is relatively low (~100 – 200 Pa), thus the dissolution of released air in the meltwater is minimal (Kawamura et al., 2003). In comparison, the melt refreeze method typically requires several tens of minutes to refreeze meltwater (~~apparatus as well as dissolution of gases in the meltwater. The much lower air pressure over the meltwater than that in the other methods also helps to lower the gas dissolution in the meltwater (Kawamura et al., 2003). ~~e.g., Brook et al., 2005; Chappellaz et al., 1997; Flückiger et al., 1999), possibly elevates trace gas concentrations in the extracted air by degassing from the inner wall of the vessel, as well as alter the air composition by gas-dependent dissolution in meltwater (at several tens of hPa) and incomplete degassing during refreezing.~~

The extracted air is homogenized in the sample tube for one night and split into two aliquots for mass spectrometric (MS) and gas chromatographic (GC) measurements. About 20 and 80 % of the sample are used for the MS and GC measurements, respectively.

2.1 Air extraction

2.1.1 Extraction line and its pre-treatment

A schematic diagram of our extraction system is shown in Fig~~.~~ure 1. The components of the extraction line (tubings, fittings, valves and vessels) are made of electropolished (EP) stainless steel except for traps~~, which are~~ made of Pyrex glass. The traps 1 – 3 have Kovar glass-to-metal transition. It has six inlet ports for stainless-steel vessels, each containing an ice core sample. The vessels and traps 1 – 3 are connected to the line with metal face-seal fittings (Fujikin UJR®, 1/2") using nickel gaskets. Diaphragm metal-seal valves (Fujikin FUDDFM-71G-9.52) are used for all stop valves (V1 – V23). All valves are manually operated. ISO-KF25 flanges are attached to both ends of the trap 4 with two-component epoxy adhesive, and Viton o-rings are used for connecting the trap to the line. The vacuum is provided by a turbomolecular pump (Pfeiffer HiPace 80) backed by an oil rotary pump (Edwards). The vessels are made of stainless steel pipe (65A) with Conflat flange (ICF114) with a volume of

~600 ~~cm^3~~mL, and the sample tubes are made of 1/4" EP stainless-steel tube with a metal-seal valve (Fujikin FUDDFM-71G-6.35) with a volume of 6.6 ~~cm^3~~mL.

After constructing~~the construction of~~ the extraction line (before actual use), we performed pre-treatment of inner surfaces of all the lines, vessels and sample tubes as follows. Pure O_2 (> 99.999 %) was humidified by bubbling through pure-water in a glass flask sealed with a silicone cap at room temperature, and flowed into the lines and vessels heated to 90 – 100 ˚C with heating tapes at a flow rate of ~20 – 50 ~~ml~~mL min^{-1} for two weeks to remove trace organic substances and hydrocarbons efficiently~~to efficiently remove trace organic substances and hydrocarbons~~. After the treatment, the line and vessels were evacuated at 90 – 100 ˚C by a turbomolecular pump for one week. The same treatment is applied to the sample tubes for air extraction. We note that we use a different set of sample tubes with a better performing treatment after splitting for $\delta O_2/N_2$ stability (GEPW tubes, see below), but the $H_2O + O_2$ pre-treatment is sufficient for the extraction step and has the advantage of low cost.

2.1.2 Preparation of apparatus and ice samples

For routine air extraction, the sample tubes and extraction line are evacuated overnight to < 1.3×10^{-4} Pa (measured at the head of the turbomolecular pump with an ionization gauge, P3). If no extraction is planned for two days or more ~~(i.e., on weekends and holidays),~~ the sample tubes and extraction line are filled with pure air (> 99.99995 %) at ~500 Pa. On the day of air extraction from ice core samples, trap 4 is cooled to -196 ˚C by liquid nitrogen to evacuate further the sample tubes and extraction line (< 10^{-4} Pa). The vessels are brought out from an oven at 50 ˚C and cooled to room temperature in ~30 min, and then brought to the cold room at -20 ˚C for further cooling. Ice core samples of ~90 – 150 g, typically 7- to 12-cm long, are cut out from bulk ice-core samples with a band saw in a cold room at -20 ˚C. The same band saw is used to trim all faces for rough decontamination, removing ~2 – 11 mm from the original surfaces. The inner ~50 – 70 g of ice is used for the air extraction, and the removed outer ice is stored for other measurements (e.g., for multiple analyses in case of measurement failures). The amount of ice may be reduced to ~35 g for all measurements with somewhat lower precisions, and to ~9 g if only MS measurements are conducted (without sample splitting).

~~As $\delta O_2/N_2$ and $\delta Ar/N_2$ ratios of the Dome Fuji ice core become highly fractionated especially near the surface of ice samples due to diffusive gas loss during ice storage, the surface must sufficiently be removed to precisely measure the air composition~~ After cutting out an ice sample from the stored ice core body, the exposed outer parts of the stored ice core sections are trimmed with a band saw, and all the sections are shaved off~~(Bereiter et al., 2009; Ikeda-Fukazawa et al., 2005; Kawamura et al., 2007)~~. ~~The gas loss also affects $\delta^{18}O$ and $\delta^{40}Ar$ because it is weakly mass-dependent (Severinghaus et al., 2009). The thickness of required surface removal depends on the storage period, storage temperature and the form of air in ice (bubbles or clathrate-hydrates). On the other hand, it is established that the gas-loss effect is not important for greenhouse gas concentrations because of their large molecular sizes, high natural variability and measurement uncertainties. The fractionation of $\delta O_2/N_2$ is the most~~

~~problematic among the measured species, thus we tested different thicknesses of surface removal from the first Dome Fuji core stored at -50˚C for 20 years by focusing on $\delta O_2/N_2$. The surface is firstly trimmed with a band saw and secondly~~ by a ceramic knife. The shaving by knife also enables the visual inspection of the ice for any cracks. We found that more than 8 mm should be removed for the Dome Fuji clathrate-hydrate ice (> ~1400 m) to eliminate gas-loss fractionation of $\delta O_2/N_2$ and $\delta Ar/N_2$ due to diffusive gas loss during ice storage (details are described in section 5.2). The cleaned ice sample is placed in a pre-cooled extraction vessel and sealed with a Conflat flange and copper gasket. The vessels are placed in a dewar ~~vessel~~ that accommodates a copper tube (o.d. = 78 mm, i.d. = 74 mm, height = 135 mm) and a eutectic refrigerant bag (~1000 g, pre-cooled to -50 ˚C)~~,~~ to keep the ice temperature below -25 ˚C.

2.1.3 Manipulations for air extraction

Up to six vessels, thus prepared, are brought to our laboratory ~~room~~ at room temperature. All valves on the extraction line are closed, and the closed-cycle refrigerator is turned on. Then, pure air is introduced from V16 to purge the manifold for vessels, and the vessels are connected to the line. The room air is evacuated from the vessels with the turbomolecular pump. After ~5 min when the pressure after two water traps (i.e., without water vapor) is below 10^{-2} Pa, the flanges and connections are leak-tested with a helium leak detector (< 10^{-8} Pa L s^{-1}). Then, pure air is introduced into the vessels and pumped out four times to further remove room air from the vessels. All the vessels are then evacuated for 90 min through the evacuation line (Fig. 1, blue). Typically, four to ~~five~~six samples are simultaneously evacuated. The evacuation is made to remove residual room air from the vessels as well as to sublimate the ice surface for further cleaning of the sample. Then, the vacuum line is switched to the sample transfer line (Fig. 1, pink), which is the line for transferring sample air during the extraction, by closing V8, V9, V14 and V17, cooling the traps 2 and 3 to -80 ˚C with ethanol, and opening V22, V13, V10 and V8. The evacuation continues for another 30 min.

After the evacuation, all ~~vessels, except for~~but one ~~for~~of the ~~first extraction,~~vessels are isolated by closing the valves above them (V2 – V7~~.~~). V19 and V21 are opened, and the open vessel and line are evacuated for another ~5 min. V22 is closed to stop the evacuation, and the valve of a sample tube is opened to establish the line for sample air transfer. The~~Then, the~~ ice sample is then melted by immersing the vessel in a hot water bath (~90 ˚C) by a few millimeters~~mm~~ from the bottom. The air released from the melting ice is continuously transferred into the sample tube at ~10 K, after passing through two water traps at −80 and −100 °C. The first trap has sufficient inner volume to condense a large amount of water vapor, and the second trap contains fine glass tubes for high trapping efficiency. Sample transfer is monitored by a Baratron Gauge (MKS, full scale = 1333 Pa) (P1 in Fig. 1), which measures the sample air pressure in the line without water vapor. The maximum pressure during the transfer is ~100 – 200 Pa. The hot water bath is removed after the completion of ice melting~~.~~ (judged by the change of noise and temperature at the bottom of the vessel sensed by the operator). When the pressure decreases below the detection limit (0.1 Pa), the sample transfer is considered to be complete, and the valve of the tube is closed. Residual pressure in the transfer line is measured using a Convectron Gauge (Granville-Phillips, P2 in Fig. 1) (typically <~~0.~~2 ~~mTorr~~×10^{-2} Pa). The ~~time~~

~~required for~~ melting of the ice sample ~~is~~takes <~3 minutes, and the ~~total time for the~~ remaining air transfer takes ~~~10~~7 min ~~(including~~after the ~~ice~~ melting~~)~~. Finally, the valve of the vessel is closed, and the line is evacuated for ~2 min to decrease the pressure to $<10^{-4}$ Pa (P3).

The pressure ~~of air released from the ice sample~~ in the next vessel ~~during the previous transfer~~ is measured with the Baratron Gauge (P1) by closing V20, V21 and V22 and opening the valve of the vessel (typically <1~~.0~~ Pa for the second vessel and ~4 Pa for the fifth vessel~~)~~., because of gradual accumulation of air released from ice samples). This ensures the absence of a leak ~~at~~through the ~~flange and fitting of~~ valve above the vessel and hence the quality of the sample air in the previous extractions. Then, V22 and V21 are opened, and the line and vessel are evacuated for ~5 min, the ice sample is melted, and the released air is transferred to the next sample tube. We repeat these procedures until all the extractions are completed.

After collecting the air from all prepared samples, the sample tubes are removed from the helium cycle cooler and laid in the laboratory room with ambient temperatures for ~~one night.~~15 – 24 hours. All the vessels and traps are also disconnected from the line, rinsed with pure water, and placed in ovens at 50°C for drying. ~~Another~~The mass of Trap 1 is measured before and after extraction to estimate the total mass of sublimated ice during the evacuations (typically 0.5 – 1.5 g from four to six samples). Finally, as the preparation for the next extractions (on the following day or after), another set of sample tubes and traps are connected to the line and evacuated with the turbomolecular pump (to $<10^{-2}$ Pa), and then the line is checked with a helium leak detector ($< 10^{-8}$ Pa L s^{-1}). After the leak check, ~~all~~ the ~~valves are opened,~~tubes and the line ~~is~~are evacuated until the next ~~extraction.~~ extractions.

2.2 Splitting

A small aliquot of air is separated from the sample tube and transferred to a second tube using the "split line" (Fig. 2) for MS analysis. We employed the general design of the line for noble gas measurements developed at SIO (Orsi, 2013; Bereiter et al., 2018). The split line is made of electropolished stainless steel except for a U-shaped cold trap~~, which is~~ made of Pyrex glass and connected to the line with bored-through 3/8" UltraTorr® fittings (Swagelok). A diaphragm metal-seal valve (Fujikin FUDDFM-71G-6.35) is placed next to the sample tube (V1) for splitting, and stainless-steel bellows valves (Swagelok SS-8BW or SS-4H) are used for other valves. The vacuum is provided by a turbomolecular pump (Pfeiffer HiPace80) backed by a dry scroll pump. The same pre-treatment with humidified O_2, as applied to the extraction line, is employed for the split line. To minimize the consumption of O_2 at the metal surfaces leading to depletion of the $\delta O_2/N_2$ ratio during the sample storage in the tube, a passivation treatment (GoldEP-White®, Nissho Astec Co. Ltd.) is employed, which forms a passive layer of oxidized chromium on the stainless-steel surface (hereafter, this type of tube is called GEPW). In our experiences, stainless-steel sample tubes with mechanical polishing or electropolishing may lead to an unacceptable depletion of $\delta O_2/N_2$ (e.g., by -

5 ‰) in less than 8 hours because of the O_2 consumption. The GEPW tubes do not deplete $\delta O_2/N_2$, and thus the storage correction is not necessary (see 4.2.1).

The experimental procedures are as follows. The split line is filled with pure air (> 99.99995 %) at ~500 Pa when not in use ~~(e.g., during nights and weekends),~~ and evacuated for more than 30 minutes before the splitting. The GEPW tubes are evacuated overnight. The sample tube containing ice-core air is connected to the split line with a 1/4" UJR® fitting using a silver-plated nickel gasket. The GEPW tube is inserted in a helium cycle cooler at <10 K and connected to an adapter with a VCR® fitting, which is then connected to the split line with a VCO® fitting (Swagelok). The whole line is evacuated for ~30 minutes, during which the pressure decreases to $< 3 \times 10^{-5}$ Pa (~~measured at the head of a turbomolecular pump with an ionization gauge).~~P3). After a leak check, V1 is closed, and the valve on the sample tube is opened to expand the sample air into the small volume (1.~~4 cm^3~~45 mL) between the valves. The time required for equilibration of the air composition in the small volume with the sample tube is > 20 minutes. During this waiting time, the sample air may be fractionated if the temperature gradient exists between the tube and the small volume. To minimize such fractionation, the sample tube and small volume are covered with a sheet of bubble wrap so that air conditioners on the laboratory ceiling do not directly blow against the splitting part. The expanded air is then split by closing the valve of the sample tube. The air in the split volume is transferred to the GEPW tube for 5 minutes, after passing through the cold trap at −196 °C~~.~~ to remove CO_2 and N_2O. The sample transfer is monitored by measuring the pressure of the line with a Baratoron Gauge (MKS, full scale = 1333 Pa) (P1 in Fig. 2). The GEPW tube is lowered by a few centimeters into the helium cycle cooler when the pressure becomes below 1.0 Pa to improve the trapping efficiency of the gas by exposing fresh metal surface. The air transfer is complete in 5 minutes, and the valve of the GEPW tube is closed. The residual pressure is measured using a Convectron Gauge (Granville-Phillips) (P2 in Fig. 2), and the GEPW tube is disconnected from the line. The GEPW tube is warmed to room temperature and allowed to homogenize the sample air for at least 3 hours before the MS analysis~~. Sometimes the samples are measured on the following day of the splitting.~~ (the longest waiting time is ~20 hours). The air remained in the original sample tube is used for measuring CH_4, CO_2 and N_2O concentrations as well as total air content.

3. Measurements of extracted air

3.1 CH_4, N_2O and CO_2 concentrations

3.1.1 Gas chromatography

After taking the aliquot of air for the mass spectrometer analysis, the remaining air ~~left~~ in the original sample tube (~80 % of the extracted air) was measured for the concentrations of CH_4, CO_2 and N_2O with two gas chromatographs (Agilent 7890A) (Fig. 3). The settings of the GCs are summarized in Table 1. Briefly, CH_4 and CO_2 are measured with one GC (GC1) equipped with two ~~Frame~~Flame Ionized Detectors (FIDs) (CO_2 is converted to CH_4 by nickel catalyst), and N_2O is measured with another

GC (GC2) equipped with an Electron Capture Detector (ECD). We employ capillary columns to obtain high separation and narrow peaks. CH_4 and CO_2 are separated with a GS-Carbon PLOT (Agilent) capillary column (L = 30 m, i.d. = 0.53 mm, film thickness = 3 μm), and N_2O is separated with a HP-PLOT Q (Agilent) column (L = 30 m, i.d. = 0.53 mm, film thickness = 40 μm). We use N_2 (> 99.99995 %, Taiyo Nissan corp., Japan) for carrier and make-up gases, and H_2 (> 99.99995 %, Taiyo Nissan corp., Japan) for FID for GC1. Hydrocarbon-free air for FID is generated by a zero-air generator (PEAK Scientific, ZA015A). For GC2, we use He carrier (> 99.99995 %, Taiyo Nissan corp., Japan) for high separation, and the mixture of Ar and CH_4 (5 %) as makeup gas for high sensitivity. We use two gas purifiers in series (a "Mini Fine Purer" from Osaka Gas Liquid and a "Big Universal Trap" from Agilent) for the carrier, makeup and H_2 gases to ensure their purity. Zero air is further purified with a Hydrocarbon/Moisture Trap (Agilent).

To measure a small amount of sample gas, we use ~~small~~0.5-mL sample loops (Loop 1~~/16" o.d., 0.5 cm^3, Valco~~ and 2 in Fig. 3) filled at sub-ambient pressure. Small sample loops are also effective in reducing baseline fluctuations when GC valves are switched. The dead volumes of the inlet, fittings and tubing need to be minimized for filling the loops at sufficient pressure. We achieve the total volume (sample loops and dead volumes) of 3.3 ~~ml~~mL by using 1/16" tubing (0.7 mm or 1.0 mm i.d.), a customized metal-seal fitting (VCR) with a small bore (1.5 mm i.d.) for the connection of the sample tube, and a customized bracket with small dead volume for the pressure transducer at the inlet (machined Valco cross fitting). This configuration allows us to fill the sample loops at 400 – 600 hPa for the first injection and 300 – 500 hPa for the second injection, for typical ice-core measurements. The third injection is necessary if the pressure for the first injection exceeds the range of calibration, or if a gas handling error occurs. To minimize the broadening of the CO_2 peak by passing through the nickel catalyst (Agilent G3440-63002), we replaced the 1/4" (o.d.) tube for packing the catalyst with a 1/8" tube. To minimize adsorption/desorption of trace gases on the inner walls of the tubing, we employ VICI® electroformed Ni tubing or mirror-polished stainless-steel tubing (~~LaboSolTec~~Labosoltech). Typical chromatograms are shown in Fig~~.~~ure 4.

A standard gas measurement at atmospheric pressure is conducted as follows. V8 is set to position 1, V1 is set to OFF, V3 is set to OFF, and V7 is opened to allow the standard gas to flow through the two sample loops at 100 ~~ml~~mL min^{-1} for 1.0 min using a mass flow controller (HORIBA STEC, SEC-E40). V7 is closed to stop the gas flow, V3 is set to ON to disconnect the two GCs, and the GC measurements are initiated by switching V1 and V4 to let the carrier gases to flow through the sample loops. In GC1, CH_4 separated by column 1 is detected with the front FID (retention time ~1.8 min). At 1.74 min, V2 is switched to ~~lead~~let CO_2 from column 1 to pass through the Ni catalyst (to convert to CH_4) and then to back FID (retention time ~ 2.3 min). Finally, at 4.6 min, V1 and V2 are switched to the original positions. In GC2, immediately after N_2O passes through column 2 (at 1.5 min), V4 is switched to back-flush column 2 to vent H_2O out from the GC during the run. It is important to prevent the accumulation of H_2O in the columns, which may cause an unstable baseline during later measurements. N_2O is further separated in column 3, and V5 is switched at 1.95 min to lead N_2O to ECD (air eluting before N_2O is vented to the

atmosphere). Finally, at 4.89 min, V5 is switched to the original position. After the run, the sample loops are evacuated to < 0.25 hPa (P1) (Paroscientific Digiquartz® Series 2000, absolute 0.16 MPa full-scale).

For a standard gas measurement at sub-ambient pressure, the sample loops are first evacuated for ~30 min by closing V11, switching V12 and V13 (to connect the sample loops and Dry Pump 1), and turning V3 ON. Then, the standard gas is allowed to flow through ~~Sample~~ Loop 1 by turning V8 to position 1~~.~~ and V7 is opened. The flow rate is 100 ~~ml~~mL min^{-1} for 1 min, and then 17 ~~ml~~mL min^{-1} for 1 min. V3 is turned OFF to isolate the pump and start filling the sample loops. When the pressure (P1) reaches a prescribed value, the flow is stopped by closing V7. Then, 15 sec is allowed to stabilize the pressure and the temperature of the sample loops, and the GC measurements are initiated by switching V1 and ~~subsequently~~ V4 ~~(1 sec after V1)~~simultaneously to introduce the carrier gases to the sample loops. The measurement procedures of the GCs are the same as above.

The routine GC calibration and measurement procedures are as follows. We use three standard gases to cover the ranges of greenhouse gas concentrations in the samples (details of our working standard gases are described in the next section and summarized in Table 2). On each day of the measurement, the standard gases in the lines (1/8" tubes) connecting the cylinders and GC inlet are first pumped out for 5 min with a dry pump, and the standard gases are freshly introduced from the cylinders into the lines. The rest of the standard gas handling and measurements are automated with a custom-made software (with LabVIEW). First, the overall stability of the GC system is assessed by measuring the three standard gases three times at atmospheric pressure. For each standard gas, the peak areas of three consecutive measurements must agree within 1 % to proceed. The linearities of the detector responses are also checked by comparing the middle standard gas concentrations calculated from linear interpolation of the concentration-area relationships of high and low standard gases with the original values. The typical differences are +1.1±1.7 ppb for CH_4, -0.3±0.2 ppm for CO_2, and +2.3±1.2 ppb for N_2O. Then, each of the three standard gases is measured at three sub-ambient pressures (i.e., nine measurements in total) to construct calibration curves for the ice-core measurements. Typical pressures are 300, ~~450~~400 and ~~600~~500 hPa to cover the pressure range for two injections of sample air from ~60 g of ice.

After all the standard gas measurements, a sample tube is connected to the GC inlet by VCR, V8 is set to position 4, V10 is switched ON to evacuate the inlet with a turbomolecular pump for ~20 sec, and the VCR connection is leak-checked with P2 (JTEKT® PMS-5M-2 pressure transducer). The inlet and two sample loops are then evacuated via V10 and V3, respectively, for 15 min to < 0.25 hPa, V10 is closed, the sample gas is expanded into the inlet by opening the stop valve on the sample tube, and the controlling software is started. Three seconds later, the two sample loops are connected and isolated from the vacuum line (V3 OFF), and the sample air is expanded into the sample loops (V8 position 3). The rest of the GC measurement sequences are the same as the standard gas measurements. After measuring~~the measurement of~~ a sample, the sample loops are evacuated

by switching V3 for ~~2~~3 min (P1 < 0.25 hPa), and the second measurement is initiated automatically. After the end of the second measurement, the sample tube is replaced with the next one.

After measuring all samples, the standard gases are measured again at the sub-ambient pressures to account for the drifts of GC signals during the sample measurements. The areas of the standard gases before and after the sample measurements were linearly interpolated to the time of the sample measurements for calculating the sample concentrations, assuming that the drift is linear with time.

The concentration of greenhouse gas in the sample air is determined ~~as follows.~~based on the calibration measurements of the three standard gases at three pressures. As an example, the calibration procedure for CH_4 concentration is schematically shown in Figure 5. First, the peak areas of the three standard gases at the sample pressure (in the sample loop) are ~~calculated~~estimated by:

$$A_{St,n,P} = a_n P^2 + b_n P + c_n, \quad (1)$$

where $A_{St,n,P}$ is peak area of standard gas n (= 1~~to~~, 3, and 5) calculated for the sample pressure (P), and a_n, b_n and c_n are coefficients obtained by second-order polynomial fit to the peak area versus pressure from the calibration measurements~~. Then, the~~ (Fig. 5a). The greenhouse gas concentration in the sample is obtained by:

$$C = dA^2 + eA + f, \quad (2)$$

where C is concentration, A is sample peak area, and d, e and f are coefficients obtained by the second-order polynomial fit to the standard gas concentrations versus $A_{St,n,P}$ (n = 1~~to~~, 3, and 5) (Fig. 5b). Each sample air is measured at least twice, and the mean values are used.

3.1.2 Standard gases

The CH_4, N_2O and CO_2 concentrations are determined against Tohoku University (TU) scales, which are based on gravimetrically prepared primary standard gases (Aoki et al., 1992; Tanaka et al., 1983). Uncertainties of the TU primary standards are < ±0.2, 0.2 and 0.03 % for CH_4, N_2O and CO_2 concentrations, respectively (Aoki et al. (1992) for CH_4, Ishijima et al. (2001) for N_2O and Tanaka et al. (1987) for CO_2). The ice-core standard gases are calibrated using the primary standard gases manufactured in 2008 for CH_4 (300.1 – 2799.1 ppb) and CO_2 (200.13 – 449.72 ppm), and those made in 1991 for N_2O (100.0 – 400.1 ppb). Working standard gases at NIPR contain CH_4, N_2O and CO_2 in purified air in 47-L aluminum cylinders (Taiyo Nissan corp., Japan), whose concentrations were calibrated at Tohoku University using their working standard gases named '2007-Ice-Work' (with 25 measurements for each cylinder). We have five working standard gases (named STD 1 – 5) with different concentrations covering from preindustrial Holocene to glacial maxima (Table 2). Two additional cylinders (STD-A and B) are prepared and calibrated against the NIPR working standard gases at NIPR and used for various tests. Uncertainty of CH_4, N_2O and CO_2 concentrations of the NIPR working standards are < ±0.6 ppb, ± 0.3 ppb and ±0.02 ppm, respectively (one standard error of the mean).

For modern atmospheric concentration levels, the TU scales are in agreement with the NOAA/WMO scales within ~2 ppb for CH_4, ~0.3 ppm for CO_2, and ~0.5 ppb for N_2O as reported in WMO/IAEA Round Robin Comparison Experiment (Dlugokencky, 2005; Tsuboi et al., 2017) (https://www.esrl.noaa.gov/gmd/ccgg/wmorr/index.html). However, at lower concentration levels, inter-calibration between TU and NOAA scales have not been conducted. For CH_4 and N_2O, we discuss the consistency of calibration scales by comparing our ice-core data with those from other laboratories (see section 5.1).

3.2 Mass spectrometry for isotopic and elemental ratios of N_2, O_2 and Ar

Isotopic and elemental ratios ($\delta^{15}N/^{14}N$ of N_2, $\delta^{18}O/^{16}O$ of O_2, $\delta O_2/N_2$ and $\delta Ar/N_2$) are analysed on a dual inlet mass spectrometer (Thermo Fisher Scientific, Delta V) with 9 Faraday cups and amplifiers to simultaneously collect ion beams of molecular masses 28, 29, 32, 33, 34, 36, 38, 40 and 44. The registers, typical beam intensities and other MS settings are given in Table 3. While we collect raw data from all of these cups, we do not use the signals of masses 33, 36 and 38 in this paper because high precisions for isotopic ratios with these masses (including appropriate corrections for interference and nonlinearity in the mass spectrometer) are not established. To achieve high precision, we control the temperature around the mass spectrometer (especially around the inlet) by isolating the mass spectrometer from the room-air temperature fluctuation with plastic sheets and introducing temperature-controlled air generated by an air conditioner (Orion PAP03B) into the booth. Two large (~45 cm diameter) and a small (~20 cm diameter) fans in the booth vigorously mix the air to maintain the temperature around the inlet at 25.7 ± 0.3 ˚C all year round.

3.2.1 Measurement procedures

Our reference gas is commercially available purified air (>99.9999 %, Taiyo Nissan Co.) in a 47-L cylinder filled in 3-~~liter~~ L electropolished stainless-steel containers (hereafter reference cans), each with two bellows-seal valves (Swagelok SS-4H) creating small pipette volume (1.3 ~~cm^3~~mL) at the exit. The inner surface of the can is preconditioned by humidified O_2 at > 120 °C as for the extraction line. The reference can attached to the standard side is rarely disconnected.

Our mass spectrometry largely follows Severinghaus et al. (2009). Prior to the daily sample measurements, a reference can is connected to the sample port of Delta V using VCO® fitting (typically on the prior evening to stabilize the can's temperature), and the ports and pipets are evacuated. The MS valves leading to the reference cans are closed, and both bellows are evacuated for 5 min. Then, the MS valves to the inlet ports are opened to check leak by an ion gauge, and all bellows and lines are further evacuated for 5 min. On both sides, the reference gas is introduced into the pipette of the can by closing the valve at the MS side and opening the other valve, and they are equilibrated for 10 min. The pipette volumes are disconnected from the cans, and the aliquots are expanded into the bellows and equilibrated for 10 min. Then, the bellows are isolated from the inlet and

compressed to reach ~~30~~ 34 mbar. The initial pressure in the fully expanded bellows is ~28 mbar from a freshly filled can. The reference can is replaced by a new one when the initial pressure decreases to ~18 mbar.

The reference gas from the sample port is measured against the standard side ("can versus can") for 4 blocks to check the standard deviations. Before each block, the acceleration voltage is optimized by centering the mass 40 peak, the background is measured after a 120-sec idle time, and the pressures are adjusted to 5000 ± 50 mV for mass 28 (3×10^8 Ω), automatically with the ISODAT software. The idle time and integration time are 10 seconds and 16 seconds, respectively. Each block consists of 17 changeover cycles, ~~but the first cycle is discarded~~ and only the latter 16 values are used. After running the 4 blocks, two blocks are run by imbalancing the sample pressure by ± 10 % against the standard side for obtaining pressure imbalance sensitivity (see below).

The GEPW tube containing the sample air is connected to the sample port, and the sample port is evacuated during the previous measurement. The procedure of the sample measurement is the same as the "can vs. can" measurement, except that the sample expansion into the bellow is made in one step by simply opening the tube valve. We run two blocks for each sample to obtain a total of 32 cycles. Typical standard deviations in 1 block (16 cycles) are 0.013, 0.029, 0.010 and 0.017 ‰ for $\delta^{15}N$, $\delta^{18}O$, $\delta O_2/N_2$ and $\delta Ar/N_2$, respectively.

3.2.2 Pressure imbalance and chemical slope corrections

The ratios of ion currents of different masses are slightly sensitive to the pressure in the ion source, thus a correction is applied with an established procedure (Severinghaus et al., 2003). The pressure imbalance sensitivity (PIS) is a slope of δ values against differences in beam intensity ($\Delta P = (I_{sa}/I_{st} - 1) \times 1000$ where I is the mean beam intensity in one block), which is determined by measuring the reference gas at the sample side at three pressures (at ΔP = 0, +~~100~~10 and ~~-100 ‰).~~10 %). The PIS is measured every day and used for correcting the sample values measured on the same day by:

$$\delta_{\text{pressure corrected}} = \delta_{\text{measured}} - (\text{PIS})\ \Delta P. \quad (3)$$

The PIS gradually changes over several weeks, and they shift after a filament replacement.

Relative ionization efficiencies of gas are also sensitive to variations in the mixing ratio of the gas in total air (the sensitivity is called "chemical slope") (Severinghaus et al., 2003). The chemical slopes are determined from the measurements of the reference gas added by pure O_2 (+10, +20 and +30 % of original O_2 amount) for $\delta^{15}N$, and pure N_2 (+10, +20 and +30 % of original N_2 amount) for $\delta^{18}O$. The correction is made by:

$$\delta^{15}\text{~~N}_{\text{slope}}\ ^{15}\text{N}_{\text{chemslope}}\ \text{corrected} = \delta^{15}\text{N}_{\text{pressure corrected}} - [\text{CS1}] \times \delta O_2/N_{2\text{measured}} \quad (4)$$

$$\delta^{18}\text{~~O}_{\text{slope}}\ ^{18}\text{O}_{\text{chemslope}}\ \text{corrected} = \delta^{18}\text{O}_{\text{pressure corrected}} - [\text{CS2}] \times \delta N_2/O_{2\text{measured}} \quad (5)$$

where CS1 and CS2 are chemical slopes for $\delta^{15}N$ and $\delta^{18}O$, respectively. The chemical slopes are fairly stable, thus are measured only a few times per year. The typical values of CS1 and CS2 are 0.0005 ‰/‰ and 0.0018 ‰/‰, respectively.

The final normalization against the modern atmosphere (the ultimate standard gas for ice cores by definition) requires through investigation of the stability of reference gases and the atmospheric ratios, which we discuss in section 4.2.

3.3 Total air content

Total air content (TAC) is the amount of occluded air in a unit mass of ice (~~ml$_{STP}$~~mL$_{STP}$ kg^{-1}) (Martinerie et al., 1992). In our system, TAC is calculated from:

$$TAC = \frac{P}{1013.25} \cdot \frac{(V_a+V_c)\cdot(V_a+V_b)}{V_a} \cdot \frac{273.15}{T} \cdot \frac{1}{m}, \quad (6)$$

where P is pressure in the sample loops upon first expansion, T is air temperature near GC, m is mass of ice sample ~~(measured with an electronic balance, SARTORIUS CP4202S),~~just before melting, and V_a, V_b and V_c are the volume of the sample tube, the volume of the pipette at the split line, and the combined volume of GC inlet and sample loops, respectively. To take into account the ice mass loss during the evacuation, m is estimated from:

$$m = m_{initial} - \frac{m_{Trap1} \cdot r_t}{n_{sample}} \quad (7)$$

where $m_{initial}$ is the initial ice mass measured in the cold room, m_{Trap1} is the ice mass in Trap 1 after all extractions for a day measured in the laboratory, r_t (= 4/3) is the ratio of total evacuation time to the time of the first evacuation through Trap 1 (120 min/90 min), and n_{sample} is the number of samples for the day. The ice loss for each sample thus estimated is 0.1 – 0.3 g.

V_a and V_b were determined manometrically against a known volume (118.7 ~~cm^3~~mL) with a pressure gauge (Paroscientific Digiquartz® Model 745-100A, absolute 0.69 MPa full-scale). The whole apparatus is first evacuated, the air is introduced from a cylinder into the glass flask at about atmospheric pressure. The air is expanded into the manifold, pipette, and tube, and the pressure measured at each step is used to calculate the volumes by the ideal gas law. The expansion and recording are repeated 10 times, and they are averaged.

Similarly, V_c was determined manometrically for each sample tube (~6.6 ~~cm^3~~mL), which was attached to the GC inlet. N_2 or air in a sample tube at a known pressure was expanded into the evacuated GC inlet and sample loops, and the pressure was recorded (valve on the sample tube is kept open). The expansions/evacuations were repeated a few times, and the gas in the sample tube was re-filled. The whole procedures were repeated a few times to obtain a total of 12 measurements for each tube.

The calibration of the volumes V_a, V_b and V_c must be made for individual sample tubes because the volumes in the valves and end connections are slightly different from each other (V_a, V_b and V_c are different by up to 0.8 %, 0.6 % and 0.5 %, respectively,

between the tubes). Average V_a, V_b and V_c are 6.6 ~~cm^3~~mL, 1.4 ~~cm^3~~mL and 3.4 ~~cm^3~~mL, respectively. The standard error of the mean for the 10 – 12 measurements of V_a, V_b and V_c are 0.04 %, 0.10 % and 0.04 %, respectively. By propagating these values and the uncertainties of temperature (assumed to be 1 K), pressure (assumed to be 16 Pa) and ice mass (assumed to be 0.1 g), 1σ uncertainty of TAC is estimated to be 0.5 ~~ml$_{STP}$~~mL$_{STP}$ kg^{-1}.

4. Evaluation of system performance using standard gas and atmosphere

During air extraction, splitting and analyses, alteration of air composition may occur for various reasons, such as gas dissolution or chemical reaction in the meltwater, degassing from inner surfaces of vessel and line, and diffusive fractionations of isotopic ratios. Below, we evaluate the performance of the tubes, apparatus and instruments by various tests and controlled measurements (mimicking ice-core analyses with standard gas and gas-free ice).

4.1 CH_4, N_2O and CO_2 concentrations

4.1.1 Tube storing test

We evaluate the concentration changes during gas storage in the sample tubes and test tubes (used for injecting standard gas to the apparatus, with metal-seal valves at both ends)~~,~~ by filling standard gas from a cylinder (STD-A) into evacuated tubes, and measuring the sample tubes on the following day and the test tubes on the same day. The changes in CH_4, N_2O and CO_2 concentrations thus obtained are insignificant with respect to the measurement precisions for both the sample tubes (+0.8±2.1 ppb, +1.3±2.1 ppb and +0.1±1.1 ppm, respectively, with n = 25) and test tubes (+0.7±2.2 ppb, +0.9±1.0 ppb and −0.2±0.1 ppm, respectively, with n = 17) (Table 4). The excellent results of the storing tests are attributable to the passivation treatment of the tubes and the use of valves with clean inner surfaces (Fujikin metal diaphragm valves). We note from our earlier experience that CH_4 is produced by up to several ppb by opening and closing metal bellows valves (Swagelok SS-4H) if they become old (after several hundred operations), and that CO_2 concentration increases by up to ~10 ppm if the passivation treatment is insufficient.

4.1.2 Standard gas transfer test

Gas-free ice for tests is made from ultra-pure water in a stainless-steel vessel (~1800 ~~cm^3~~mL) sealed with a Conflat blank flange. The water is boiled for 20 – 30 min with an open outlet port on the flange, and cooled to room temperature after closing the outlet, and then put in a freezer at -20 ˚C. The side of the vessel is surrounded by insulation so that the water is frozen from the bottom over a few days. The ice is removed from the vessel, and ice with visible cracks and bubbles are removed (more than half of the ice).

Standard gas from a cylinder is flushed through a pre-evacuated line and test tube (volume is 3 or 5 ~~cm^3~~mL) at 50 ~~ml~~mL min^{-1} for 5 min, and sampled at atmospheric pressure after ceasing the flow by closing an upstream valve. The relatively low flow rate for flushing prevents thermal fractionation of the gas due to adiabatic expansion at the pressure regulator (important for isotopic analyses), and the pre-evacuation and >200 ~~ml~~mL of total flow ensure clean sampling.

The test tube with standard gas and vessel with ~50 g of gas-free ice are attached to the extraction line, and the vessel is evacuated for 120 min. The ice is melted while the vessel is evacuated (for 15 min) to remove any air degassed from the melt. We also use ice-core melt instead of gas-free ice melt for the blank test. In this case, the vessel with ice-core melt is evacuated for 30 min after a sample extraction to pump out any residual air. Then, the standard gas from the test tube is slowly injected into the extraction system and transferred continuously over the gas-free water into a sample tube, maintaining the pressure similar to that of ice-core extraction.

The standard gas thus transferred to the sample tubes ~~are~~ is measured on the following day, after handling it with the split line (see below for the results of isotopic analyses). No significant changes in CH_4, N_2O and CO_2 concentrations are observed with respect to the mean values of the test tubes' storing tests (+0.8±2.7 ppb -0.1±1.7 ppb and +1.3±0.7 ppm, Table 4). Based on the above results, we apply no corrections for CH_4, N_2O and CO_2 concentrations.

4.2 Isotopic and elemental ratios of N_2, O_2 and Ar

4.2.1 Storing test of GEPW tubes

To evaluate the possible effect of gas storage in the GEPW tubes for one day, the reference gas was transferred to the tubes using the split line and measured the following day, and the results were compared with those measured on the same day. They are identical within the measurement uncertainties for all ratios (-0.002 ± 0.003 ‰ for $\delta^{15}N$, -0.002 ± 0.010 ‰ for $\delta^{18}O$, -0.012 ± 0.056 ‰ for $\delta O_2/N_2$, -0.013 ± 0.042 ‰ for $\delta Ar/N_2$, with n=14), thus no corrections are applied for the storage duration in the GEPW tubes.

4.2.2 Standard gas transfer test

The standard gas filled in a test tube was transferred to a sample tube with the extraction line and gas-free water (the same experiment as in section 4.1.2), and an aliquot was taken with the split line and transferred to a GEPW tube as the ice-core analyses (Fig. ~~5~~6). On the other hand, the same standard gas filled in the same test tube was attached directly to the split line, and its aliquot was transferred to a GEPW tube, skipping the extraction line and overnight storage (Fig. ~~5~~6). Comparison of the measured values from these two experiments gives the changes in the isotopic and elemental ratios during the ice-core air extraction and overnight storage, denoted as $\Delta\delta_{extraction}$. The values of $\Delta\delta_{extraction}$ are -0.005 ± 0.001, -0.003 ± 0.002 and -0.102 ± 0.011 for $\delta^{15}N$, $\delta^{18}O$ and $\delta Ar/N_2$, respectively (errors are standard error, n > 100). The signs of changes are negative for all

gases, suggesting~~which may suggest~~ a slightly less effective transfer of heavier isotopes with our extraction line. Based on these results, we employ the above values for $\delta^{15}N$ and $\delta Ar/N_2$ as constant corrections, and no correction for $\delta^{18}O$, for the ice-core data. We also conducted similar tests with ~1 ~~ml$_{STP}$~~mL$_{STP}$ sample size using a small test tube, in which whole gas was transferred to a GEPW tube without splitting. The changes are not significantly different from those of the larger sample sizes (-0.002 ± 0.002, +0.004 ± 0.006 and -0.113 ± 0.048 ‰ for $\delta^{15}N$, $\delta^{18}O$ and $\delta Ar/N_2$, respectively (errors are standard error with n = 9)).

Relatively large decrease and dependence on the sample size are found for $\delta O_2/N_2$ in the above tests (-0.193 ± 0.015, -0.293 ± 0.029 and -0.482 ± 0.048 ‰ for 5, 3 and 1 ~~cm^3~~mL, respectively). We interpret the result as O_2 consumption by the inner walls of the extraction line and sample tubes, whose magnitude (number of O_2 molecules consumed) might be only weakly dependent on the sample size. We use an exponential fit to the above data (Fig. ~~6~~7),

$$\Delta\delta_{extraction,\ O2/N2} = 0.\text{~~55362~~554}\ \exp(-0.\text{~~31606~~316} \times V) - 0.\text{~~078802 (‰),~~} \quad \text{~~(7~~0788 (‰),} \quad (8)$$

where V is the sample size of air in ~~ml$_{STP}$~~mL$_{STP}$ for correcting the ice core data.

4.2.3 Long-term stability of standard gas and atmosphere, and normalization of sample ratios

For normalization of the ice-core data and monitoring its long-term stability, standard gas in a cylinder (STD-A) and atmosphere (sampled outside the NIPR building) have been regularly measured against the reference can.

The atmospheric sampling and measurement procedures follow Headly (2008) and Orsi (2013). Briefly, the atmosphere is collected in a 1.5 L glass flask with a metal piston pump (Senior Aerospace, MB-158), aspirated air intake and two water traps. The flow rates of the sampling and aspiration lines are 4 and 15 L min^{-1}, respectively, with a flushing time of > 10 min before sampling. In the laboratory, the flask air is expanded into three volumes in series (~4, ~1.5 and ~2 ~~ml~~mL) and allowed for 30 min to equilibrate, and the air in the middle volume is transferred to a GEPW tube. The STD-A is filled in a test tube~~,~~ (3 or 5 mL), and an aliquot of it (~1 mL$_{STP}$) is transferred to a GEPW tube using the split line (see section 4.1.2).

The $\delta^{15}N$, $\delta^{18}O$, $\delta O_2/N_2$, and $\delta Ar/N_2$ of STD-A and atmosphere for 2016 to 2019 are shown in Fig. ~~5~~6 and Fig. ~~7~~8, and the values of the STD-A against the atmosphere is summarised in Table 5. Shifts in the ratios are commonly seen when the ion source filament or reference can is renewed (as indicated by vertical lines in the figure). However, there are no discernible trends and seasonal variations during the use of one reference can for all ratios except for $\delta O_2/N_2$. Typical standard deviations of a set of atmospheric measurements (~10 replicates) using two flasks within a few days are 0.003, 0.007, 0.020, and 0.034 ‰ for $\delta^{15}N$, $\delta^{18}O$, $\delta O_2/N_2$, and $\delta Ar/N_2$, respectively, while those of the STD-A measurements are 0.004, 0.008, 0.058, and 0.033 ‰, respectively. Comparison of $\delta^{15}N$, $\delta^{18}O$ and $\delta Ar/N_2$ between STD-A and atmosphere indicate slightly better

reproducibilities for the atmospheric measurements, possibly due to fractionations during the filling of STD-A into the test tubes. Therefore, the atmosphere is the best choice for the normalization of those ratios.

General trends towards more positive values are seen for $\delta O_2/N_2$ (Fig. ~~5d~~6d and Fig. ~~7d~~8d), presumably because O_2 in the reference can is gradually consumed by oxidation of organic matter on the inner wall. Moreover, atmospheric $\delta O_2/N_2$ in urban areas may show spikes and seasonal variations (Ishidoya and Murayama, 2014), which are much larger than our measurement precision. Indeed, $\delta O_2/N_2$ of STD-A only shows linear trends (due to the drift in the reference can), but the atmospheric $\delta O_2/N_2$ sometimes deviates from its linear trend by up to ~0.5 ‰ (e.g., in Dec. 2017, Jan. 2018, April 2018, Mar. 2019 and Dec. 2019). Thus, the use of a standard gas in the cylinder (STD-A) for normalization, rather than the atmosphere sampled at the time of calibrations, is the better choice for precise $\delta O_2/N_2$ measurements. We here define our "modern air" for $\delta O_2/N_2$ as the annual average $\delta O_2/N_2$ in 2017 observed over Minamitorishima island (hereafter MTS air) (24°17'N, 153°59'E) observed by National Institute of Advanced Industrial Science and Technology (AIST) in cooperation with Japan Meteorological Agency ~~(JMA)~~ (Ishidoya, 2017), and determined $\delta O_2/N_2$ in STD-A against it (+2.595 ± 0.008 ‰). We note that AIST recently developed a gravimetric $\delta O_2/N_2$ calibration scale for precise and long-term atmospheric monitoring (Aoki et al., 2019).

~~The values of~~ In each month, the atmosphere ~~or STD-A~~ is sampled in two flasks on the same day, and a total of 10 or more aliquots are measured and averaged. The STD-A is measured every week, and the values in the same month are averaged. The monthly atmospheric or STD-A values thus assigned against the reference can ~~within a few weeks immediately before and after the sample measurements are averaged and used for normalizations.~~are averaged over two consecutive months, and the ice-core samples are normalized against the nearest two-month average values. The final corrected and normalized δ ~~value~~values of an ice core sample ~~is~~are:

~~$$\delta_{\text{normalized}} = \left[\frac{(\delta_{\text{slope corrected}} - \Delta\delta_{\text{extraction}})\cdot 10^{-3} + 1}{\delta_{\text{ATM}}\cdot 10^{-3} + 1} - 1\right]\cdot 10^3 \text{ (‰)}, \quad (8)$$~~

$$\delta^{15}N_{\text{normalized}} = \left[\frac{(\delta^{15}N_{\text{chemslope corrected}} - \Delta\delta_{\text{extraction},\delta 15N})\cdot 10^{-3} + 1}{\delta^{15}N_{\text{ATM}}\cdot 10^{-3} + 1} - 1\right]\cdot 10^3 \text{ (‰)}, \quad (9)$$

$$\delta^{18}O_{\text{normalized}} = \left[\frac{\delta^{18}O_{\text{chemslope corrected}}\cdot 10^{-3} + 1}{\delta^{18}O_{\text{ATM}}\cdot 10^{-3} + 1} - 1\right]\cdot 10^3 \text{ (‰)}, \quad (10)$$

$$\delta O_2/N_{2\text{normalized}} = \left[\frac{\left(\delta O_2/N_{2\text{pressure corrected}} - \Delta\delta_{\text{extraction,O2N2}}\right) + 1}{\delta O_2/N_{2\,ATM}\cdot 10^{-3} + 1} - 1\right]\cdot 10^3 \text{ (‰)}, \quad (11)$$

$$\delta Ar/N_{2\text{normalized}} = \left[\frac{\left(\delta Ar/N_{2\text{pressure corrected}} - \Delta\delta_{\text{extraction,ArN2}}\right) + 1}{\delta Ar/N_{2\,ATM}\cdot 10^{-3} + 1} - 1\right]\cdot 10^3 \text{ (‰)}, \quad (12)$$

where ~~$\Delta\delta_{extraction}$ is the correction for air extraction and overnight storage (only for $\delta^{15}N$, $\delta O_2/N_2$ and $\delta Ar/N_2$, see section 4.2.2), and~~ δ_{ATM} is the two-month-average atmospheric value against the reference can corrected for PIS and chemical slope~~.~~ (for effectively correcting for the drifts in the reference can).

5. Ice core analyses and comparison with published records

We analysed the Dome Fuji (hereafter DF) ice core, Antarctica, and NEEM ice core, Greenland, and compared the results with other records to evaluate the overall reliabilities of our methods. The reproducibilities of ice-core measurements are also assessed using the pooled standard deviation of duplicates (measurements of two ice samples from the same depth, Severinghaus et al. (2003)) for some depths. The number of samples and depths are as follows: 49 samples from 40 depths in 112.88 – 157.81 m (bubbly ice, 0.2~~.0~~ – 2.0~~.2~~ kyr BP), and 70 samples from 35 depths in 1245.00 – 1918.59 m (clathrate ice, 79 – 150 kyr BP) from the DF core, and 75 samples from 47 depths in 112.68 – 449.10 m (bubbly ice and above brittle zone, 0.2~~.0~~ – 2.0~~.2~~ kyr BP) from the NEEM core.

We employed the following age scales and synchronizations. For the preindustrial late Holocene (~0 to ~1800 year C.E.), the GICC05 chronology was used for the NEEM core as published by Rasmussen et al. (2013), and a WAIS Divide Core gas chronology (WDC05A) (Mitchell et al., 2013; Mitchell et al., 2011) was transferred to the DF core by CH_4 synchronization (the tie points are shown in Fig. ~~9~~10 and Table 6). For the other ice cores for comparisons (including GISP2, WDC, Law Dome cores), we employed their own published time scales (Table A1).

The following data were rejected or not acquired due to experimental errors. The DF sample at 144.75 m lost CH_4, CO_2 and N_2O concentrations and TAC because of a connection failure between the GC and computer. $\delta^{15}N$, $\delta^{18}O$, $\delta O_2/N_2$ and $\delta Ar/N_2$ from the DF core at 1521.06, 1540.56 and 1712.10 m were rejected because of the leaky valve on the GEPW tube. The NEEM sample at 217.15 m showed anomalous CO_2 and N_2O concentrations as compared with another sample at the same depth (+83 ppm and +47 ppb, respectively); all GC data including CH_4 were rejected for this sample. The NEEM sample at 229.80 m and 438.83 m showed anomalously low $\delta^{15}N$ and $\delta^{18}O$ (half of the typical values, or lower), possibly due to gas handling error or leak. As all the anomalous NEEM data were acquired within 2 months after establishing the method, there would have been experimental errors that slipped from our attention.

5.1 CH_4, N_2O and CO_2 concentrations

The pooled standard deviations of the CH_4, N_2O and CO_2 concentrations are ± 3.2 ppb, ± 1.3 ppb and ± 3.2 ppm for the DF bubbly ice (number of pairs = 8), ± 3.3 ppb, ± 2.2 ppb and ± 3.1 ppm for the DF clathrate ice (n = 29), and ± 2.9 ppb, ± 3.0 ppb and ± 5.5 ppm for the NEEM bubbly ice (n = 25) (Table 7). The pooled standard deviations of CH_4 and N_2O are similar

to those reported from most precise measurements by other laboratories (± 2.8 ppb for CH_4 by OSU (Mitchell et al., 2013), and ± 1.5 ppb for N_2O by ~~Seoul National University~~SNU (Ryu et al., 2018)).

Our new CH_4, N_2O and CO_2 data from the DF core agree with the previous data from Tohoku University (Fig. ~~8~~9) (Kawamura, 2001), indicating consistency of the TU concentration scales for ice core analyses over the past ~ 20 years. We compare our results for the preindustrial late Holocene (~0 to ~1800 C.E.) at ~50-year resolution with other ice core records from other groups on the NOAA concentration scales (Fig. ~~9~~10). The DF CH_4 data agree well with those from the WAIS Divide core by OSU (Mitchell et al., 2013) and Law Dome cores by CSIRO (Rubino et al., 2019), which are currently the best Antarctic records in terms of precision and resolution (see Fig. A1 in Appendix for comparison with other records). We note that multi-decadal variations are smoothed out in the DF core because of the slow bubble-trapping process. For Greenland, our NEEM data show good agreement with the GISP2 data from OSU (Mitchell et al., 2013), including multi-decadal~~multidecadal~~ to centennial-scale variations.

We note that unrealistically high CH_4 variabilities were found at two depths in the NEEM core (417.60 – 418.00 m and 361.05 – 361.35 m; gas ages are ~218 C.E. and ~532 C.E., respectively) (Fig. ~~10~~11). The change of ~20 to 50 ppb between the neighbouring depths (only < 1 year apart in age) is impossible to be ~~an~~of atmospheric origin considering diffusive mixing in firn. The good agreements between the duplicate measurements for these depths exclude the possibility of ~~analytical error.~~experimental failure. The N_2O concentrations at the same depths are not significantly different from those in the neighbouring depths, suggesting that the CH_4 anomalies are not due to ice-sheet surface melt and associated gas dissolution, which should elevate both CH_4 and N_2O. ~~In any case, we exclude these anomalously high concentrations from the calculation of pooled standard deviation and comparison with other ice core records.~~Anomalously high CH_4 concentrations with similar magnitudes have been reported from GISP2 and NEEM cores measured at other laboratories, and the reasons may be CH_4 production after bubble close-off (in the ice sheet) or during air extraction from dusty glacial-period ice (Mitchel et al., 2013; Rhodes et al., 2013, 2016; Lee et al., 2020). For the purpose of evaluating our system, we exclude the anomalous values from the calculation of pooled standard deviations and quantitative comparison with other records because they are extremely inhomogeneous. We speculate that the CH_4 anomalies in our data originate in in-situ production because we used the Holocene (low dust) ice, and full investigation of our system on CH_4 production (as found by Lee et al., 2020) would require higher-resolution analyses of dusty ice and inter-comparison with other laboratories, which is beyond the scope of this paper. The CH_4 concentration of 723.7 ppb at 961 C.E. (the mean of four discrete measurements), in the middle of an increase over a century, is also higher than the GISP2 data by ~30 ppb~~.~~, whereas the N_2O concentration does not appear to be anomalous. The four discrete values agree within 12 ppb (717.6, 724.9, 729.5 and 722.9 ppb), ~~indicating~~excluding again ~~that the large deviation from~~ the ~~GISP2 data is not due to analytical error. The reason~~possibility of major experimental failure for ~~this~~the anomaly. This discrepancy ~~is not clear, but it~~ could be due to uncertainty in age synchronization between the cores, a reversal of the NEEM gas age by firn layering (the possibility that the bubbles were closed-off in the last stage of firn-ice transition, Rhodes

et al. (2016)) or ~~natural artefacts (e.g., gas dissolution by surface melt, or biological~~ CH_4 production within the ice sheet~~).~~ as discussed above.

N_2O concentrations from both polar regions should agree with each other within the uncertainty of ice core analyses. ~~Our data from the NEEM core agree with those from the Law Dome core by CSIRO within ~5 ppb without systematic bias (Rubino et al., 2019) (see Fig. A1 in Appendix for comparison with other records). The DF data also agree with the NEEM data within ~5 ppb.~~Our datasets from the NEEM and DF cores agree with each other within ~5 ppb without systematic bias, and they also agree with the Law Dome data by CSIRO within ~5 ppb (Rubino et al., 2019). We also compare our data with the Monte Carlo spline fit through the NGRIP, TALDICE, EDML, and EDC data by the University of Bern (Fischer et al., 2019; see Fig. A1 for individual data points) and high-resolution data from the NEEM and Styx Glacier ice cores by SNU (Ryu et al., 2020). Multi-centennial-scale variations (i.e., relatively low concentrations around 600 C. E. and high concentrations around 1100 C.E.) are commonly seen in all the datasets. However, there appear to be some offsets between the data from NIPR, University of Bern, and SNU. The NEEM and Styx Glacier data by SNU are systematically lower by ~5 ppb than our data. Because the NEEM core is measured by both laboratories, the offset cannot be explained by the difference in the original N_2O concentration in the ice. We examine here the possibility that our method overestimates the N_2O concentration. Based on the standard-gas transfer tests, we do not apply extraction correction for N_2O concentration. This raises the possibility that, if our tests indeed underestimate the N_2O dissolution, then our ice-core data should become lower than the true values. This scenario leads to an upward correction of our dataset and thus does not explain the offset. Therefore, the causes of the systematic offset between the two datasets may be the differences in standard gas scales and calibration methods employed by the two laboratories. The spline curve by the University of Bern shows depth-dependent offset relative to other datasets. The 2σ error band of the spline curve overlaps well with our data between ~1000 and 1800 C.E., but it is systematically lower than our data and agree with the SNU data for ~0 – 1000 C.E. We measure the ice samples in random order to avoid any apparent trends in the data that might originate in the drifts in the standard gases or instruments (on weekly to monthly timescales). The sample at 1076 C.E. (129.16 m) of the DF core shows very high concentration (~20 ppb higher than the neighbouring depths), which is unlikely to be due to experimental errors because the CH_4 and CO_2 concentrations of the same sample are not elevated. Anomalous N_2O concentrations were also found in late Holocene DF samples in previous measurements (Kawamura, 2001), and they are possibly natural artifacts~~artefacts~~ (N_2O production in ice sheet) (Kawamura, 2001; Sowers, 2001).

The overall agreements of our CH_4 and N_2O data with the other datasets suggest the reliability of our method and consistency of the TU scales at low concentrations with the NOAA scales. We note that our method does not apply experimental corrections for CH_4 and N_2O concentrations. For reference, the OSU method (wet extraction with refreezing) applies solubility correction of 1 % (~3 – 8 ppb) and blank correction of 2.5 ppb for CH_4 (Mitchell et al., 2011), and the CSIRO method (dry extraction) applies blank corrections of 4.1 ppb and 1.8 ppb for CH_4 and N_2O, respectively (MacFarling Meure et al., 2006). The negligible

effect of gas dissolution in our method is explained by the immediate removal of the released air from the ice vessel, maintaining low pressure above the meltwater.

The CO_2 concentration is generally measured with mechanical dry extraction techniques ~~methods~~ (e.g., ~~(~~Ahn et al., 2009; Barnola et al., 1987; Monnin et al., 2001; Nakazawa et al., 1993a) and sublimation (Schmitt et al. 2011), because wet extraction method has a risk of contamination by acid-carbonate reaction and oxidation of organic materials in meltwater. While CO_2 production in the meltwater indeed occurs, its magnitude is up to 20 ppm, and the glacial-interglacial CO_2 variations are well captured in the DF record for the last 340 kyr BP (Kawamura et al., 2003). Our new wet-extraction CO_2 values of the DF core for the last 2000 years agree with the Law Dome (MacFarling Meure et al., 2006), EDML (Siegenthaler et al., 2005) and WAIS Divide (Ahn et al., 2012) ice cores mostly within 0 to +10 ppm, with several ~20-ppm deviations. The NEEM wet-extraction CO_2 data are higher than those of DF and other ice cores by ~10 – 30 ppm (maximum ~60 ppm), which is much larger than the pooled standard deviation (5.3 ppm for the NEEM dataset). ~~The primary reason for the high CO_2 values in the NEEM ice core is high impurity contents in the core, which cause in-situ CO_2 production in the ice sheet (Anklin et al., 1995).~~This result is not surprising because it is well known that reliable CO_2 reconstructions are only possible from Antarctic ice cores owing to in-situ CO_2 production in the Greenland ice sheet with high impurity concentrations (Anklin et al., 1995). Anklin et al. (1995) measured Eurocore (Greenland) late Holocene ice with both dry and wet extraction methods, and found that the wet extraction values were higher (by ~30 to 100 ppm) than the dry extraction values, which in turn are higher than the Antarctic records by up to ~20 ppm. Their results thus suggest that the excess CO_2 in our NEEM dataset might be partly produced during the extraction by chemical reactions in the meltwater.

5.2 Elemental and isotopic compositions of N_2, O_2 and Ar

5.2.1 Gas-loss fractionation and surface removal

Previous studies have indicated that gases can slightly be lost from ice cores during storage, causing size- and mass-dependent fractionations in $\delta O_2/N_2$, $\delta^{18}O$ and $\delta Ar/N_2$ (Bender et al., 1995; Bereiter et al., 2009; Huber et al., 2006a; Ikeda-Fukazawa et al., 2005; Kawamura et al., 2007; Severinghaus et al., 2009). Greenhouse-gas concentrations could also be biased (presumably to higher values, Ikeda-Fukazawa et al., 2004, 2005; Bereiter et al., 2009; Eggleston et al. 2016), but it would not be detected in most cases with the current measurement precisions. As the $\delta O_2/N_2$, $\delta^{18}O$ and $\delta Ar/N_2$ ratios become fractionated especially in the exposed outer part of the core, the surface must sufficiently be removed to precisely measure the air composition and accurately reconstruct the ratios as originally archived in the ice sheet (Bereiter et al., 2009; Ikeda-Fukazawa et al., 2005; Kawamura et al., 2007; Severinghaus et al., 2009). The thickness of sufficient surface removal should depend on the storage period, storage temperature and the form of air in ice (bubbles or clathrate-hydrates). To examine whether those ratios as originally recorded in the ice sheet can be ~~obtained from~~found in the long-stored DF core~~, which had been stored~~ (at -50 °C

for ~20 years~~,~~), we measured samples from the same depths ~~but~~ with different thickness of surface removal (~~for example~~e.g., 8 and 5 mm) (Fig. ~~11~~12). The outer ice pieces were also measured, and the results were compared with ~~the values~~those from the inner ice.

First, we compare the data from the outer ice and inner ice to validate the magnitude of gas-loss ~~induced~~ fractionation. For both the bubbly ice and clathrate ice (note that bubble-clathrate transition zone is not investigated), all the measured samples show lower $\delta O_2/N_2$ and $\delta Ar/N_2$ in the outer ice than those in the inner ice (Fig. ~~12). The outer ice has more depleted $\delta O_2/N_2$ and $\delta Ar/N_2$ than the inner ice, and~~13). In addition, $\delta O_2/N_2$ is more depleted than $\delta Ar/N_2$, ~~indicating significant~~consistent with the gas-loss fractionations found in earlier studies, which proposed that the gas-loss fractionation is largely size-dependent ~~fractionation in the outer ice.~~(molecular diameter of O_2 is smaller than Ar) with weak mass dependency (Bender et al., 1995; Huber et al., 2006a; Severinghaus et al., 2009). Most samples show higher $\delta^{18}O$ in the outer ice than in the inner ice. In contrast,~~,~~ ~~while~~ $\delta^{15}N$ from the outer and inner ice agree to each other, suggesting that ~~significant~~detectable mass-dependent fractionation ~~also~~ occurred for O_2, but not for N_2, ~~in~~by the gas loss from the outer ice.

Next, we examine the $\delta O_2/N_2$ data from the inner ice with different thicknesses of surface removal. Below 1380 m (pure clathrate ice), the $\delta O_2/N_2$ values from the inner ice with the outer removal of 5 mm are mostly lower than those from the adjacent pieces with 8-mm removal (Fig. ~~13~~14), suggesting that gas loss affects the gas composition to more than 5 mm from the surface. On the other hand, no significant differences are observed between $\delta O_2/N_2$ values from the inner ice (with ~~the~~ different outer removal ~~of more than~~) if the removal is 8 mm or more (we tested with combinations of 8, 9, 11, and 13 mm) (Fig. ~~14~~15). The $\delta Ar/N_2$, $\delta^{15}N$ and $\delta^{18}O$ data from the inner ice with surface removal of 5 mm and 8 mm are not different from each other, suggesting insignificant mass-dependent gas-loss fractionation in ice > 5 mm away from the surface. From these results, we conclude that the removal of ~~more than~~ 8 mm is sufficient to obtain the gas composition as originally trapped in the DF1 core. For our routine measurements of the DF core, we decided to cut 9 mm to include an extra margin.

5.2.2 Reproducibility and comparison with previous data

The pooled standard deviations for the DF clathrate hydrate ice with removal thickness of >8 mm are 0.006, 0.010, 0.089 and 0.115 ‰ for $\delta^{15}N$, $\delta^{18}O$, $\delta O_2/N_2$ and $\delta Ar/N_2$, respectively (Table 7). The reproducibility of $\delta O_2/N_2$ is one order of magnitude better than those previously reported (Bender, 2002; Extier et al., 2018). The reproducibility for $\delta^{15}N$ and $\delta^{18}O$ are comparable to but slightly worse than the most precise measurements by SIO (Seltzer et al., 2017; Severinghaus et al., 2009).

We compare our new DF data with previous data from Tohoku University (Fig. ~~15~~16) (Kawamura, 2001; Kawamura et al., 2007). The previous $\delta O_2/N_2$ data were significantly depleted due to gas loss during the sample storage at -25 °C (Fig. ~~15c~~16c, grey marks), thus they were corrected for effect~~for effect~~ by assuming a linear relationship between the storage duration and $\delta O_2/N_2$ (Fig. ~~15c~~16c, red marks). Our new $\delta O_2/N_2$ data agree with the gas-loss corrected old data, suggesting that $\delta O_2/N_2$ as

originally trapped in the DF core can be ~~measured~~reconstructed from the 20-year old samples, and that the relatively large gas-loss correction by Kawamura et al. (2007) was rather accurate. The new $\delta^{15}N$ and $\delta^{18}O$ data generally agree with those of Kawamura (2001) and Kawamura et al. (2007) within the uncertainty of the old data, although the large uncertainties of the old datasets do not permit precise comparisons.

The duplicate measurements of bubbly ice of the NEEM core (by removing more than 3 mm from the surface) produced pooled standard deviations for $\delta^{15}N$ and $\delta^{18}O$ (0.006 and 0.008 ‰) similar to those for the DF clathrate ice (Table 7). This suggests that the removal of 3 mm is sufficient for the bubbly ice at least for the isotopic ratios, possibly due to generally low pressure of bubbly ice (because it is shallower) compared with clathrate ice. On the other hand, pooled standard deviations for $\delta O_2/N_2$ and $\delta Ar/N_2$ of the bubble ice are much larger than those for the DF clathrate ice (0.235 and 0.119 ‰ for the DF core, and 0.775 and 0.450 ‰ for the NEEM core, respectively), possibly related with the natural variability of pressure and composition of individual air bubbles with different trapping histories (Ikeda-Fukazawa et al., 2001; Kobashi et al., 2015). The larger pooled standard deviations for the NEEM core than those of the DF core possibly reflect natural difference within the ice sheets, or artifacts~~artefacts~~ (gas loss) during drilling, handling and storage at the NEEM site associated with the warmer environment than the Dome Fuji drilling site. We also note that, due to the small number of duplicates for the bubbly ice, it is difficult at this stage to assess whether there are small systematic lowering of $\delta O_2/N_2$ and $\delta Ar/N_2$ with the 3-mm removal.

5.3 Total air content

The pooled standard deviations for TAC are 0.66 and 0.67 ~~ml$_{STP}$~~mL$_{STP}$ kg^{-1} for both DF bubbly ice and clathrate ice. The data from the clathrate ice agree with those from previous measurements using ~300 g of ice (Kawamura, 2001), while the data from the bubbly ice appear to be lower than the previous data, especially for the shallowest depths (Fig. ~~15~~16). These results may be explained by the fact that TAC of bubbly ice is biased towards lower values due to the so-called "cut-bubble effect" (Martinerie et al., 1990), in which bubbles intersecting the sample surfaces are cut and lose air. The cut-bubble effect is larger for samples with a smaller surface-to-volume ratio and samples from shallower depths.

6. Conclusions

We presented a new analytical ~~technic~~technique for high-precision, simultaneous measurements of CH_4, N_2O and CO_2 concentrations, isotopic and elemental ratios of N_2, O_2 and Ar, and total air content, from a single ice core sample with relatively small size (50 – 70 g) by a wet extraction. The ice sample is melted under a vacuum in 3 min, and the released air is continuously transferred and cryogenically trapped into a sample tube, with the total duration for extraction of about 10 minutes. The rapid and continuous transfer minimizes contaminations due to degassing from the inner walls of the apparatus, as well as dissolution of the sample air into the meltwater. The extracted air is homogenized in the sample tube for one night, and split

into two aliquots for mass spectrometric measurement (~20 % of the sample) and gas chromatographic measurement (~80 % of the sample).

The system performance was evaluated by measuring the standard gas after treating it as the ice-core air extraction, by passing it through the extraction and split lines with gas-free water in the extraction vessel. We do not observe significant changes in the mean CH_4, N_2O and CO_2 concentrations, possibly because of the long evacuation, rapid and continuous gas transfer at low pressure over meltwater, and passivation treatments of the extraction lines and sample tubes. Thus, we do not apply corrections (e.g., so-called blank correction and solubility correction) for the greenhouse gas concentrations. For the mass spectrometry, we do not observe significant changes in $\delta^{18}O$, while we observe changes in $\delta^{15}N$, $\delta O_2/N_2$, $\delta Ar/N_2$. Moreover, the change in $\delta O_2/N_2$ is dependent on the sample size. Thus, we apply constant corrections for $\delta^{15}N$ and $\delta Ar/N_2$, and sample-size-dependent correction for $\delta O_2/N_2$.

Standard deviations of duplicate measurements for DF clathrate ice are 3.2 ppb, 2.2 ppb, and 3.1 ppm for CH_4, N_2O and CO_2 concentrations, respectively, and 0.006, 0.010, 0.09 and 0.12 ‰ for $\delta^{15}N$, $\delta^{18}O$, $\delta O_2/N_2$ and $\delta Ar/N_2$, respectively. The CH_4 and N_2O data from the DF and NEEM ice cores for the last 2,000 years agree well with those from the GISP2, WAIS Divide and Law Dome cores. We also demonstrate significant gas-loss induced depletion of $\delta O_2/N_2$ in the ice near the sample surface of the DF clathrate ice, which has been stored at -50 °C over ~20 years. The original $\delta O_2/N_2$, $\delta Ar/N_2$, $\delta^{15}N$ and $\delta^{18}O$ in the ice sheet may still be obtained by removing the sample surface by > 8 mm.

Our new method will have many paleoclimatic applications, such as detecting subtle variations in greenhouse gas cycles (in particular CH_4 inter-polar difference and N_2O variations), hydrological cycles ($\delta^{18}O$ of O_2), insolation signals for dating ($\delta O_2/N_2$ and $\delta Ar/N_2$), and local climatic and glaciological conditions ($\delta^{15}N$ and TAC) from deep ice cores with high temporal resolution.

Appendix A: Comparison with other available records

Table A1: Ice cores and time scales shown in this study.

	Ice core	Reference	Offset (ppb)	Time scale
CH_4	NEEM	This study		GICC05 (Rasmussen et al., 2013)
	Dome Fuji	This study		WDC05A (Mitchell et al., 2013; Mitchell et al., 2011)
	Dome Fuji	Kawamura (2001)		WDC05A (Mitchell et al., 2013; Mitchell et al., 2011)
	GISP2	Mitchell et al. (2013)		WDC05A (Mitchell et al., 2013; Mitchell et al., 2011)
	GISP2	Brook (2009)		WDC05A (Mitchell et al., 2013; Mitchell et al., 2011)
	GRIP	Blunier et al. (1995); Chappellaz et al. (1997); Chappellaz et al. (1993)	+23.84[a]	GICC05 (Rasmussen et al., 2014; Seierstad et al., 2014)
	NGRIP	Beck et al. (2018)	+6.15[a]	GICC05 (Rasmussen et al., 2014; Seierstad et al., 2014)
	WAIS Divide	Mitchell et al. (2013)		WDC05A (Mitchell et al., 2013; Mitchell et al., 2011)
	Law Dome	Rubino et al. (2019)		Rubino et al. (2019)
	EDC	Flückiger et al. (2002)	+10.38[a]	Beck et al. (2018)
	EDML	Schilt et al. (2010)	+1.52[a]	Beck et al. (2018)
	TALDICE	Beck et al. (2018)	+6.15[a]	Beck et al. (2018)
	TALDICE	Bock et al. (2017)	+6.15[a]	Beck et al. (2018)
	TALDICE	Schilt et al. (2010)	+4.06[a]	Beck et al. (2018)
	Siple Dome	Brook (2009)		Beck et al. (2018)
N_2O	NEEM	This study		GICC05 (Rasmussen et al., 2013)
	Dome Fuji	This study		WDC05A (Mitchell et al., 2013; Mitchell et al., 2011)
	Dome Fuji	Kawamura (2001)		WDC05A (Mitchell et al., 2013; Mitchell et al., 2011)
	NEEM	Prokopiou et al. (2018)		GICC05 (Rasmussen et al., 2013)
	NEEM	Ryu et al. (2020)		WD2014 (Buizert et al., 2015)
	GISP2	Sowers et al. (2003)		WDC05A (Mitchell et al., 2013; Mitchell et al., 2011)
	NGRIP	Fischer et al. (2019)		Fischer et al. (2019)
	EDC	Schilt et al. (2010)		Beck et al. (2018)
	TALDICE	Schilt et al. (2010)		Beck et al. (2018)
	TALDICE	Fischer et al. (2019)		Fischer et al. (2019)
	EDML	Schilt et al. (2010)		Beck et al. (2018)
	Law Dome	Rubino et al. (2019)		Rubino et al. (2019)
	Styx Glacier	Ryu et al. (2020)		WD2014 (Buizert et al., 2015)
	Monte Carlo spline	Fischer et al. (2019)		Fischer et al. (2019)
CO_2	NEEM	This study		GICC05 (Rasmussen et al., 2013)
	Dome Fuji	This study		WDC05A (Mitchell et al., 2013; Mitchell et al., 2011)
	Dome Fuji	Kawamura et al. (2007)		WDC05A (Mitchell et al., 2013; Mitchell et al., 2011)
	Law Dome	Rubino et al. (2019)		Rubino et al. (2019)
	WDC	Ahn et al. (2012)		Ahn et al. (2012)
	EDML	Siegenthaler et al. (2005)		Siegenthaler et al. (2005)
	South Pole	Siegenthaler et al. (2005)		Siegenthaler et al. (2005)

[a] Offset correction was made to CH_4 concentrations by following Beck et al. (2018).

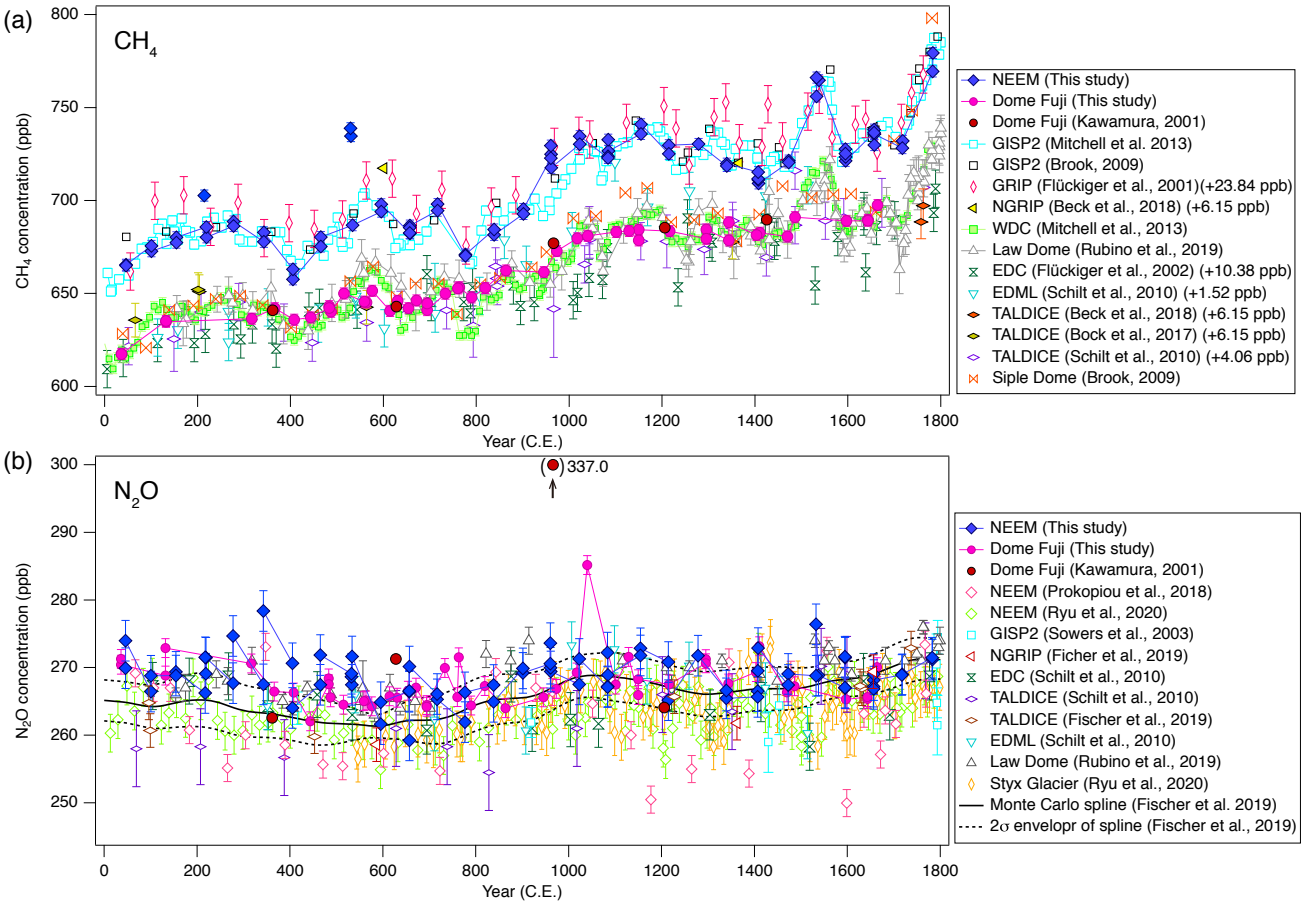

Figure A1: (a) CH_4 and (b) N_2O concentrations for 0 – 1800 C.E. from the DF and NEEM ice cores measured with our new method, and the comparison with published records from other groups (Beck et al., 2018; Bock et al., 2017; Brook, 2009; Fischer et al., 2019; Flückiger et al., 2002; Kawamura, 2001; Mitchell et al., 2013; Prokopiou et al., 2018; Rubino et al., 2019; Ryu et al., 2020; Schilt et al., 2010; Sowers et al., 2003). The DF data is placed on the WDC05A chronology (see Fig. 10), and all the other data are placed on the respective (published) time scales (details are summarized in Table A1). The GRIP, NGRIP, EDC, EDML, and TALDICE data are corrected for systematic offsets relative to the WDC data, as reported by Beck et al. (2018).

Data availability

Gas data of the Dome Fuji and NEEM ice cores are available at the NIPR ADS data repository (~~https://ads.nipr.ac.jp/dataset/A20200501-001~~https://ads.nipr.ac.jp/dataset/A20200501-001) and will be available on the NOAA paleoclimate database~~; for inquiry: oyabu.ikumi@nipr.ac.jp)~~.

Author contribution

K. Kawamura designed the wet extraction apparatus and mass spectrometer configuration, and developed the overall concept of the splitting and multiple-species analyses. K. Kawamura, SS and AK designed the GC configurations. JPS and RB developed the calibration protocols for atmospheric normalization of mass spectrometer measurements except for $\delta O_2/N_2$, and customized ISODAT scripts. AO designed the split line. RD developed GC controlling software with a discussion with K. Kawamura. SI provided the $\delta O_2/N_2$ standard scale. DDJ provided the NEEM ice core samples. KGA provided funding for the mass spectrometer, and the NEEM samples as the national representative. SA and TN provided the greenhouse gas concentration scales and funding for the wet extraction apparatus and cryostat. IO and K. Kitamura made the measurements. IO, K. Kitamura and K. Kawamura established the detailed procedures of ice core measurements and calibrations. CS contributed to the early stages of development. IO and K. Kawamura wrote the manuscript, and all authors contributed to the discussion.

Competing interests

The authors declare that they have no conflict of interest.

Acknowledgments

We thank Yumiko Miura for a part of the data reduction, Akito Tanaka, Satoko Nakanishi, Mariko Hayakawa, and Satomi Oda for the measurements and Shinji Morimoto for providing the Tohoku University scales and assisting our standard gas calibrations. We acknowledge the Dome Fuji drilling projects led by Okitsugu Watanabe, Yoshiyuki Fujii and Hideaki Motoyama and participants in the Japanese Antarctic Research Expedition and Ice Core Consortium related to the Dome Fuji fieldworks and managements. NEEM is directed and organized by the Center of Ice and Climate at the Niels Bohr Institute and US NSF, Office of Polar Programs. It is supported by funding agencies and institutions in Belgium (FNRS-CFB and FWO), Canada (NRCan/GSC), China (CAS), Denmark (FIST), France (IPEV, CNRS/INSU, CEA and ANR), Germany (AWI), Iceland (RannIs), Japan (NIPR), Korea (KOPRI), The Netherlands (NWO/ALW), Sweden (VR), Switzerland (SNF), United Kingdom (NERC), and the USA (US NSF, Office of Polar Programs). This study was supported by Japan Society for the Promotion of Science (JSPS) and Ministry of Education, Culture, Sports, Science and Technology-Japan (MEXT) KAKENHI Grant Numbers 17K12816, 17J00769 and 20H04327 to IO, 20H00639, 17H06316, 15KK0027, 26241011, 21671001 and 18749002 to K. Kawamura, 22221002 to KGA, 18K01129 to SI, 22310003 to TN, the GRENE Arctic Climate Change Research Project of the MEXT to SA, the Global Environment Research Coordination System from the Ministry of the Environment to SI, and Project Research KP305 and Senshin Project from National Institute of Polar Research., and partially carried out in the Arctic Challenge for Sustainability II (ArCS II), Program Grant Number JPMXD1420318865. We are grateful for constructive comments, remarks and advice from Jochen Schmitt and an anonymous reviewer.

References

Ahn, J., Brook, E. J., and Howell, K.: A high-precision method for measurement of paleoatmospheric CO_2 in small polar ice samples, J. Glaciol., 55, 499-506, https://doi.org/10.3189/002214309788816731, 2009.

Ahn, J., Brook, E. J., Mitchell, L., Rosen, J., McConnell, J. R., Taylor, K., Etheridge, D., and Rubino, M.: Atmospheric CO_2 over the last 1000 years: A high-resolution record from the West Antarctic Ice Sheet (WAIS) Divide ice core, Global Biogeochem. Cycles, 26, https://doi.org/10.1029/2011GB004247, 2012.

Anklin, M., Barnola, J. M., Schwander, J., Stauffer, B., and Raynaud, D.: Processes Affecting the CO_2 Concentrations Measured in Greenland Ice, Tellus B, 47, 461-470, https://doi.org/10.1034/j.1600-0889.47.issue4.6.x, 1995.

Aoki, N., Ishidoya, S., Matsumoto, N., Watanabe, T., Shimosaka, T., and Murayama, S.: Preparation of primary standard mixtures for atmospheric oxygen measurements with less than 1 μmol mol^{-1} uncertainty for oxygen molar fractions, Atmos. Meas. Tech., 12, 2631-2646, https://doi.org/10.5194/amt-12-2631-2019, 2019.

Aoki, S., Nakazawa, T., Murayama, S., and Kawaguchi, S.: Measurements of atmospheric methane at the Japanese Antarctic Station, Syowa, Tellus, 44, 273-281, https://doi.org/10.3402/tellusb.v44i4.15455, 1992.

Barnola, J. M., Raynaud, D., Korotkevich, Y. S., and Lorius, C.: Vostok Ice Core Provides 160,000-Year Record of Atmospheric CO_2, Nature, 329, 408-414, https://doi.org/10.1038/329408a0, 1987.

Bazin, L., Landais, A., Lemieux-Dudon, B., Toyé Mahamadou Kele, H., Veres, D., Parrenin, F., Martinerie, P., Ritz, C., Capron, E. F. N., Lipenkov, V., Loutre, M. F., Raynaud, D., Vinther, B., Svensson, A., Rasmussen, S. O., Severi, M., Blunier, T., Leuenberger, M., Fischer, H., Masson-Delmotte, V., Chappellaz, J., and Wolff, E.: An optimized multi-proxy, multi-site Antarctic ice and gas orbital chronology (AICC2012): 120-800 ka, Clim. Past, 9, 1715-1731, https://doi.org/10.5194/cp-9-1715-2013, 2013.

Beck, J., Bock, M., Schmitt, J., Seth, B., Blunier, T., and Fischer, H.: Bipolar carbon and hydrogen isotope constraints on the Holocene methane budget, Biogeosciences, 15, 7155-7175, https://doi.org/10.5194/bg-15-7155-2018, 2018.

Bender, M., Sowers, T., and Lipenkov, V.: On the concentrations of O_2, N_2, and Ar in trapped gases from ice cores, J. Geophys. Res., https://doi.org/10.1029/94JD02212, 1995.

Bender, M. L.: Orbital tuning chronology for the Vostok climate record supported by trapped gas composition, Earth Planet. Sci. Lett, 204, 275-289, https://doi.org/10.1016/S0012-821X(02)00980-9, 2002.

Bereiter, B., Kawamura, K., and Severinghaus, J. P.: New methods for measuring atmospheric heavy noble gas isotope and elemental ratios in ice core samples, Rapid Commun. Mass Spectrom., 32, 801-814, doi/10.1002/rcm.8099, 2018.

Bereiter, B., Schwander, J., Luthi, D., and Stocker, T. F.: Change in CO_2 concentration and O_2/N_2 ratio in ice cores due to molecular diffusion, Geophys. Res. Lett., 36, L05703-05705, https://doi.org/10.1029/2008GL036737, 2009.

Blunier, T. and Brook, E. J.: Timing of millennial-scale climate change in Antarctica and Greenland during the last glacial period, Science, 291, 109-112, https://doi.org/10.1126/science.291.5501.109, 2001.

Blunier, T., Chappellaz, J., Schwander, J., Stauffer, B., and Raynaud, D.: Variations in atmospheric methane concentration during the Holocene epoch, Nature, 374, 46-49, https://doi.org/10.1038/374046a0, 1995.

Bock, M., Schmitt, J., Beck, J., ~~Seth, B., Chappellaz, J~~Schneider, R., and Fischer, H.~~: Glacial/interglacial wetland, biomass burning,~~: Improving accuracy and ~~geologic methane emissions constrained by dual stable isotopic CH_4~~precision of ice core ~~records, Proc. Natl. Acad. Sci. USA., 114, E5778-E5786, https~~δD(CH4) analyses using methane pre-pyrolysis and hydrogen post-pyrolysis trapping and subsequent chromatographic separation, Atmos. Meas. Tech., 7(7), 1999–2012. http://doi.org/10.~~1073/pnas.1613883114, 2017~~5194/amt-7-1999-2014, 2014.

~~Author:~~Bock, M., Schmitt, J., Beck, J., Seth, B., Chappellaz, J., and Fischer, H.: Glacial/interglacial wetland, biomass burning, and geologic methane emissions constrained by dual stable isotopic CH_4 ice core records, Proc. Natl. Acad. Sci. USA., 114, E5778-E5786, https://doi.org/10.1073/pnas.1613883114, 2017.

Brook, E. J.: Methane measurements from the GISP2 and Siple Dome ice cores, U.S. Antarctic Program (USAP) Data Center, https://doi.org/10.7265/N58P5XFZ, 2009.

Brook, E. J., Sowers, T., and Orchardo, J.: Rapid variations in atmospheric methane concentration during the past 110,000 years, Science, 273, 1087-1091, https://doi.org/10.1126/science.273.5278.1087, 1996.

Brook, E. J., White, J. W. C., Schilla, A. S. M., Bender, M. L., Barnett, B., Severinghaus, J. P., Taylor, K. C., Alley, R. B., and Steig, E. J.: Timing of millennial-scale climate change at Siple Dome, West Antarctica, during the last glacial period, Quat. Sci. Rev., 24, 1333-1343, https://doi.org/10.1016/j.quascirev.2005.02.002, 2005.

Buizert, C., Cuffey, K. M., Severinghaus, J. P., Baggenstos, D., Fudge, T. J., Steig, E. J., Markle B. R., Winstrup, M., Rhodes, R. H., Brook, E. J., Sowers, T. A., Clow, G. D., Cheng, H., Edwards, R. L., Sigl, M., McConnell, J. R., and Taylor, K. C.: The WAIS Divide deep ice core WD2014 chronology -Part 1: Methane synchronization (68–31 ka BP) and the gas age–ice age difference, Clim. Past, 11(2), 153–173. http://doi.org/10.5194/cp-11-153-2015, 2015.

Chappellaz, J., Blunier, T., Kints, S., Dällenbach, A., Barnola, J.-M., Schwander, J., Raynaud, D., and Stauffer, B.: Changes in the atmospheric CH_4 gradient between Greenland and Antarctica during the Holocene, J. Geophys. Res., 102, 15987-15997, https://doi.org/10.1029/97JD01017, 1997.

Chappellaz, J. A., Fung, I. Y., and Thompson, A. M.: The atmospheric CH_4 increase since the Last Glacial Maximum, Tellus, 45, 228-241, https://doi.org/10.3402/tellusb.v45i3.15726, 1993.

Dlugokencky, E. J.: Conversion of NOAA atmospheric dry air CH_4 mole fractions to a gravimetrically prepared standard scale, J. Geophys. Res., 110, https://doi.org/10.1029/2005JD006035, 2005.

Eggleston, S., Schmitt, J., Bereiter, B., Schneider, R., and Fischer, H.: Evolution of the stable carbon isotope composition of atmospheric CO_2 over the last glacial cycle, Paleoceanography, 31(3), 434–452, http://doi.org/10.1002/2015PA002874, 2016.

Extier, T., Landais, A., Bréant, C., Prié, F., Bazin, L., Dreyfus, G., Roche, D. M., and Leuenberger, M.: On the use of $\delta^{18}O_{atm}$ for ice core dating, Quat. Sci. Rev., 185, 244-257, https://doi.org/10.1016/j.quascirev.2018.02.008, 2018.

Flückiger, J., Dällenbach, A., Blunier, T., Stauffer, B., Stocker, T. F., Raynaud, D., and Barnola, J. M.: Variations in atmospheric N_2O concentration during abrupt climatic changes, Science, 285, 227-230, https://doi.org/10.1126/science.285.5425.227, 1999.

Flückiger, J., Moon, J., Stauffer, B., Schwander, J., and Stocker, T. F.: High-resolution Holocene N_2O ice core record and its relationship with CH_4 and CO_2, Global Biogeochem. Cycles, 16, 1010, https://doi.org/10.1029/2001GB001417, 2002.

Headly, M.: Krypton and xenon in air trapped in polar ice cores: paleo-atmospheric measurements for estimating past mean ocean temperature and summer snowmelt frequency, Ph. D thesis, UC San Diego, USA, ProQuest ID: umi-ucsd-2223. Merritt ID: ark:/20775/bb7065849g, Retrieved from https://escholarship.org/uc/item/7065845jv7065849j7065846kw, 2008.

Huber, C., Beyerle, U., Leuenberger, M., Schwander, J., Kipfer, R., Spahni, R., Severinghaus, J. P., and Weiler, K.: Evidence for molecular size dependent gas fractionation in firn air derived from noble gases, oxygen, and nitrogen measurements, Earth Planet. Sci. Lett, 243, 61-73, https://doi.org/10.1016/j.epsl.2005.12.036, 2006a.

Huber, C., Leuenberger, M., Spahni, R., Flückiger, J., Schwander, J., Stocker, T. F., Johnsen, S., Landais, A., and Jouzel, J.: Isotope calibrated Greenland temperature record over Marine Isotope Stage 3 and its relation to CH_4, Earth Planet. Sci. Lett, 243, 504-519, https://doi.org/10.1016/j.epsl.2006.01.002, 2006b.

Ikeda-Fukazawa, T., Fukumizu, K., Kawamura, K., Aoki, S., Nakazawa, T., and Hondoh, T.: Effects of molecular diffusion on trapped gas composition in polar ice cores, Earth Planet. Sci. Lett, 229, 183-192, https://doi.org/doi/10.1016/j.epsl.2004.11.011, 2005.

Ikeda-Fukazawa, T., Kawamura, K., and Hondoh, T.: Mechanism of molecular diffusion in ice crystals, Molecular Simulation, 30(13-15), 973–979, http://doi.org/10.1080/08927020410001709307, 2004.

Ikeda-Fukazawa, T., Hondoh, T., Fukumura, T., Fukazawa, H., and Mae, S.: Variation in N_2/O_2 ratio of occluded air in Dome Fuji Antarctic ice, J. Geophys. Res., 106, 17799-17810, https://doi.org/10.1029/2000JD000104, 2001.

Ishidoya, S. and Murayama, S.: Development of a new high precision continuous measuring system for atmospheric O_2/N_2 and Ar/N_2 and its application to the observation in Tsukuba, Japan, Tellus B, 66, 22574, https://doi.org/10.3402/tellusb.v66.22574, 2014.

Ishidoya, S., Tsuboi, K., Murayama, S., Matsueda, H., Aoki, N., Shimosaka, T., Kondo, H., and Saito, K.: Development of a continuous measurement system for atmospheric O_2/N_2 ratio using a Paramagnetic analyzer and its application in Minamitorishima Island, Japan, SOLA, 13, 230-234, https://doi.org/10.2151/sola.2017-042, 2017.

Ishijima, K., Nakazawa, T., Sugawara, S., Aoki, S., and Saeki, T.: Concentration variations of tropospheric nitrous oxide over Japan, Geophys. Res. Lett., 28, 171-174, https://doi.org/10.1029/2000GL011465, 2001.

Kawamura, K.: Variations of atmospheric components over the past 340000 years from Dome Fuji deep ice core, Antarctica, Ph. D thesis, Tohoku University, Japan, http://hdl.handle.net/10097/38833, 2001.

Kawamura, K., Nakazawa, T., Aoki, S., Sugawara, S., Fujii, Y., and Watanabe, O.: Atmospheric CO_2 variations over the last three glacial-interglacial climatic cycles deduced from the Dome Fuji deep ice core, Antarctica using a wet extraction technique, Tellus B, 55, 126-137, https://doi.org/10.1034/j.1600-0889.2003.00050.x, 2003.

Kawamura, K., Parrenin, F., Lisiecki, L., Uemura, R., Vimeux, F., Severinghaus, J. P., Hutterli, M. A., Nakazawa, T., Aoki, S., Jouzel, J., Raymo, M. E., Matsumoto, K., Nakata, H., Motoyama, H., Fujita, S., Goto-Azuma, K., Fujii, Y., and Watanabe, O.: Northern Hemisphere forcing of climatic cycles in Antarctica over the past 360,000years, Nature, 448, 912-916, https://doi.org/10.1038/nature06015, 2007.

Kobashi, T., Ikeda-Fukazawa, T., Suwa, M., Schwander, J., Kameda, T., Lundin, J., Hori, A., Motoyama, H., Döring, M., and Leuenberger, M.: Post-bubble close-off fractionation of gases in polar firn and ice cores: effects of accumulation rate on permeation through overloading pressure, Atmos. Chem. Phys., 15, 13895-13914, https://doi.org/10.5194/acp-15-13895-2015, 2015.

Kobashi, T., Kawamura, K., Severinghaus, J. P., Barnola, J.-M., Nakaegawa, T., Vinther, B. M., Johnsen, S. J., and Box, J. E.: High variability of Greenland surface temperature over the past 4000 years estimated from trapped air in an ice core, Geophys. Res. Lett., 38, https://doi.org/10.1029/2011GL049444, 2011.

Kobashi, T., Severinghaus, J. P., and Barnola, J.-M.: 4±1.5 °C abrupt warming 11,270 yr ago identified from trapped air in Greenland ice, Earth Planet. Sci. Lett, 268, 397-407, https://doi.org/10.1016/j.epsl.2008.01.032, ~~2008~~2008a.

Kobashi, T., Severinghaus, J. P., and Kawamura, K.: Argon and nitrogen isotopes of trapped air in the GISP2 ice core during the Holocene epoch (0 – 11,500 B.P.): Methodology and implications for gas loss processes, Geochim. Cosmochim. Acta,, 72(1), 4675–4686, http://doi.org/10.1016/j.gca.2008.07.006, 2008b.

Landais, A., Dreyfus, G., Capron, E., Masson-Delmotte, V., Sanchez-Goni, M. F., Desprat, S., Hoffmann, G., Jouzel, J., Leuenberger, M., and Johnsen, S.: What drives the millennial and orbital variations of $\delta^{18}O_{atm}$?, Quat. Sci. Rev., 29, 235-246, https://doi.org/10.1016/j.quascirev.2009.07.005, 2010.

Lee, J. E., Edwards, J. S., Schmitt, J., Fischer, H., Bock, M., and Brook, E. J.: Excess methane in Greenland ice cores associated with high dust concentrations, Geochim. Cosmochim. Acta, 270, 409–430. http://doi.org/10.1016/j.gca.2019.11.020, 2020.

Lipenkov, V., Candaudap, F., Ravoire, J., Dulac, E., and Raynaud, D.: A new device for the measurement of air content in polar ice, J. Glaciol., 41(138), 423–429, http://doi.org/10.1017/S0022143000016294, 1995.

Lipenkov, V. Y., Raynaud, D., and Loutre, M. F.: On the potential of coupling air content and O_2/N_2 from trapped air for establishing an ice core chronology tuned on local insolation, Quat. Sci. Rev., 30, 3280-3289, https://doi.org/10.1016/j.quascirev.2011.07.013, 2011.

MacFarling Meure, C., Etheridge, D., Trudinger, C., Steele, P., Langenfelds, R., van Ommen, T., Smith, A., and Elkins, J.: Law Dome CO_2, CH_4 and N_2O ice core records extended to 2000 years BP, Geophys. Res. Lett., 33, L14810, https://doi.org/10.1029/2006GL026152, 2006.

Machida, T., Nakazawa, T., Fujii, Y., Aoki, S., and Watanabe, O.: Increase in the atmospheric nitrous oxide concentration during the last 250 years, Geophys. Res. Lett., 22, 2921-2924, https://doi.org/10.1029/95GL02822, 1995.

Martinerie, P., Lipenkov, V. Y., and Raynaud, D.: Air content paleo record in the Vostok ice core (Antarctica): A mixed record of climatic and glaciological parameters, J. Geophys. Res., 99, 10565-10576, https://doi.org/10.1029/93JD03223, 1994.

Martinerie, P., Lipenkov, V. Y., and Raynaud, D.: Correction of air-content measurements in polar ice for the effect of cut bubbles at the surface of the sample, J. Glaciol., 36, 299-303, https://doi.org/10.3189/002214390793701282, 1990.

Martinerie, P., Raynaud, D., Etheridge, D. M., Barnola, J. M., and Mazaudier, D.: Physical and climatic parameters which influence the air content in polar ice, Earth Planet. Sci. Lett, 112, 1-13, https://doi.org/10.1016/0012-821X(92)90002-D, 1992.

Mitchell, L., Brook, E., Lee, J. E., Buizert, C., and Sowers, T.: Constraints on the late Holocene anthropogenic contribution to the atmospheric methane budget, Science, 342, 964-966, https://doi.org/10.1126/science.1238920, 2013.

Mitchell, L. E., Brook, E. J., Sowers, T., McConnell, J. R., and Taylor, K.: Multidecadal variability of atmospheric methane, 1000-1800 C.E, Journal of Geophysical Research: Biogeosciences, 116, G02007, https://doi.org/10.1029/2010JG001441, 2011.

Monnin, E., Indermühle, A., Dällenbach, A., Flückiger, J., Stauffer, B., Stocker, T. F., Raynaud, D., and Barnola, J.-M.: Atmospheric CO_2 Concentrations over the Last Glacial Termination, Science, 291, 112-114, https://doi.org/10.1126/science.291.5501.112, 2001.

Nakazawa, T., Machida, T., Esumi, K., Tanaka, M., Fujii, Y., Aoki, S., and Watanabe, O.: Measurements of CO_2 and CH_4 concentrations a polar ice core, J. Glaciol., 39, 209-215, https://doi.org/10.3189/S0022143000015860, 1993a.

Nakazawa, T., Machida, T., Tanaka, M., Fujii, Y., Aoki, S., and Watanabe, O.: Differences of the atmospheric CH_4 concentration between the Arctic and Antarctic regions in pre-industrial/pre-agricultural era, Geophys. Res. Lett., 20, 943-946, https://doi.org/10.1029/93GL00776, 1993b.

NEEM community members: Eemian interglacial reconstructed from a Greenland folded ice core, Nature, 493, 489-494, https://doi.org/10.1038/nature11789, 2013.

Orsi, A. J.: Temperature reconstruction at the West Antarctic Ice Sheet Divide, for the last millennium, from the combination of borehole temperature and inert gas isotope measurements, Ph. D thesis, UC San Diego, USA, ProQuest ID: Orsi_ucsd_0033D_13075, Merritt ID: ark:/20775/bb4779580x, Retrieved from https://escholarship.org/uc/item/4779502g4779583c4779585fq, 2013.

Orsi, A. J., Cornuelle, B. D., and Severinghaus, J. P.: Magnitude and temporal evolution of Dansgaard–Oeschger event 8 abrupt temperature change inferred from nitrogen and argon isotopes in GISP2 ice using a new least-squares inversion, Earth Planet. Sci. Lett, 395, 81-90, https://doi.org/10.1016/j.epsl.2014.03.030, 2014.

Parrenin, F., Cavitte, M. G. P., Blankenship, D. D., Chappellaz, J., Fischer, H., Gagliardini, O., Masson-Delmotte, V., Passalacqua, O., Ritz, C., Roberts, J., Siegert, M. J., and Young, D. A.: Is there 1.5-million-year-old ice near Dome C, Antarctica?, The Cryosphere, 11, 2427-2437, https://doi.org/10.5194/tc-11-2427-2017, 2017.

Prokopiou, M., Sapart, C. J., Rosen, J., Sperlich, P., Blunier, T., Brook, E., van de Wal, R. S. W., and Röckmann, T.: Changes in the isotopic signature of atmospheric nitrous oxide and its global average source during the last three millennia, J. Geophys. Res., 123, 10,757-710,773, https://doi.org/10.1029/2018JD029008, 2018.

Rasmussen, S. O., Abbott, P. M., Blunier, T., Bourne, A. J., Brook, E., Buchardt, S. L., Buizert, C., Chappellaz, J., Clausen, H. B., Cook, E., Dahl-Jensen, D., Davies, S. M., Guillevic, M., Kipfstuhl, S., Laepple, T., Seierstad, I. K., Severinghaus, J. P., Steffensen, J. P., Stowasser, C., Svensson, A., Vallelonga, P., Vinther, B. M., Wilhelms, F., and Winstrup, M.: A first

chronology for the North Greenland Eemian Ice Drilling (NEEM) ice core, Clim. Past, 9, 2713-2730, https://doi.org/10.5194/cp-9-2713-2013, 2013.

Rasmussen, S. O., Bigler, M., Blockley, S. P., Blunier, T., Buchardt, S. L., Clausen, H. B., Cvijanovic, I., Dahl-Jensen, D., Johnsen, S. J., Fischer, H., Gkinis, V., Guillevic, M., Hoek, W. Z., Lowe, J. J., Pedro, J. B., Popp, T., Seierstad, I. K., Steffensen, J. P., Svensson, A. M., Vallelonga, P., Vinther, B. M., Walker, M. J. C., Wheatley, J. J., and Winstrup, M.: A stratigraphic framework for abrupt climatic changes during the Last Glacial period based on three synchronized Greenland ice-core records: refining and extending the INTIMATE event stratigraphy, Quat. Sci. Rev., 106, 14-28, https://doi.org/10.1016/j.quascirev.2014.09.007, 2014.

Raynaud, D., Lipenkov, V., Lemieux-Dudon, B., Duval, P., Loutre, M.-F., and Lhomme, N.: The local insolation signature of air content in Antarctic ice. A new step toward an absolute dating of ice records, Earth Planet. Sci. Lett, 261, 337-349, https://doi.org/10.1016/j.epsl.2007.06.025, 2007.

Rhodes, R. H., Faïn, X., Brook, E. J., McConnell, J. R., Maselli, O. J., Sigl, M., Edwards, J., Buizert, C., Blunier, T., Chappellaz, J., and Freitag, J.: Local artifacts in ice core methane records caused by layered bubble trapping and in situ production: a multi-site investigation, Clim. Past, 12, 1061-1077, https://doi.org/10.5194/cp-12-1061-2016, 2016.

Rhodes, R. H., Faïn, X., Stowasser, C., Blunier, T., Chappellaz, J., McConnell, J. R., Romanini, D., Mitchell, L. E., and Brook, E. J.: Continuous methane measurements from a late Holocene Greenland ice core: Atmospheric and in-situ signals, Earth Planet. Sci. Lett., 368, 9–19. http://doi.org/10.1016/j.epsl.2013.02.034, 2013.

Rubino, M., Etheridge, D. M., and System, D. P. T. E.: Revised records of atmospheric trace gases CO_2, CH_4, N_2O, and $\delta_{13}C$-CO_2 over the last 2000 years from Law Dome, Antarctica, Earth Syst. Sci. Data, 11, 473-492, https://doi.org/10.5194/essd-11-473-2019, 2019.

Ryu, Y., Ahn, J., and Yang, J.-W.: High-Precision Measurement of N_2O Concentration in Ice Cores, Environ. Sci. Technol., 52, 731-738, https://doi.org/10.1021/acs.est.7b05250, 2018.

Ryu, Y., Ahn, J., Yang, J.-W., Brook, E. J., Timmermann, A., Blunier, T., Hur, S., and Kim, S.-J.: Atmospheric nitrous oxide variations on centennial time scales during the past two millennia. Glob. Biogeochem. Cycles, 34(9), http://doi.org/10.1029/2020GB006568, 2020.

Schilt, A., Baumgartner, M., Blunier, T., Schwander, J., Spahni, R., Fischer, H., and Stocker, T. F.: Glacial-interglacial and millennial-scale variations in the atmospheric nitrous oxide concentration during the last 800,000 years, Quat. Sci. Rev., 29, 182-192, https://doi.org/10.1016/j.quascirev.2009.03.011, 2010.

Seierstad, I., Abbott, M. B., Bigler, M., Blunier, T., Bourne, A. J., Brook, E., Buchardt, S. L., Buizert, C., Clausen, H., Cook, E., Dahl-Jensen, D., Davies, S. M., Guillevic, M., Johnsen, S., Pedersen, D. S., Popp, T., Rasmussen, S. O., Severinghaus, J. P., Svensson, A., and Vinther, B.: Consistently dated records from the Greenland GRIP, GISP2 and NGRIP ice cores for the past 104 ka reveal regional millennial-scale $\delta^{18}O$ gradients with possible Heinrich event imprint, Quat. Sci. Rev., 106, 29-46, https://doi.org/10.1016/j.quascirev.2014.10.032, 2014.

Seltzer, A. M., Buizert, C., Baggenstos, D., Brook, E. J., Ahn, J., Yang, J.-W., and Severinghaus, J. P.: Does $\delta^{18}O$ of O_2 record meridional shifts in tropical rainfall?, Clim. Past, 13, 1323-1338, https://doi.org/10.5194/cp-13-1323-2017, 2017.

Severinghaus, J. P., Beaudette, R., Headly, M. A., Taylor, K., and Brook, E. J.: Oxygen-18 of O_2 Records the Impact of Abrupt Climate Change on the Terrestrial Biosphere, Science, 324, 1431-1434, https://doi.org/10.1126/science.1169473, 2009.

Severinghaus, J. P. and Brook, E.: Abrupt climate change at the end of the last glacial period inferred from trapped air in polar Ice, Science, 286, 930-934, https://doi.org/10.1126/science.286.5441.930, 1999.

Severinghaus, J. P., Grachev, A., Luz, B., and Caillon, N.: A method for precise measurement of argon 40/36 and krypton/argon ratios in trapped air in polar ice with applications to past firn thickness and abrupt climate change in Greenland and at Siple Dome, Antarctica, Geochim. Cosmochim. Acta, 67, 325-343, https://doi.org/10.1016/S0016-7037(02)00965-1, 2003.

Severinghaus, J. P., Sowers, T., Brook, E., Alley, R. B., and Bender, M.: Timing of abrupt climate change at the end of the Younger Dryas interval from thermally fractionated gases in polar ice, Nature, 391, 141-146, https://doi.org/10.1038/34346, 1998.

Schmitt, J., Schneider, R., and Fischer, H.: A sublimation technique for high-precision measurements of $\delta^{13}CO_2$ and mixing ratios of CO_2 and N_2O from air trapped in ice cores, Atmos. Meas. Tech., 4, 1445–1461, http://doi.org/10.5194/amt-4-1445-2011, 2011.

Schmitt, J., Seth, B., Bock, M., and Fischer, H.: Online technique for isotope and mixing ratios of CH_4, N_2O, Xe and mixing ratios of organic trace gases on a single ice core sample, Atmos. Meas. Tech., 7(8), 2645–2665, http://doi.org/10.5194/amt-7-2645-2014, 2014.

Siegenthaler, U., Monnin, E., Kawamura, K., Spahni, R., Schwander, J., Stauffer, B., Stocker, T. F., Barnola, J.-M., and Fischer, H.: Supporting evidence from the EPICA Dronning Maud Land ice core for atmospheric CO_2 changes during the past millennium, Tellus B, 57, 51-57, https://doi.org/10.3402/tellusb.v57i1.16774, 2005.

Sowers, T., Bender, M., and Raynaud, D.: Elemental and isotopic composition of occluded O_2 and N_2 in polar ice, J. Geophys. Res., 94, D4, 5137–5150, http://doi.org/10.1029/JD094iD04p05137, 1989.

Sowers, T.: N_2O record spanning the penultimate deglaciation from the Vostok ice core, J. Geophys. Res., 106, 31903-31914, https://doi.org/10.1029/2000JD900707, 2001.

Sowers, T., Alley, R. B., and Jubenville, J.: Ice core records of atmospheric N_2O covering the last 106,000 years, Science, 301, https://doi.org/10.1126/science.1085293, 2003.

Tanaka, M., Nakazawa, T., and Aoki, S.: High Quality Measurements of the Concentration of Atmospheric Carbon Dioxide, Journal of the Meteorological Society of Japan. Ser. II, 61, 678-685, https://doi.org/10.2151/jmsj1965.61.4_678, 1983.

Tanaka, M., Nakazawa, T., Shiobara, M., Ohshima, H., Aoki, S., Kawaguchi, S., Yamanouchi, T., Makino, Y., and Murayama, H.: Variations of atmospheric carbon dioxide concentration at Syowa Station (69°00'S, 39°35'E), Antarctica, Tellus B, 39, 72, doi/10.3402/tellusb.v39i1-2.15324, 1987.

Tsuboi, K., Nakazawa, T., Matsueda, H., Machida, T., Aoki, S., Morimoto, S., Goto, D., Shimosaka, T., Kato, K., Aoki, N., Watanabe, T., Mukai, H., Thojima, Y., Katsumata, K., Murayama, S., Ishidoya, S., Fujitani, T., Koide, H., Takahashi, M., Kawasaki, T., Takizawa, A., and Sawa, Y.: InterComparison Experiments for Greenhouse Gases Observation (iceGGO) in 2012–2016, Technical Reports of the Meteorological Research Institute, 79, https://doi.org/10.11483/mritechrepo.79, 2017.

WAIS Divide Project Members: Precise interpolar phasing of abrupt climate change during the last ice age, Nature, 520, 661-665, https://doi.org/10.1038/nature14401, 2015.

Figures

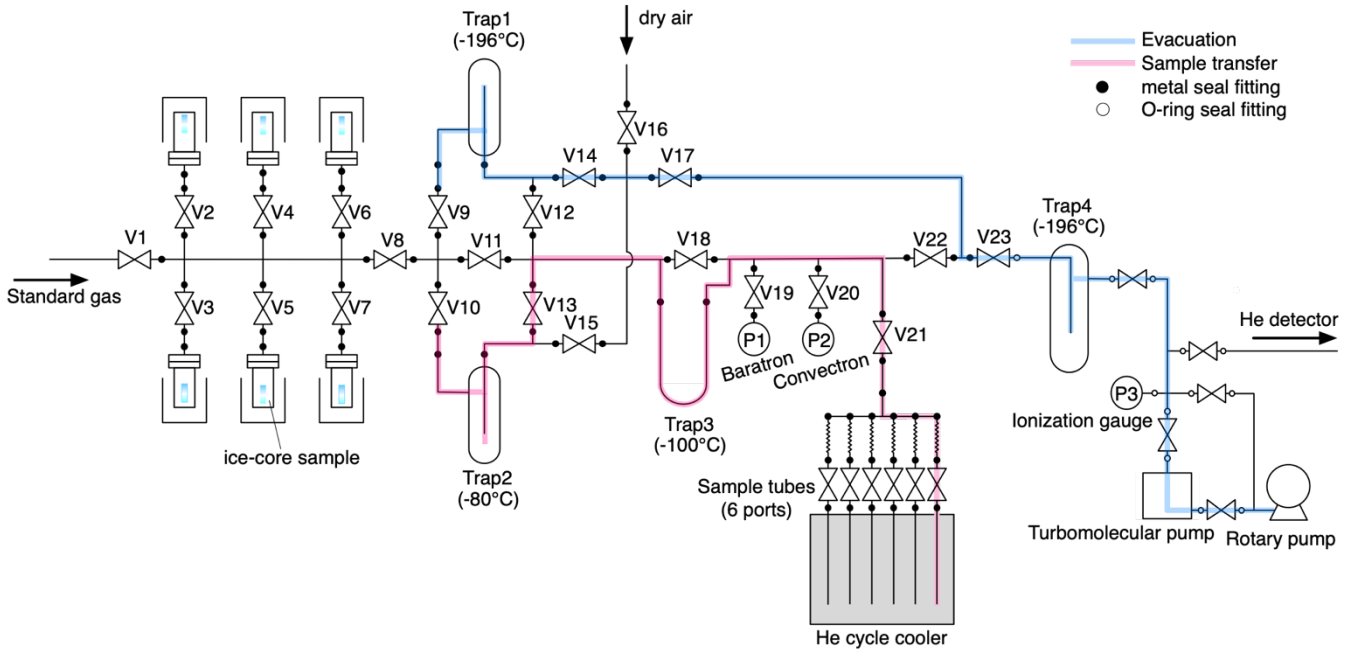

Figure 1: Schematic diagram of the wet extraction system.

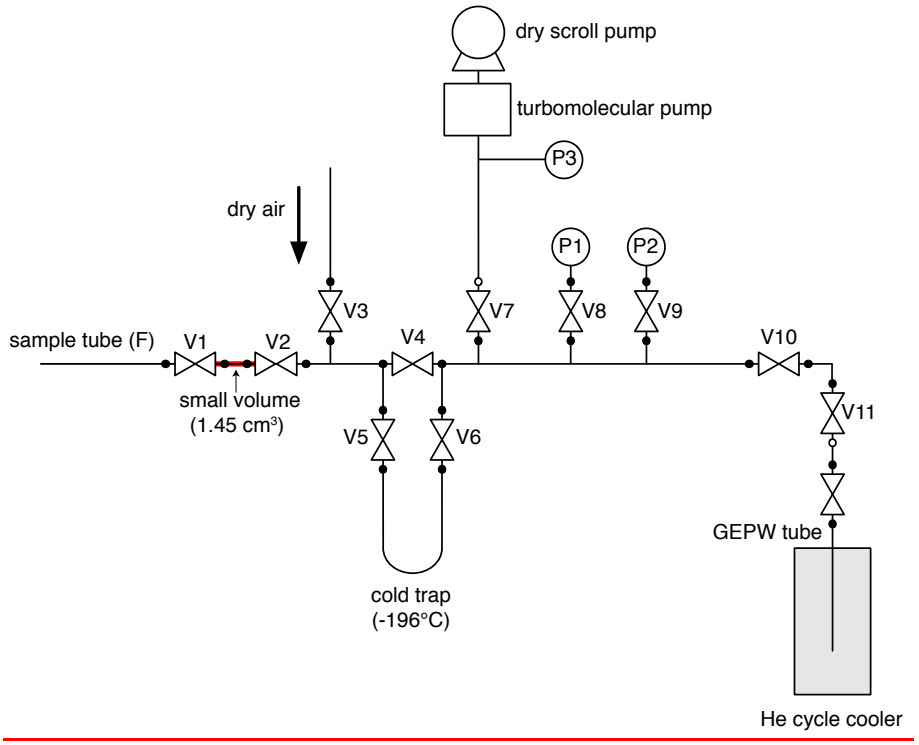

Figure 2: Schematic diagram of the split line.

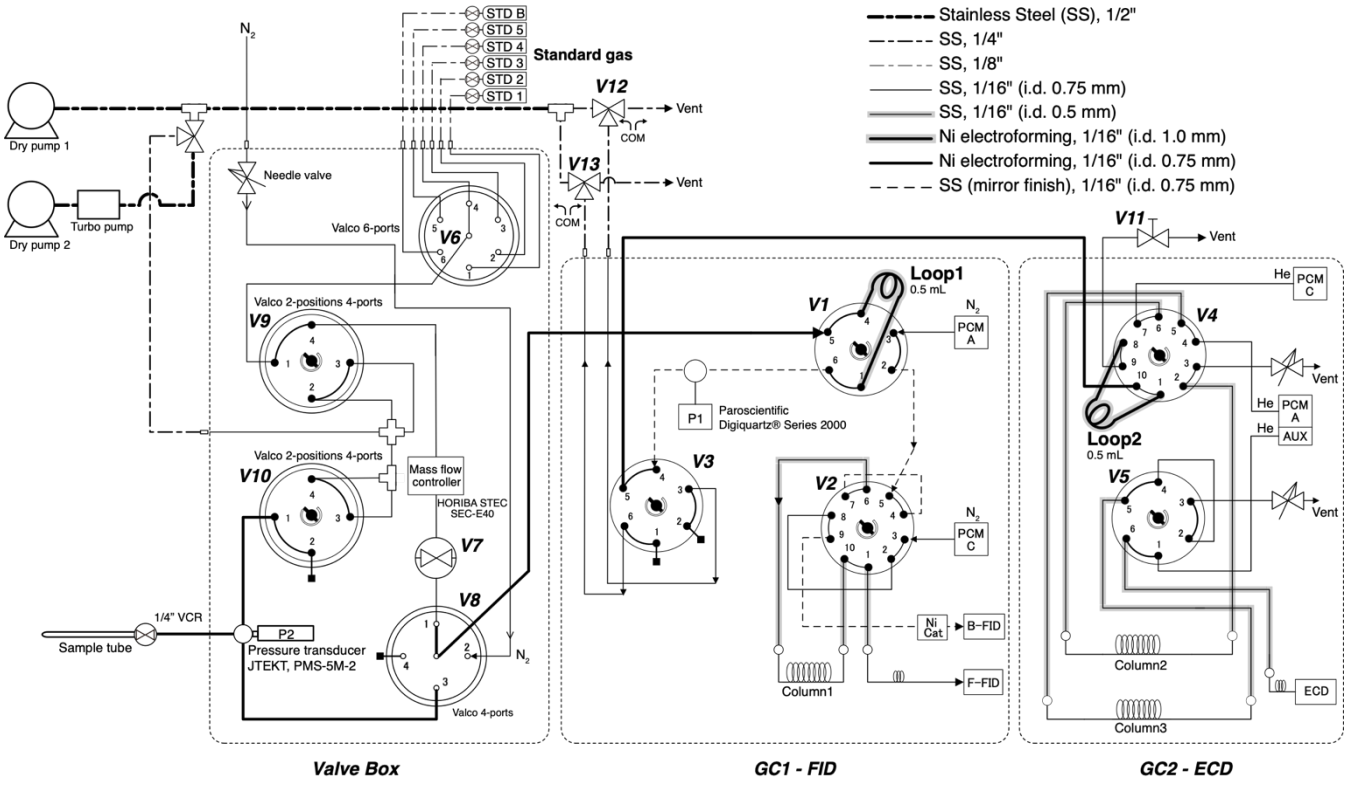

Figure 3: Schematic diagram of gas chromatographs and inlet. All two-position valves are in "OFF" positions.

1090

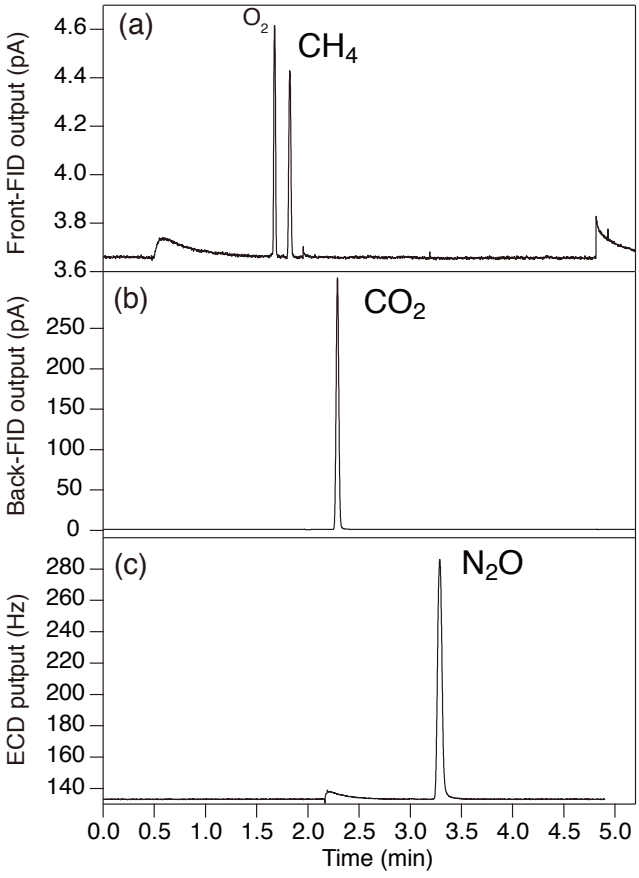

Figure 4: Typical chromatogram of (a) Front FID for CH_4 (the largest peak is O_2, and the second-largest peak is CH_4), (b) Back FID for CO_2, and (c) ECD for N_2O.

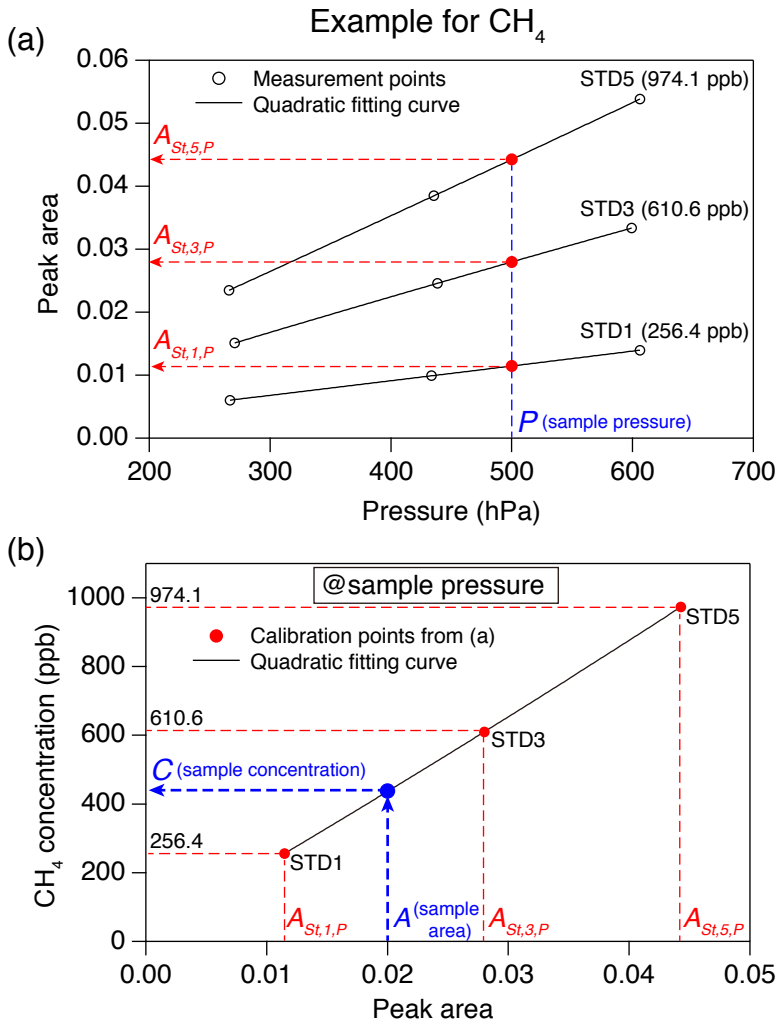

~~Figure 5~~Figure 5: Example of a calibration procedure for greenhouse gas concentration. (a) Peak areas for three standard gases measured at three pressures (black circles), with quadratic fits (black lines). Peak areas of the standard gases ($A_{St,1,P}$, $A_{St,3,P}$, and $A_{St,5,P}$, red circles) estimated at the sample pressure (blue dashed line) are also shown. (b) Calibration curve at the sample pressure (black line) from the peak areas from (a). The numbers in the panel are CH_4 concentrations of the standard gases, A is the peak area of the sample, and C is the CH_4 concentration of the sample.

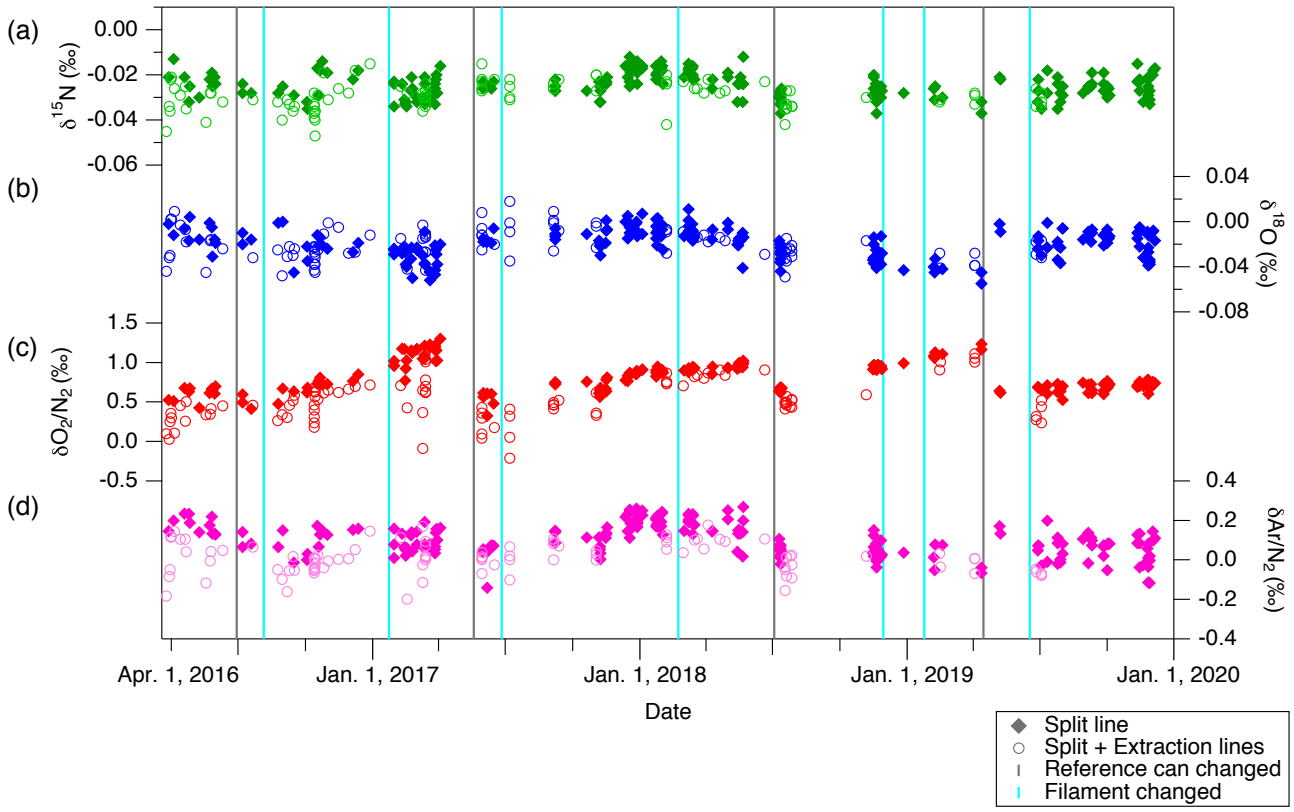

Figure 6: Standard gas (STDA) composition measured against reference gas for (a) $\delta^{15}N$, (b) $\delta^{18}O$, (c) $\delta O_2/N_2$, and (d) $\delta Ar/N_2$. Filled markers represent samples transferred only through the split line, and open markers represent samples transferred through both extraction and split lines. Vertical grey lines indicate the timing of replacements of reference can, and vertical light blue lines indicate the timing of filament replacements.

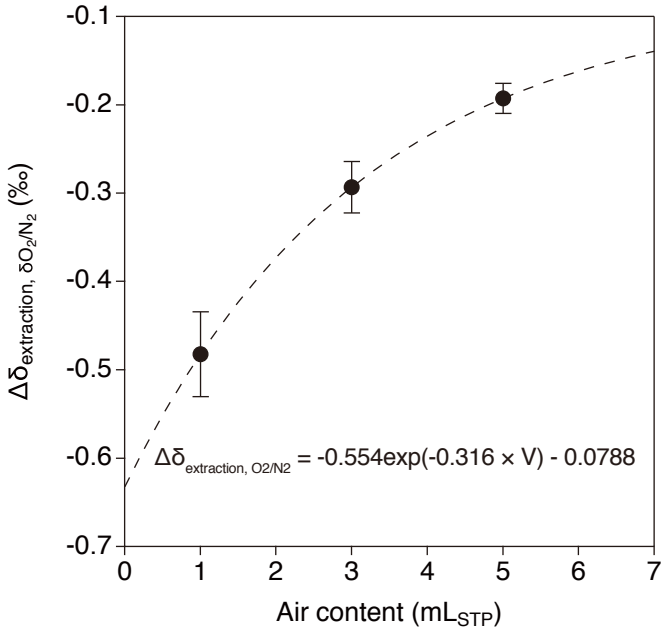

Figure ~~6~~7: Change of $\delta O_2/N_2$ by wet extraction and overnight storage. Dashed line represents exponential fit to the data ($\Delta\delta_{extraction,\ O2/N2}$ = -0.~~55362~~554 exp(-0.~~31606~~316 × *V*) ~~+ -~~ 0.~~0788020~~0788).

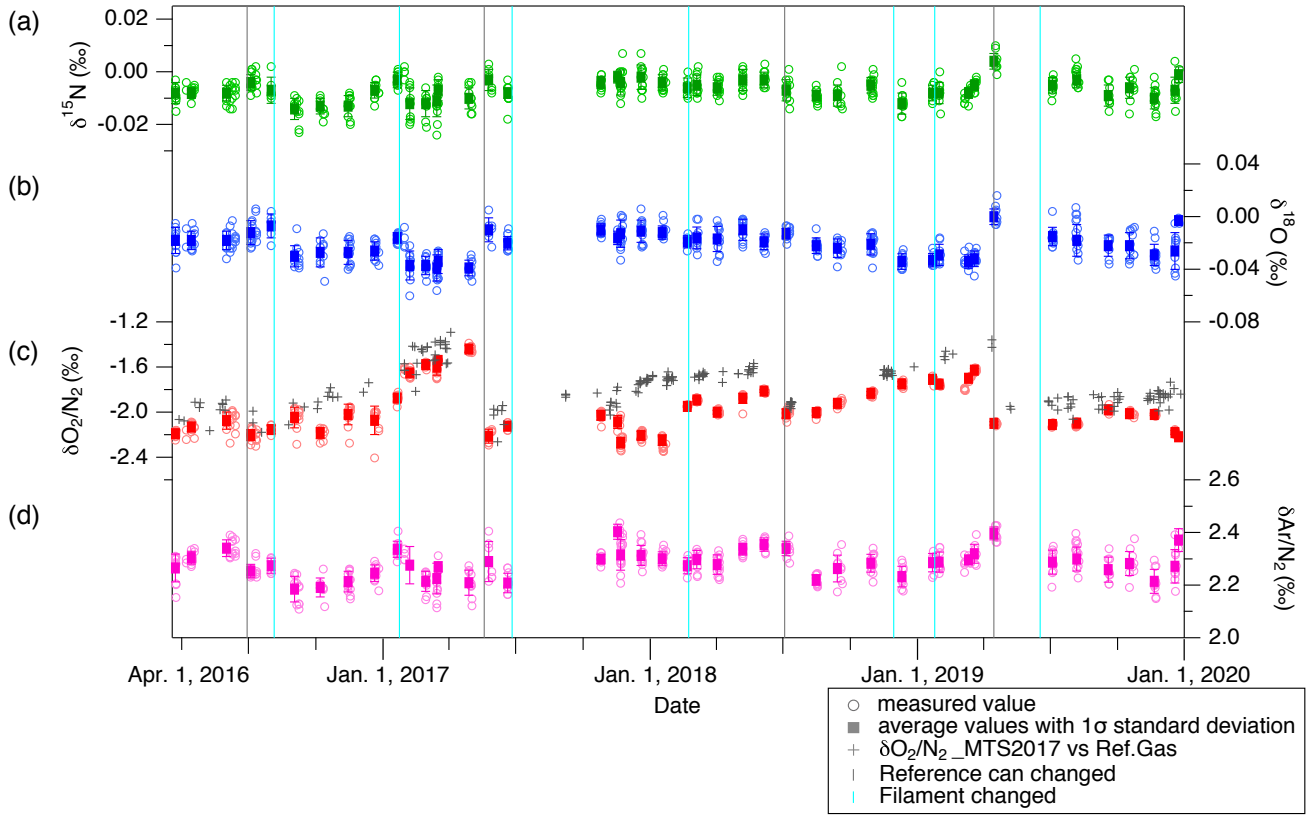

Figure ~~7~~8: Atmospheric composition measured against reference gas for (a) $\delta^{15}N$, (b) $\delta^{18}O$, (c) $\delta O_2/N_2$, and (d) $\delta Ar/N_2$. Open markers represent individual data points, whereas filled markers represent the means of values measured within several days (error bars are one standard deviation~~deviations~~). Grey plus (+) markers in (d) represent estimated $\delta O_2/N_2$ of MTS-2017 against reference gas through the measurements of STD-A against the reference gas, assuming that $\delta O_2/N_2$ of STD-A has not changed. Vertical grey lines indicate the timing of replacements of reference can, and vertical light blue lines indicate the timing of filament replacements.

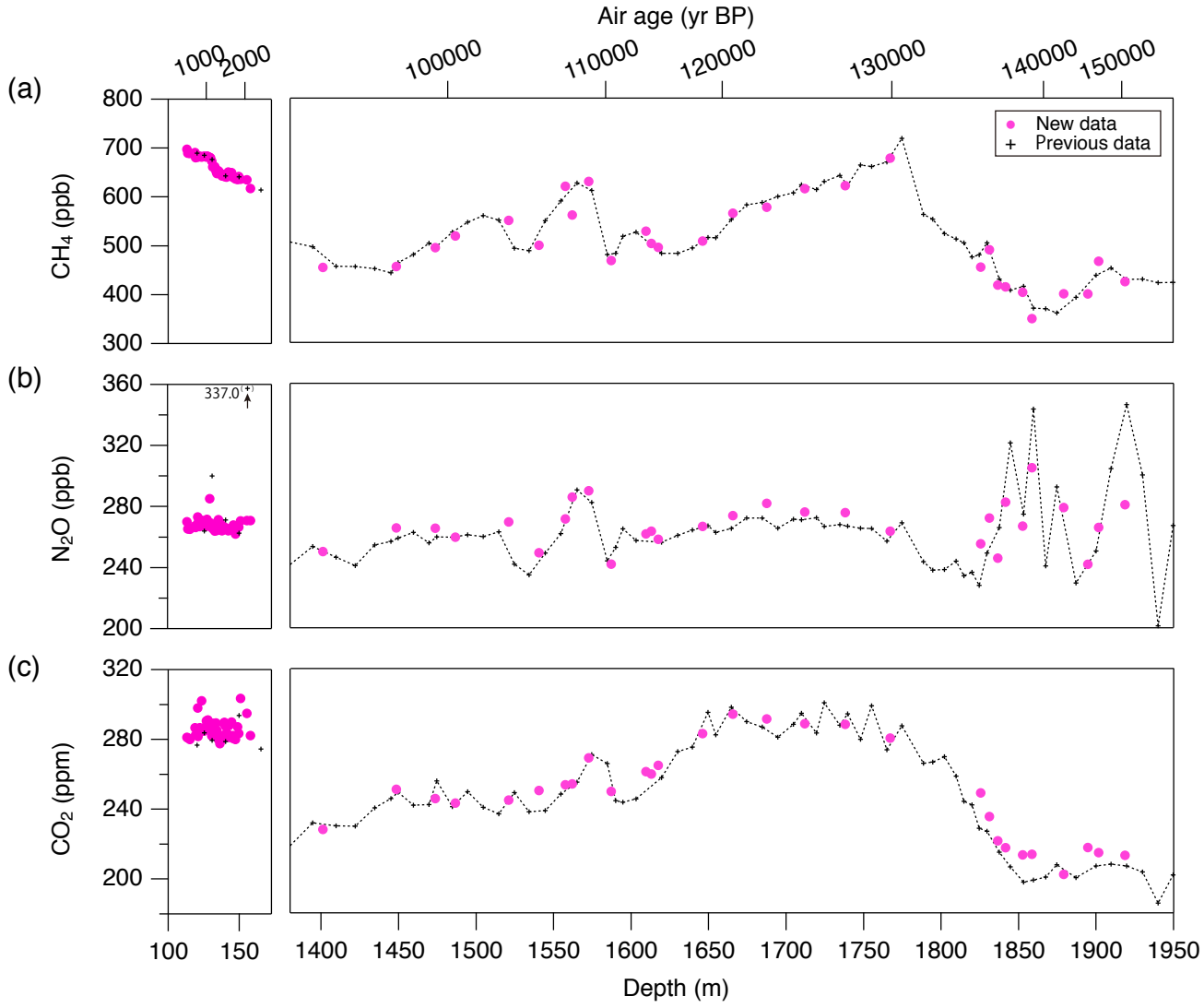

125 **Figure 89:** CH_4, N_2O and CO_2 concentrations of the Dome Fuji ice core, and comparison with previous records from the same core (Kawamura, 2000 and Kawamura et al., 2007).

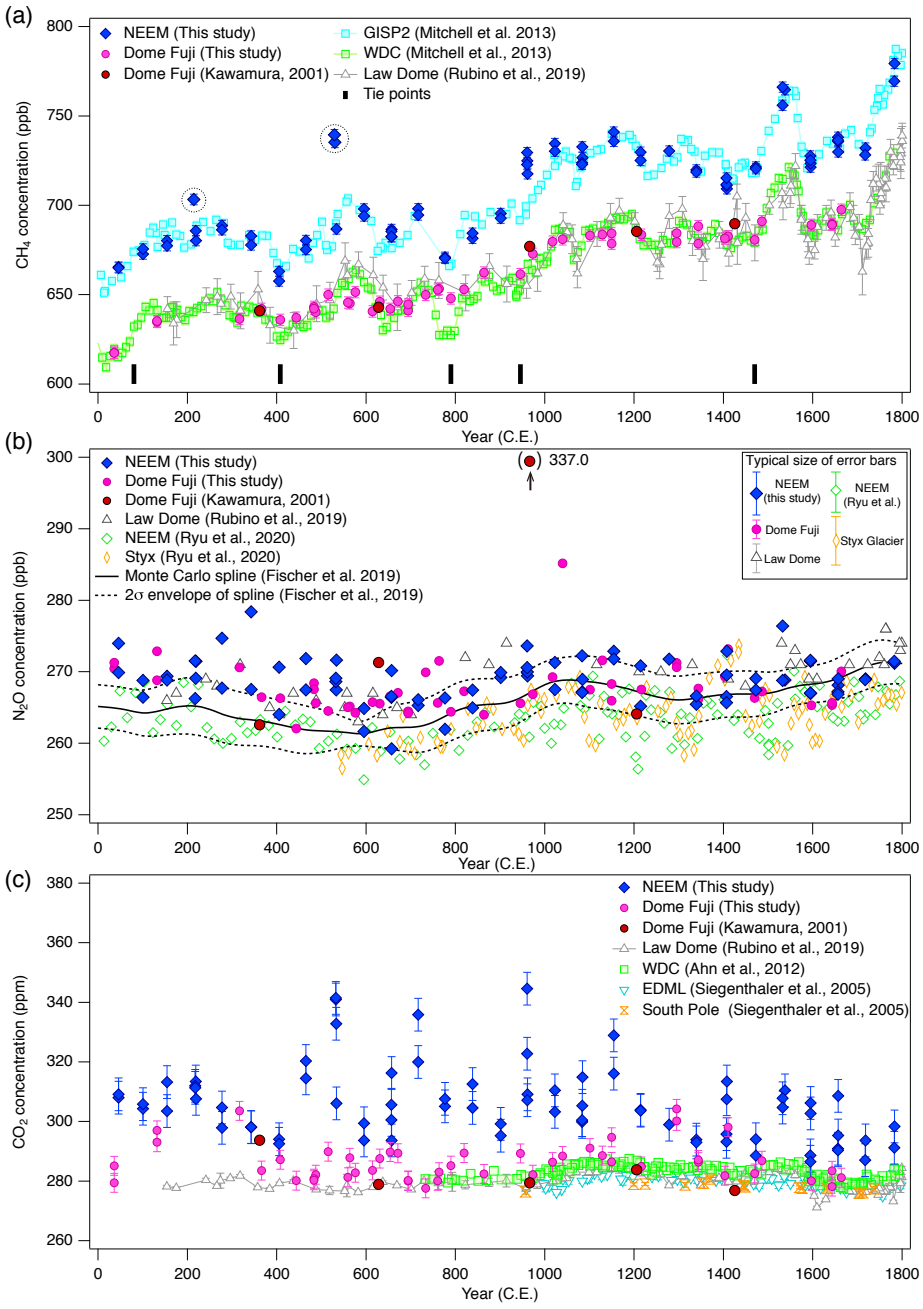

Figure ~~9~~10: (a) CH_4, (b) N_2O and (c) CO_2 concentrations for 0 – 1800 C.E. from the DF and NEEM ice cores measured with our new method, and the comparison with published records ~~from other groups~~ (Ahn et al., 2012; Kawamura, 2001; Kawamura et al., 2007; Mitchell et al., 2013; Rubino et al., 2019; Ryu et al., 2020; Siegenthaler et al., 2005). Details are summarized in Table A1. The DF data is placed on the WDC05A chronology by placing 5 tie points between the CH_4 variations of the DF and WD cores (thick tick marks at the bottom of (a)), and all the other data are placed on the respective (published) time scales. ~~Details are summarized in Table A1.~~ Five CH_4 outliers at two depths in the NEEM core, highlighted by dotted-line circles, are interpreted as natural artifacts (see text and Fig. 11).

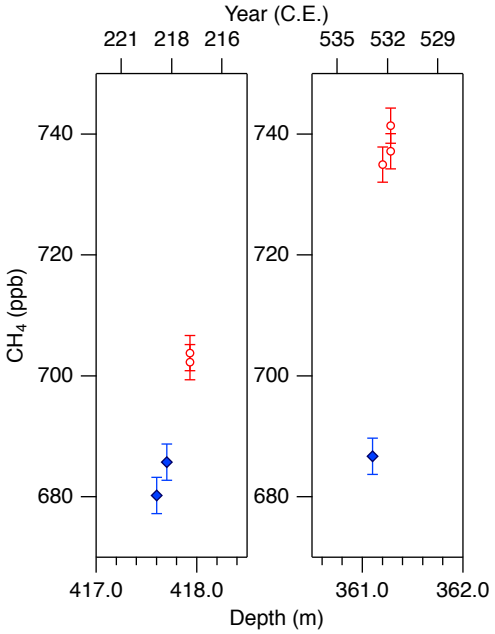

Figure ~~10~~11: Detailed views of individual CH_4 data for the abrupt (non-atmospheric) increases in the NEEM core at ~418 and 361 m. Data shown in blue agree with the GISP2 data, and those in red are unrealistically high (interpreted as natural artifacts~~artefacts~~). ~~The dotted line (blue) connects the blue markers (mean of two data for 417 m and one data for 361 m) with their neighbouring data points.~~

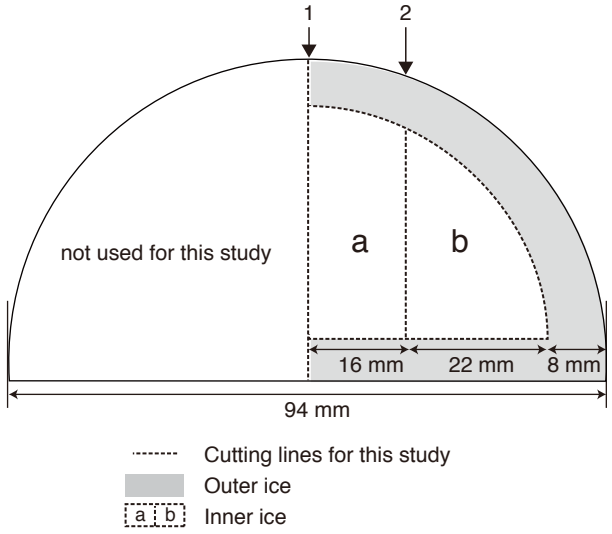

Figure~~s~~ ~~11~~12: Typical cross-sectional cutting plan of the DF core for duplicate measurements and outer-inner comparisons for mass spectrometer analyses. The sample length is ~12 cm. The original outer surface (black line) has been exposed to the atmosphere for ~20 years. ~~Dotted~~The ice is first cut at line 1, then the outer part is removed, and finally the inner ice is cut at line 2 into "a" and "b" pieces. Dashed lines indicate the boundaries between "a," "b," and "outer" pieces. For a single (non-duplicate) ~~measurements, "a" piece~~measurement, the ice is not cut~~.~~ at line 1 (only cut at line 2 to produce "b" piece).

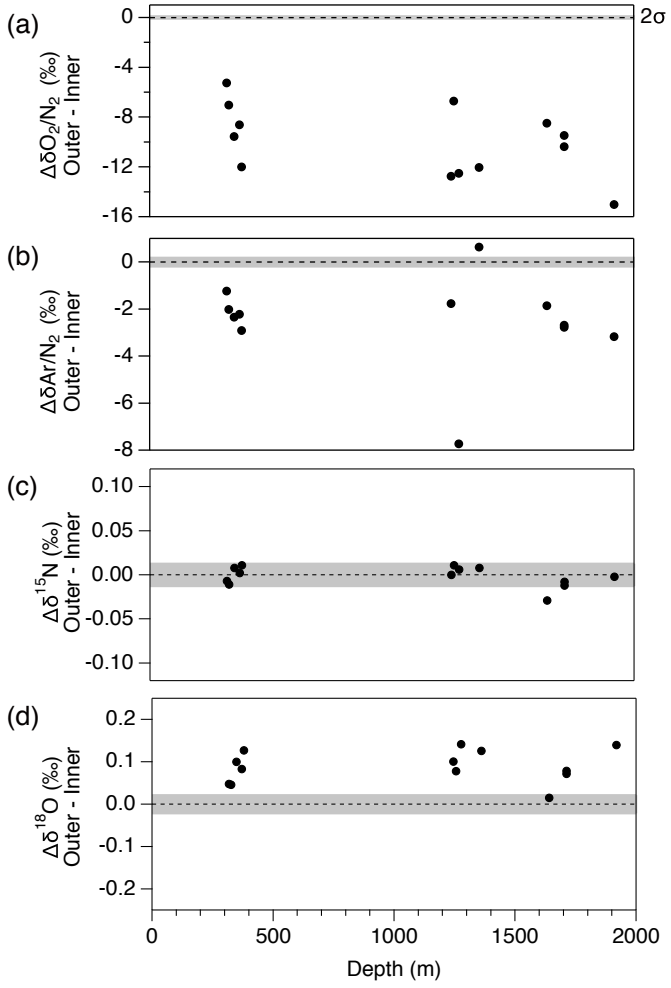

Figure ~~12:~~ ~~Difference~~13: Pair difference (Δ) between outer ice and inner ice for (a) $\delta O_2/N_2$, (b) $\delta Ar/N_2$, (c) $\delta^{15}N$, and (d) $\delta^{18}O$. Grey shadings indicate the estimated 2σ uncertainty for clathrate ice (from pooled standard deviations of duplicates with > 8 mm of outer removal).

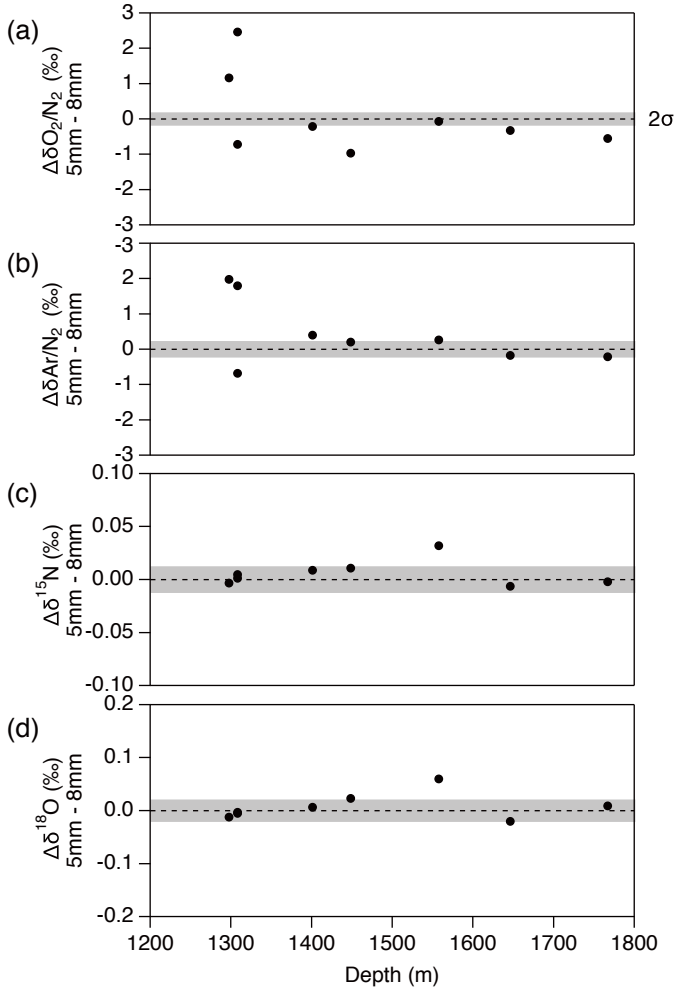

Figure ~~13~~14: Pair difference between the two inner ice pieces with the thickness of outer removal of 5 mm and 8 mm for (a) $\delta O_2/N_2$, (b) $\delta Ar/N_2$, (c) $\delta^{15}N$, and (d) $\delta^{18}O$. Grey shadings indicate the estimated 2σ uncertainty for clathrate ice (from pooled standard deviations of duplicates with > 8 mm of outer removal).

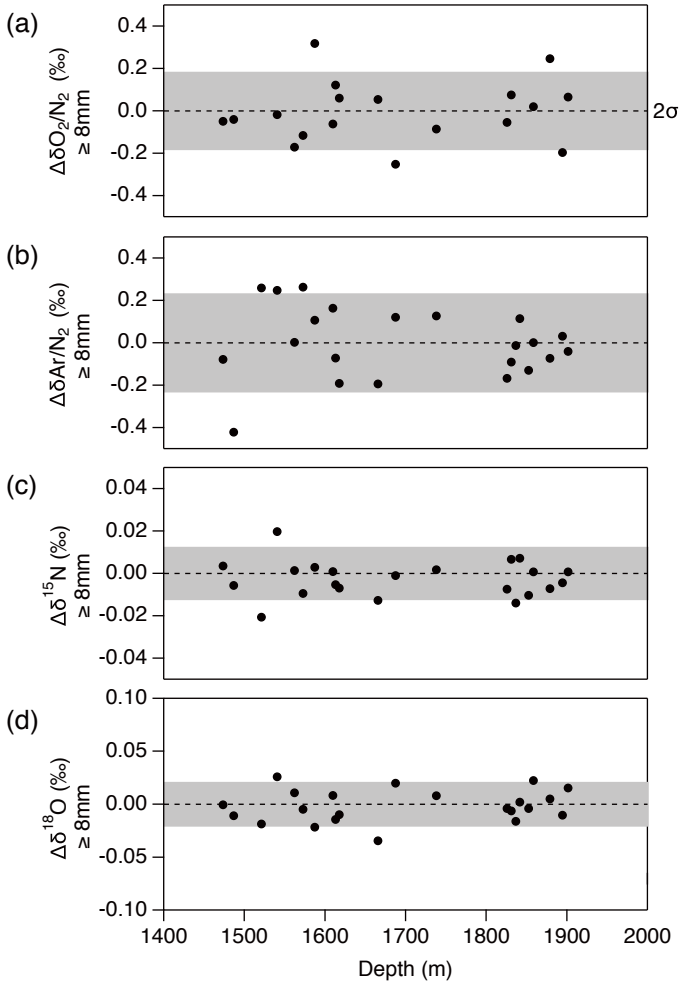

Figure ~~14~~15: Pair difference between the two inner ice ~~with the thickness of~~pieces (data from "b" piece minus that from "a" piece) whose outer ~~removal of >~~parts are removed by 8 mm or more for (a) $\delta O_2/N_2$, (b) $\delta Ar/N_2$, (c) $\delta^{15}N$, and (d) $\delta^{18}O$. Grey shadings indicate the estimated 2σ uncertainty for clathrate ice (from pooled standard deviations of duplicates ~~with > 8 mm of outer removal~~).

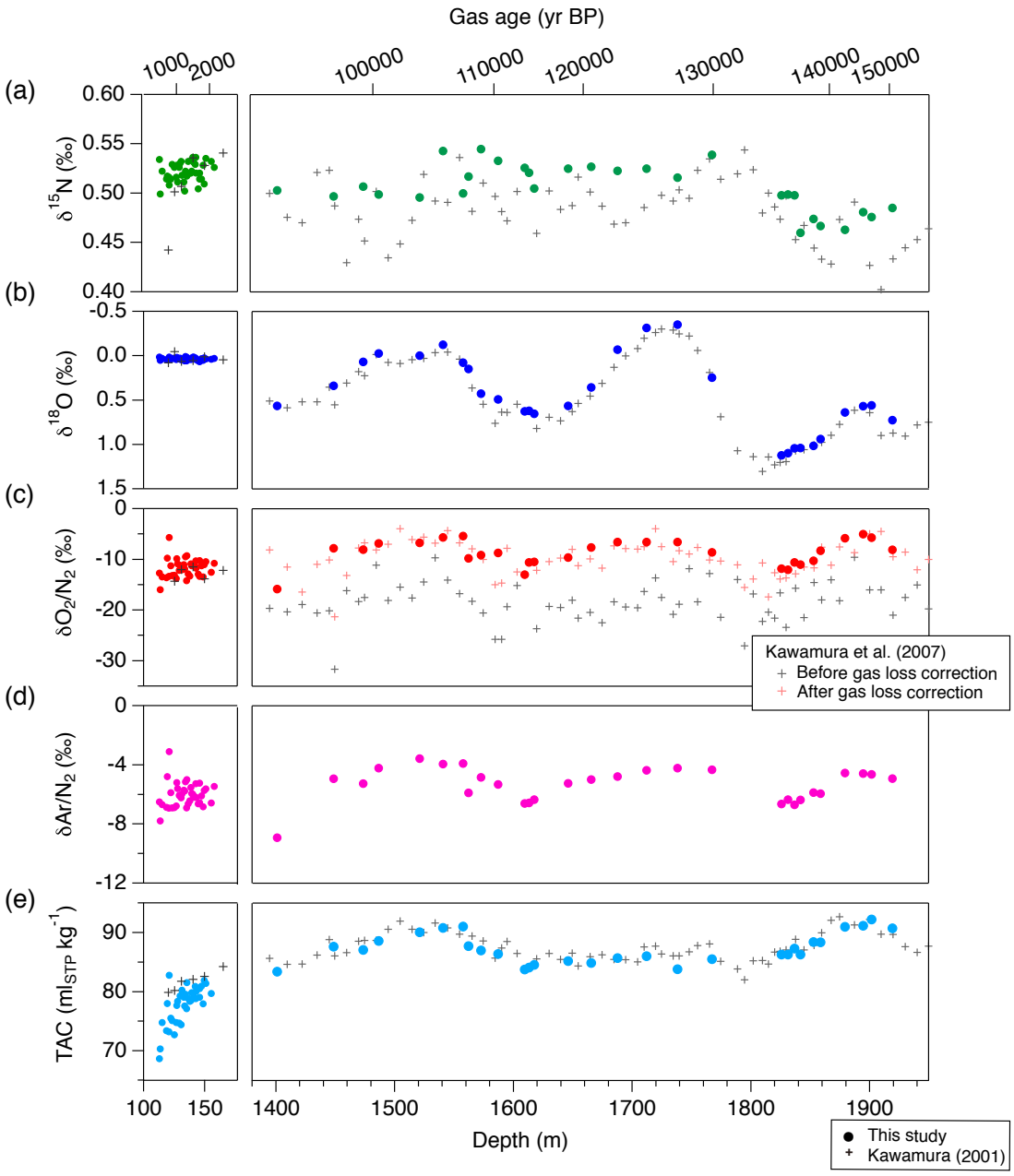

~~Figure15~~Figure16: The DF records of mass spectrometer measurements and TAC from this study (filled markers), and comparison with previous records from the same core (crosses ~~connected with dotted lines~~, Kawamura, 2000; Kawamura et al., 2007). (a) $\delta^{15}N$, (b) $\delta^{18}O$, (c) $\delta O_2/N_2$, (d) $\delta Ar/N_2$, and (e) TAC. For the previous $\delta O_2/N_2$ records in the right panel of (c), both raw data (black) and corrected data for gas-loss fractionation during core storage at -25 °C (red) are shown.

Tables

Table 1: Settings of gas chromatographs.

	GC1		GC2
	CH_4	CO_2	N_2O
Carrier gas	N_2, 10 ~~ml~~mL min^{-1}		He, 7 ~~ml~~mL min^{-1}
Sample loop volume	0.5 ~~ml~~mL		0.5 ~~ml~~mL
Oven temperature	30 ˚C		30 ˚C
Column	GS-CarbonPLOT		HP-PLOT/Q
Length	30 m		30 m
Internal diameter	0.53 mm		0.53 mm
Film thickness	3 µm		40 µm
Ni-catalyst temperature	None	400 ˚C	None
Detector	FID	FID	ECD
Temperature	200 ˚C	200 ˚C	325 ˚C
H_2 flow rate	35 ~~ml~~mL min^{-1}	40 ~~ml~~mL min^{-1}	None
Air flow rate	400 ~~ml~~mL min^{-1}	400 ~~ml~~mL min^{-1}	None
Make-up gas	N_2, 20 ~~ml~~mL min^{-1}	N_2, 20 ~~ml~~mL min^{-1}	Ar+CH_4 (5 %), 10 ~~ml~~mL min^{-1}

Table: 2: Standard gases.

	STD 1	STD 2	STD 3	STD 4	STD 5	STD A	STD B	scale
Cylinder ID	~~CQB09303~~ CQB06571	~~CQB12403~~ CQB06572	~~CQB09309~~ CQB06573	~~CQB07938~~ CQB08455	~~CQB09336~~ CQB08456	CRC00059	CRC00057	
CH_4 [ppb]	~~255.3~~256.4	~~430.9~~436.8	~~609.9~~610.6	~~796~~791.2	~~968.8~~974.1	526.7	720.2	TU-2008
N_2O [ppb]	~~186.2~~189.6	~~222.9~~221.0	259.7	~~298.1~~286.5	~~317.9~~329.7	241.3	273.2	TU-2006
CO_2 [ppm]	169.~~79~~33	~~209.25~~208.88	249.~~64~~65	289.~~37~~30	~~330.71~~328.90	229.04	269.21	TU-2008

Table 3: Collector configurations of the mass spectrometer.

Mass	Slit width (mm)	Resistor (Ω)	Typical ion current (A)
28	2.0	3×10^{8}	2×10^{-8}
29	3.8	3×10^{10}	1×10^{-10}
32	3.8	1×10^{9}	4×10^{-9}
33	1.4	1×10^{12}	3×10^{-12}
34	3.8	3×10^{11}	2×10^{-11}
36	2.0	1×10^{12}	1×10^{-12}
38	1.4	1×10^{12}	2×10^{-13}
40	2.0	3×10^{9}	3×10^{-10}
44	2.4	1×10^{10}	4×10^{-12}

Table 4: Test results using a standard gas (STD-A) for greenhouse gases.

		CH_4 (ppb)	N_2O (ppb)	CO_2 (ppm)	n
Sample tubes	Average	+0.8	+1.3	+0.1	25
(overnight storing)	Std. dev.	2.1	2.1	1.1	
Test tubes	Average	+0.7	+0.9	-0.2	17
(immediate measurement)	Std. dev.	2.2	1.0	0.1	
Extraction line	Average	+1.5	+0.8	+1.1	9
(mimicking ice core extraction)	Std. dev.	1.6	1.3	0.7	

Values are differences from the calibrated concentrations of the STD-A cylinder (Table 3)

Table 5: Composition of STD-A for mass spectrometer measurements.

	$\delta^{15}N$ (‰)	$\delta^{18}O$ (‰)	$\delta O_2/N_2$ (‰)	$\delta Ar/N_2$ (‰)	n
Mean	-0.018	0.002	2.595	-2.171	214 (18 for $\delta O_2/N_2$)
Std. error	<0.001	<0.001	0.008	0.006	

$\delta O_2/N_2$ is determined in ~~Jul.~~July 2019 against the 2017 annual mean $\delta O_2/N_2$ over Minamitorishima island provided by AIST. Other ratios are determined against outside air sampled monthly at NIPR over Feb. 2016 – Dec. 2019.

Table 6: Age control points for the DF core from CH_4 matching to the WDC core (0 – 1800 C.E.)

DF depth (m)	WDC05A age (C.E.)	Approximate 1σ error [a] (year)
119.23	1470	42
131.29	945	42
134.17	790	33
148.65	408	41
156.515	80	44

[a] estimated as ~~the~~ half of the mean age intervals from the tie point to the neighbouring CH_4 data points (uncertainty of WDC05A itself is also considered).

Table 7: Pooled standard deviations for the NEEM and Dome Fuji ice cores.

	CH_4 (ppb)	N_2O (ppb)	CO_2 (ppm)	TAC (~~ml~~$_{STP}$mL$_{STP}$ kg^{-1})	Number of pairs	$\delta^{15}N$ (‰)	$\delta^{18}O$ (‰)	$\delta O_2/N_2$ (‰)	$\delta Ar/N_2$ (‰)	Number of pairs
NEEM (bubble)	2.9	3.0	5.5		25	0.006	0.008	0.775	0.450	23
DF (bubble)	3.2	1.3	3.2	0.66	8	0.009	0.018	0.235	0.119	8
DF (clathrate)	3.2	2.2	3.1	0.67	29	0.006	0.010	0.089	0.115	22